




12-2015

## Spontaneously Generated Inhomogeneous Phases via Holography

Kübra Yeter Aydeniz

*University of Tennessee - Knoxville, kyeter@vols.utk.edu*

Follow this and additional works at: [https://trace.tennessee.edu/utk\\_graddiss](https://trace.tennessee.edu/utk_graddiss)

 Part of the [Condensed Matter Physics Commons](#), and the [Elementary Particles and Fields and String Theory Commons](#)

---

### Recommended Citation

Yeter Aydeniz, Kübra, "Spontaneously Generated Inhomogeneous Phases via Holography. " PhD diss., University of Tennessee, 2015.  
[https://trace.tennessee.edu/utk\\_graddiss/3621](https://trace.tennessee.edu/utk_graddiss/3621)

This Dissertation is brought to you for free and open access by the Graduate School at TRACE: Tennessee Research and Creative Exchange. It has been accepted for inclusion in Doctoral Dissertations by an authorized administrator of TRACE: Tennessee Research and Creative Exchange. For more information, please contact [trace@utk.edu](mailto:trace@utk.edu).

To the Graduate Council:

I am submitting herewith a dissertation written by Kübra Yeter Aydeniz entitled "Spontaneously Generated Inhomogeneous Phases via Holography." I have examined the final electronic copy of this dissertation for form and content and recommend that it be accepted in partial fulfillment of the requirements for the degree of Doctor of Philosophy, with a major in Physics.

George Siopsis, Major Professor

We have read this dissertation and recommend its acceptance:

John J. Quinn, Norman Mannella, Fernando A. Schwartz

Accepted for the Council:

Carolyn R. Hodges

Vice Provost and Dean of the Graduate School

(Original signatures are on file with official student records.)

# Spontaneously Generated Inhomogeneous Phases via Holography

A Dissertation Presented for the  
Doctor of Philosophy  
Degree

The University of Tennessee, Knoxville

Kübra Yeter-Aydeniz

December 2015

© by Kübra Yeter-Aydeniz, 2015  
All Rights Reserved.



*To my parents, grandparents, to my beloved husband Mehmet and to my brother...*

# Acknowledgements

This PhD thesis is the last stop of my five-year-long journey at The University of Tennessee, Knoxville. I am grateful to my advisor, Professor George Siopsis for always being there to answer my questions, for his patience, guidance and support. Without his support I could not have come this far. I would also like to thank my committee members Professors John J. Quinn, Norman Mannella, Fernando Schwartz for their time, guidance and support. I am also grateful to Professors James E. Parks and Yuri Kamyshkov for their guidance.

I would like to thank my collaborators James Alsup and Eleftherios Papanonopoulos as well. I am especially grateful to James Alsup for answering my questions, invaluable discussions, and support. I would also like to thank to my colleagues Savan Kharel, Suman Ganguli, Mostafa Sherif Derbala Aly, Eleftherios Moschandreou, Marouanne Salhi, Jason Therrien for their valuable discussions, help and for being great group mates.

I am grateful to the University of Tennessee, Knoxville, Department of Physics and Astronomy, Department of Energy Grant No. DE-FG05-91ER40627, Turkish Higher Education Council, and Anadolu University, Eskisehir for their financial support.

I would like to thank all of my teachers who encouraged me go through this process. Special thanks go to my professors Sebnem Kandil Ingec, Pervin Unlu, Uygur Kanli, Kudret Ozdas, Murat Tanisli, Cem Yuce, Hakan Cebeci, who inspired, encouraged, and supported me to continue my career in academia.

The last but not the least, I am indebted to my family for their infinite support. I am grateful to my parents Fahriye and Mustafa Yeter for always being with me, for their love, encouragement, dedication, and the most important for being my parents. I would like to thank my grandparents. I believe that their confidence in me and support throughout my education encouraged me to go through all this process. My brother, Mustafa Yasin Yeter, has been a role model for me in my educational and personal life, so I would like to thank him for guiding my thinking, and challenging me to become successful. My last thanks go to the smallest member of our family, my nephew, Mustafa Ilter Yeter. Thank you for making me smile everytime I hear your cute stories no matter how busy or tired I am.

And my husband Mehmet Aydeniz . . . I am grateful for your encouragement and support throughout this process. I am so lucky to have you in my life.

*“And now here is my secret, a very simple secret: It is only with the heart that one can see rightly; what is essential is invisible to the eye.”*

*Antoine de Saint-Exupery, The Little Prince*

# Abstract

We discuss a holographic model consisting of a  $U(1)$  gauge field and a scalar field coupled to a charged AdS (anti-de Sitter) black hole under a spatially homogeneous chemical potential. By turning on a higher-derivative interaction term between the  $U(1)$  gauge field and the scalar field, a spatially dependent profile of the scalar field is generated spontaneously. We calculate the critical temperature at which the transition to the inhomogeneous phase occurs for various values of the parameters of the system. We solve the equations of motion below the critical temperature, and show that the dual gauge theory on the boundary spontaneously develops a spatially inhomogeneous charge density. In addition to that we discuss the zeroes and poles of the determinant of the retarded Green function ( $\det G_R$ ) at zero frequency in a holographic system of charged massless fermions interacting via a dipole coupling. For large negative values of the dipole coupling constant  $p$ ,  $\det G_R$  possesses only poles pointing to a Fermi liquid phase. We show that a duality exists relating systems of opposite  $p$ . This maps poles of  $\det G_R$  at large negative  $p$  to zeroes of  $\det G_R$  at large positive  $p$ , indicating that the latter corresponds to a Mott insulator phase. This duality suggests that the properties of a Mott insulator can be studied by mapping the system to a Fermi liquid and then for small values of  $p$ ,  $\det G_R$  contains both poles and zeroes (pseudo-gap phase). Finally, we study holographic fermions in the spontaneously generated holographic lattice background defined above. We solve the equations of motion below  $T_c$  (critical temperature) and analyze the change in Fermi surface due to introduction of the holographic lattice. The band structure of this

fermionic system was also analyzed numerically and it was found that a band gap was formed due to lattice effects.

# Table of Contents

|          |   |           |
|----------|---|-----------|
| <b>1</b> | <b>Introduction</b>   | <b>1</b>  |
| 1.1      | Background: Superconductivity, Charge Density Waves, and Holography   | 3         |
| 1.1.1    | Superconductivity . . . . .   | 3         |
| 1.1.2    | Charge Density Waves (CDW) . . . . .  | 10        |
| 1.1.3    | Electrons in periodic potential . . . . .   | 12        |
| 1.2      | AdS/CFT Correspondence and Holography . . . . .   | 16        |
| 1.2.1    | Holographic Superconductors . . . . .   | 23        |
| <b>2</b> | <b>Spontaneously Generated Inhomogeneous Phases via Holography</b>  | <b>30</b> |
| 2.1      | Introduction . . . . .  | 30        |
| 2.2      | The setup . . . . .   | 34        |
| 2.3      | The critical temperature . . . . .  | 36        |
| 2.4      | Below the critical temperature . . . . .  | 42        |
| 2.5      | Conclusions . . . . .   | 49        |
| <b>3</b> | <b>Duality between zeroes and poles in holographic systems with massless fermions and a dipole coupling</b> | <b>51</b> |
| 3.1      | Introduction . . . . .  | 51        |
| 3.2      | Gravitational Bulk . . . . .  | 56        |
| 3.3      | Solutions of the Dirac Equations . . . . .  | 59        |
| 3.4      | Duality of poles and zeroes . . . . .   | 61        |
| 3.5      | Conclusions and discussion . . . . .  | 64        |

|          |   |            |
|----------|---|------------|
| <b>4</b> | <b>Holographic Fermions with Spontaneously Generated Inhomogeneous Phases</b> | <b>67</b>  |
| 4.1      | Introduction . . . . .  | 67         |
| 4.2      | The Holographic Setup . . . . .   | 69         |
| 4.2.1    | Below the critical temperature . . . . .                                      | 72         |
| 4.3      | The Dirac Equation . . . . .  | 76         |
| 4.4      | Perturbation Theory for Dirac Equations . . . . .                             | 78         |
| 4.4.1    | Numerical Solution to Dirac Equation at Finite Temperature .                  | 78         |
| 4.4.2    | Analytical Solution to Dirac Equation at Finite Temperature .                 | 81         |
| 4.4.3    | Zeroth Order Solution to Dirac Equations . . . . .                            | 84         |
| 4.4.4    | First Order Solution to Dirac Equations . . . . .                             | 98         |
| 4.4.5    | Second Order Solution to Dirac Equations . . . . .                            | 107        |
| 4.4.6    | The Far Region . . . . .  | 116        |
| 4.5      | Conclusion . . . . .  | 118        |
| <b>5</b> | <b>Conclusion and Outlook</b>   | <b>119</b> |
|          | <b>Bibliography</b>   | <b>123</b> |
|          | <b>Appendix</b>   | <b>136</b> |
| <b>A</b> | <b>Calculation of the metric functions</b>                                    | <b>137</b> |
| <b>B</b> | <b>The first order scalar equation below <math>T_c</math></b>                 | <b>142</b> |
| <b>C</b> | <b>Details of Spinor Rotation</b>   | <b>144</b> |
|          | <b>Vita</b>   | <b>146</b> |



# List of Figures

|     |   |    |
|-----|---|----|
| 1.1 | Temperature dependence of the critical magnetic field of a typical superconducting material [1]. . . . .  | 4  |
| 1.2 | Quantum criticality in heavy-fermion systems. The temperature is plotted with respect to the control parameter, e.g. pressure. Figure taken from [22]. . . . .                                | 9  |
| 1.3 | Doping temperature phase diagram of the hole-doped cuprate superconductors. Figure taken from [22]. . . . .   | 10 |
| 1.4 | Various broken symmetry ground states of one-dimensional metals. Figure is taken from [25]. . . . .   | 11 |
| 1.5 | One dimensional energy band structure for free electron model on the left side. Band gap formation in the presence of periodic lattice on the right side. Figures are taken from [1]. . . . . | 14 |
| 1.6 | Nearly-free-electron model band structure for reduced and extended-zone scheme respectively. Figures are taken from [2]. . . . .  | 15 |
| 1.7 | The dictionary of AdS/CFT correspondence taken from [36]. . . . .   | 23 |
| 1.8 | The condensate as a function of temperature. The critical temperature is proportional to the chemical potential. Figure is taken from [37]. . . . .   | 27 |
| 1.9 | Condensates with different dimension, $\lambda$ , as a function of temperature. The condensate tends to increase with $\lambda$ . Figure is taken from [37]. . . . .                          | 29 |

|     |  |    |
|-----|--|----|
| 2.1 | Dependence of the transition temperature $T_0/\mu$ on the wavenumber $k/\mu$ for $\Delta = 2$ in the absence of higher-derivative interactions ( $\frac{\eta}{\mu^2} = \frac{\eta'}{\mu^4} = 0$ ). From left-to-right the lines correspond to $q = 0, 1, 1.5, 3, 5, 10$ . The maximum transition temperature (i.e., the critical temperature) occurs at $k = 0$ and the homogeneous configuration is dominant. . . .   | 39 |
| 2.2 | Dependence of the transition temperature $\frac{T_0}{\mu}$ on the wavenumber $\frac{k}{\mu}$ for $\frac{\eta}{\mu^2} = 1$ , $\frac{\eta'}{\mu^4} = 0.005$ , $q = 1$ , and $\Delta = 1.7$ (solid line), 2 (dash-dotted line), and 2.5 (dotted line). . . . .  | 40 |
| 2.3 | The critical temperature $\frac{T_c}{\mu}$ (left panel) and corresponding wavenumber $\frac{k}{\mu}$ (right panel) as functions of $q$ with $\frac{\eta}{\mu^2} = 1$ , $\frac{\eta'}{\mu^4} = 0.005$ , and $\Delta = 2$ . When $q \lesssim 3.2$ , the charge is small enough that the higher-derivative couplings spontaneously generate inhomogeneity. Above that range, the homogeneous scalar is dominant. . . . .  | 41 |
| 2.4 | Dependence of the critical temperature $\frac{T_c}{\mu}$ (left panel) and corresponding wavenumber $\frac{k}{\mu}$ (right panel) on the second higher-derivative coupling constant $\frac{\eta'}{\mu^4}$ , for $\frac{\eta}{\mu^2} = 1$ , $q = 1$ , $\Delta = 1.7$ (solid), 2 (dash-dotted), and 2.5 (dashed). The inset is shown only for $\Delta = 2$ because, at the scale shown, no difference can be seen between the three different conformal dimensions of the full graph. . . . . | 42 |
| 3.1 | Scaling dimension $\nu_{k_F}$ vs. $p$ for $q = 1$ . . . . .  | 61 |
| 3.2 | Plots of $\Re \det G_R$ ( $\Im \det G_R = 0$ ) with $q = 1$ for $p = -5$ (first panel) showing a pole at $k = k_F \approx 1.5$ , and $p = 5$ (second panel) showing a zero at $k = k_L \approx 1.5$ . . . . .  | 62 |
| 3.3 | Plots of $\Re \det G_R$ (solid lines) and $\Im \det G_R$ (dashed lines) with $q = 1$ for $p = -0.1$ (first panel) showing a pole at $k = k_F \approx 0.8$ and a zero at $k = k_L \approx 1.0$ , and $p = 0.1$ (second panel) showing a pole at $k = k_F \approx 1.0$ and a zero at $k = k_L \approx 0.8$ . . . . .   | 63 |

|     |  |     |
|-----|--|-----|
| 3.4 | Poles at $k = k_F$ (blue lines) and zeroes at $k = k_L$ (red lines) <i>vs.</i> $p$ with $q = 1$ . Notice the symmetry under $k \rightarrow -k$ , and the duality of poles and zeroes under $p \rightarrow -p$ . . . . .  | 64  |
| 4.1 | Numerical solutions for $Q_{tt11}(x, z)$ , $Q_{zz11}(x, z)$ , $Q_{yy11}(x, z)$ , and $A_{t11}(x, z)$ for $\frac{\eta}{\mu_0^2} = 0.41$ , $\frac{\eta'}{\mu_0^4} = 0.005$ , $q = 0$ , $\Delta = 1$ . . . . .  | 75  |
| 4.2 | The charge density of the system for $\frac{\eta}{\mu_0^2} = 0.41$ , $\frac{\eta'}{\mu_0^4} = 0.005$ , $q = 0$ , $\Delta = 1$ , and $\xi = 0.1$ . . . . .  | 76  |
| 4.3 | The plot of the peak of spectral function $A(\omega, k_x, k_y = 0)$ at $k_F = 2.573$ for $q_f = 1.7$ , $\mu = 2.35$ , $\Delta = 1$ above the critical temperature, $T_c$ . . . . .   | 87  |
| 4.4 | The plot of the peak of spectral function $A(\omega, k_x, k_y = 2k_x)$ at $k_F = 2.4548$ for $q_f = 1.7$ , $\mu_0 = 2.257$ , $\Delta = 1$ above the critical temperature, $T_c$ , as a function of $\omega$ calculated from (4.72). . . . .  | 89  |
| 4.5 | The plot of the peak of spectral function $A(\omega = -0.0001, k_x = 1.098, k_y)$ at $k_F = 2.4548$ for $q_f = 1.7$ , $\mu_0 = 2.257$ , $\Delta = 1$ above the critical temperature, $T_c$ , calculated from (4.72). . . . .   | 90  |
| 4.6 | The plot of the peak of spectral function $A(\omega = -0.0001, k_x + Kl, k_y)$ for $q_f = 1.56$ , $\mu_0 = 2.257$ , $\Delta = 1$ above the critical temperature, $T_c$ , calculated from (4.72). . . . .   | 91  |
| 4.7 | Plot of spectral function $A(\omega, k_x = k, k_y = 2.8538)$ <i>vs.</i> $\omega$ for parameters $\frac{\eta}{\mu_0^2} = 0.25$ , $\frac{\eta'}{\mu_0^4} = 0.005$ , $q = 0$ , $\Delta = 1$ , $q_f = 2$ , $\mu_0 = 2.25072$ , $\frac{T}{\mu_0} = 0.0613$ and for $\xi = 0.0, 0.05, 0.07, 0.1$ respectively. . . . . | 108 |
| 4.8 | Plot of spectral function $A(\omega = 0.0005, k_x = k, k_y)$ <i>vs.</i> $k_y$ for parameters $\frac{\eta}{\mu_0^2} = 0.25$ , $\frac{\eta'}{\mu_0^4} = 0.005$ , $q = 0$ , $\Delta = 1$ , $q_f = 1.8$ , $\mu_0 = 2.25072$ , $\frac{T}{\mu_0} = 0.0613$ and for $\xi = 0.0, 0.07, 0.075$ respectively. . . . .      | 110 |

# Chapter 1

## Introduction

Recently ongoing studies have revealed that gauge/gravity duality makes possible to understand the strongly coupled quantum systems. Gauge/gravity duality relates string theory with the observable world by using the Maldacena's idea of the correspondence of strongly coupled gauge theories to weakly coupled gravity. The correspondence is defined by using two different ways of defining the string theory structures, branes. One perspective is to consider the branes as solutions to supergravity, low-energy theory of open strings and the other perspective is to consider them as low-energy theory of closed strings in which the gauge theory lives on the brane. The origin of gauge/gravity duality is string theory but it has become a powerful tool to study the strongly coupled systems such that rather than focusing on string theory itself it focuses on the properties of strongly coupled systems like condensed matter systems, and heavy-ion collisions. In this thesis gauge/gravity duality is used to analyze condensed matter systems. Since the gauge theory lives in a higher dimensional space the word holographic is used for these kind of condensed matter systems, e.g. holographic superconductors, holographic superfluids, holographic charge density waves etc.

In this thesis some particular condensed matter applications of gauge/gravity duality are presented in the following organized fashion. In Chapter 1 we start

with providing some background information about the condensed matter systems like superconductors, charge density waves, and the band structure of the electrons moving in periodic potential. The purpose of this introduction is to give the readers of this dissertation an opportunity to understand the fundamental concepts and theories related to work presented in this dissertation. Then we continue with a brief overview of gauge/gravity duality and AdS/CFT correspondence. In Chapters 2 and 3 we present our previously published work in *Physical Review D* [12], [13] and in Chapter 4 our work in presubmit stage in collaboration with James Alsup, Eleftherios Papantonopoulos, and George Siopsis. In Chapter 2 a holographic superfluid with spatially inhomogeneous background was explored. The inhomogeneous phases were spontaneously generated by the higher order derivative coupling between the electromagnetic and the scalar field. The system was studied above and below the critical temperature. In Chapter 3 the zeroes and poles of the Green's function were studied in a holographic system whose bulk has an AdS-Reissner-Nordström black hole with a dipole coupling. As a result, we show that the dipole coupling acts as an order parameter in Mott physics. As we vary the dipole coupling parameter we observe the transfer of the spectral density between bands. In Chapter 4 we put holographic fermions to the system that we studied in Chapter 2. We study the spectral functions of the system to see holographic lattice effect which is spontaneously generated by high-derivative coupling between the electromagnetic and scalar field. To be able to analyze the system we solve the equations both analytically and numerically by using perturbation theory. The findings of our study reveals the band gap structure at the Brillouin zone boundary which is discussed in section 1.1.3.

# 1.1 Background: Superconductivity, Charge Density Waves, and Holography

## 1.1.1 Superconductivity

In 1911 Kamerlingh Onnes observed the disappearance of the electrical resistance of some metals like mercury, lead, and tin in a small temperature range at a critical temperature  $T_c$ , which depends on the type of the metal. There are two important indications of the superconductivity. The one which might lead to the potential applications of superconductivity, such as high-current transmission lines or high-field magnets is the *perfect conductivity*. The second one is the *perfect diamagnetism* which was discovered by Meissner and Ochsenfeld in 1933 [14]. The *Meissner effect* is defined through perfect diamagnetism which means that any magnetic field that is present in the bulk of the sample when  $T > T_c$  is expelled when  $T$  is lowered through the transition temperature [1]. The transition from the superconducting state to the normal state can occur at a critical magnetic field  $H_c$ , which depends on the difference between the free energies of the normal and superconducting states. This energy difference is called the condensation energy of the superconducting state and given by

$$\frac{H_c^2(T)}{8\pi} = f_n(T) - f_s(T) \quad (1.1)$$

Also experiments showed that

$$H_c(T) \approx H_c(0) \left[ 1 - \left( \frac{T}{T_c} \right)^2 \right] \quad (1.2)$$

as seen in Fig.(1.1).

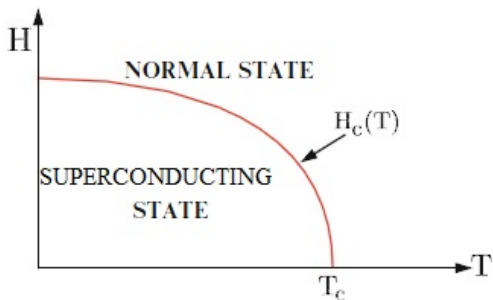


**Figure 1.1:** Temperature dependence of the critical magnetic field of a typical superconducting material [1].

### London Equations

In 1935 London brothers published a paper to give a theoretical explanation to the persistent electric currents in the superconductors [15]. The derivation of London equations is the following. The equation of motion of a dissipationless electron in superfluid is

$$m \frac{d\vec{v}_S}{dt} = -e\vec{E} \quad (1.3)$$

then the current density is given by

$$\vec{j} = -n_s e \vec{v}_S \quad (1.4)$$

then we obtain,

$$\frac{d\vec{j}}{dt} = -n_s e \frac{d\vec{v}_S}{dt} = \frac{n_s e^2}{m} \vec{E} . \quad (1.5)$$

Eq.(1.5) tells us that in stationary conditions there is no electric field in the superconductor and this equation is called the *First London Equation* . Then from Faraday's Law,

$$\vec{\nabla} \times \vec{E} = -\frac{1}{c} \frac{d\vec{B}}{dt} \quad (1.6)$$

by integrating Eq.(1.5) we obtain the solution

$$\vec{\nabla} \times \vec{j} + \frac{n_s e^2}{mc} \vec{B} = \vec{C} \quad (1.7)$$

where the constant vector  $\vec{C}$  is to be determined from the initial conditions. To satisfy the Meissner effect London brothers proposed this constant vector  $\vec{C}$  to be a zero vector. This leads to so called *London gauge*, i.e.  $\vec{j} = -\frac{n_S e^2}{mc} \vec{A}$ . Using this information we find the *Second London Equation*.

$$\vec{\nabla} \times \vec{j}_s = -\frac{n_S e^2}{mc} \vec{B} \quad (1.8)$$

Here the constant  $\lambda_L = \frac{n_S e^2}{mc}$  is a phenomenological parameter which only depends on the type of the material. This parameter is called the *London penetration depth*. The applied magnetic field to the superconductor decreases exponentially with the distance from the surface of the superconductor with an exponential factor of the London penetration depth, i.e.  $\vec{B}(x) = B_{app} \hat{y} e^{-x/\lambda_L}$ . The temperature dependence of this penetration depth is experimentally found as the following.

$$\lambda_L(T) \approx \lambda_L(0) \left[ 1 - \left( \frac{T}{T_c} \right)^4 \right]^{-1/2} \quad (1.9)$$

where  $\lambda_L(0) = \frac{n_S e^2}{mc}$ .

## Landau-Ginzburg Theory of Superconductors

Although London and Pippard theory was good enough to explain the phenomenological behavior of the superconductors these theories also had some deficiencies to be fixed. For instance, in London's theory the superfluid density  $n_S$  was assumed to be constant in time and uniform in space and since it is treated to be given there was no way to understand the dependence of  $n_S$  on parameters like temperature or applied magnetic field within these theories.

In 1937 to resolve these deficiencies of London theory Landau introduced the idea of order parameter to describe the phase transitions [16]. This order parameter that Landau introduced was constant in time and space. The main point of the Landau's theory was to describe the free energy in terms of the order parameter and



then find the phase transitions by minimizing the free energy with respect to the order parameter. To cover the spatially non-uniform densities Ginzburg and Landau included the gradient terms in the free energy as well [17]. We write the functional for superconductors as the following.

$$F[\psi, \mathbf{A}] \cong \int d^3r \left[ \alpha |\psi|^2 + \frac{\beta}{2} |\psi|^4 + \frac{1}{2m^*} \left| \left( \frac{\hbar}{i} \nabla - \frac{q}{c} \mathbf{A} \right) \psi \right|^2 + \frac{B^2}{8\pi} \right] \quad (1.10)$$

where the kinetic momentum and energy density of the magnetic field term are the terms added to the *Landau functional*. Minimizing this functional  $F$  with respect to the order parameter  $\psi$  and the vector potential  $\mathbf{A}$  respectively we obtain the *Ginzburg-Landau equations* as the following.

$$\frac{1}{2m^*} \left( \frac{\hbar}{i} \nabla - \frac{q}{c} \mathbf{A} \right)^2 \psi + \alpha \psi + \beta |\psi|^2 \psi = 0 \quad (1.11)$$

$$\mathbf{j} = \frac{c}{4\pi} \nabla \times \mathbf{B} = i \frac{q\hbar}{2m^*} ([\nabla \psi^*] \psi - \psi^* \nabla \psi) - \frac{q^2}{m^* c} |\psi|^2 \mathbf{A} . \quad (1.12)$$

As one can see from Eq.(1.12) in the case of uniform  $\psi(\mathbf{r})$  current  $\mathbf{j}$  reduces to the form of the London equation, i.e.  $\mathbf{j} = -\frac{e^2 n_S}{mc} \mathbf{A}$ ,

$$\mathbf{j} = -\frac{q^2 |\psi|^2}{m^* c} \mathbf{A} , \quad (1.13)$$

Therefore, we can deduce that

$$\frac{q^2 |\psi|^2}{m^*} = \frac{e^2 n_S}{m} \quad (1.14)$$

Setting  $q = -2e$  and  $m^* = 2m_e$  the superfluid density  $n_S$  becomes

$$n_S = \frac{m q^2 |\psi|^2}{e^2 m^*} = \frac{m 4e^2 |\psi|^2}{e^2 2m} = 2|\psi|^2 . \quad (1.15)$$

Finally, the penetration depth is

$$\lambda = \sqrt{\frac{mc^2}{4\pi e^2 n_s}} \quad (1.16)$$

There are two characteristic length scales in Ginzburg-Landau theory of superconductors and superfluids. The penetration depth ( $\lambda$ ) is associated with the vector potential  $\mathbf{A}$  and the coherence length ( $\xi$ ) is associated with the order parameter field  $|\psi(\mathbf{r})|$ . They are the minimal spatial scales over which they can vary with their respective fields. The dimensionless ratio of these two length scales is called *Ginzburg-Landau parameter* ( $\kappa := \frac{\lambda(T)}{\xi(T)}$ ). Depending on whether  $\kappa$  is less than or greater than  $1/\sqrt{2}$  superconductors are called Type-I or Type-II superconductors respectively.

### BCS Theory of Superconductors

In 1957 Bardeen, Cooper, and Schrieffer [18] published a paper on the theory of superconductivity which is also known as BCS theory. In the BCS theory, they showed that there is an instability in the Fermi-sea ground state of the electron gas due to the weak attractive interaction between electrons. This instability occurs for the formation of bound pairs of electrons which are in the states with equal and opposite momentum and spin [14]. These bound pairs form charged bosons which are called the *Cooper pairs*. BCS theory predicted the minimum energy to break a pair is  $E_g = 2\Delta(T)$  and as a result two quasi-particle excitations are produced. The value of  $\Delta(T)$  increases from zero at  $T_c$  to

$$E_g(0) = 2\Delta(0) = 3.528k_B T_c \quad (1.17)$$

in the limit of  $T \ll T_c$ , where  $k_B$  is Boltzmann constant. This value of gap is close to the values measured for simple elementary superconductors. On the other hand, the superconductors with stronger coupling and for unconventional superconductors

this value do not match with the experimental results. For instance, for mercury the gap ratio  $2\Delta(0)/k_B T_c \approx 4.4$ .

### High $T_c$ Superconductors

In 1986 high temperature superconductivity in layered materials dominated by copper oxide ( $CuO_2$ ) planes was discovered by Bednorz and Müller [20]. After this discovery superconductors with  $T_c$  higher than 40K are classified as high- $T_c$  superconductors. Although BCS theory, which is based on the weakly-coupled Fermi liquid description [29], suggests that the superconductivity is induced by the electron-phonon interactions in high- $T_c$  superconductors it is believed that strong electronic correlations play the key role. The underlying physical mechanism for high- $T_c$  superconductivity is not clear yet but some models (e.g. Hubbard model) are used to study these type of materials. So far the highest critical temperature measured is  $T_c \approx 133K$  [21] for a mercury, barium, calcium, copper, oxide ( $HgBa_2Ca_2Cu_3O_8$ ).

For cuprates, a type of high  $T_c$  superconductors, the crystal structures share the two-dimensional Cu-O planes. Although the mechanism behind it is not well understood yet for high  $T_c$  superconductors the superconducting state is formed by Cooper pairs. Another difference between the conventional superconductors and the high  $T_c$  superconductors is that they former has  $s$ -wave and the latter has  $d$ -wave symmetry for their Cooper pair wave function.

In the presence of many competing and mutually frustrating interactions a rich phase diagram can appear in quantum many-body systems. For example, the quantum critical behavior of the heavy fermion systems is summarized in Fig.(1.2). In these systems, the ordered phase that terminates at the quantum critical point (QCP) is magnetic, and is clearly visible in experiments. The phase diagram of cuprate high- $T_c$  superconductors (see Fig.(1.3)) is another example of one of the richest and most interesting phase structures has been known to appear in strongly correlated materials. The phase diagram of a hole-doped high- $T_c$  superconductor starts with an insulator phase with the antiferromagnetic order (Mott insulator) in the

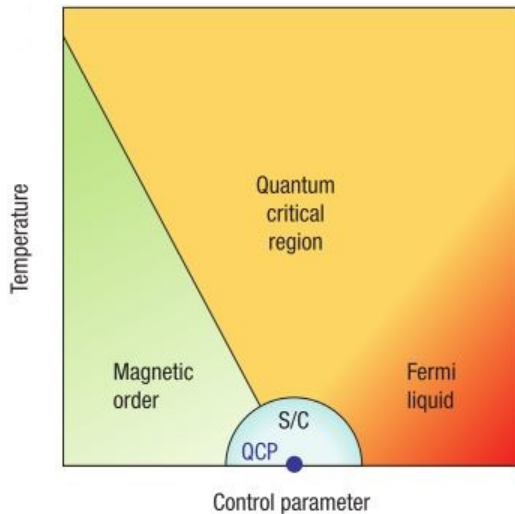


**Figure 1.2:** Quantum criticality in heavy-fermion systems. The temperature is plotted with respect to the control parameter, e.g. pressure. Figure taken from [22].

underdoped regime which has strong electron-electron correlations is then followed by the superconductor phase. Adjacent to the Mott insulator and superconductor phases, there appear the pseudogap and strange metal phases, where transport properties are highly unusual. For example, strange metals or non-Fermi liquid show linear resistivity which makes weakly coupled description insufficient [29]. The underdoped regime also exhibits a variety of spin and charge orders that can be static or fluctuate in addition to the pseudogap phase, which suppresses spin and charge excitations below a temperature  $T^*$ . As we increase doping  $x$  beyond the superconductivity phase, there is the fermi-liquid phase. One of the properties of the Fermi liquid phase is that the resistivity is proportional to  $T^2$ . Due to short superconducting coherence length, low carrier densities, and quasi-two dimensionality the transition temperature relative to its mean field value due to phase fluctuations favor a suppression. It is hard to identify which competing orders are essential to the description of high- $T_c$  superconductivity. Some questions still beg for an answer in understanding the pseudogap phase [22].

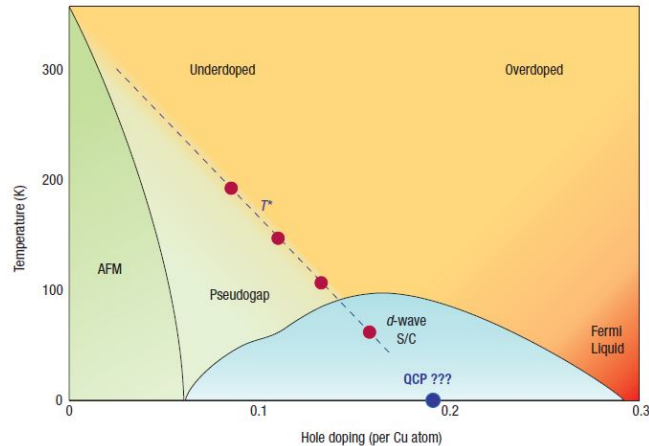


**Figure 1.3:** Doping temperature phase diagram of the hole-doped cuprate superconductors. Figure taken from [22].

### 1.1.2 Charge Density Waves (CDW)

Electron-phonon or electron-electron interactions result in the development of the density waves ground state in low-dimensional metals [23]. A periodic spatial variation of the charge or spin density can be observed in the ground states which are coherent superposition of electron-hole pairs. The spatial variation of charge density is called the *charge density wave (CDW)*. The resulting ground state consists of a periodic charge density modulation accompanied by a periodic lattice distortion. Both periods are determined by the Fermi wavevector  $k_F$ . The charge density of the collective mode is given by [24]

$$\rho(\mathbf{r}) = \rho_0 + \rho_1 \cos(2\mathbf{k}_F \cdot \mathbf{r} + \phi) \quad (1.18)$$

where  $\rho_0$  is the unperturbed electron density of the metal. The formation of the charge density waves results in a strong modification in both the electron and phonon spectra. The phenomenon is usually described by discussing the behavior of a one-dimensional coupled electron-lattice system, with the electrons forming a one-dimensional electron gas, and the ions forming a linear chain.

|                        | Pairing  | Total spin | Total momentum | Broken symmetry |
|------------------------|--|------------|----------------|-----------------|
| Singlet superconductor | electron–electron<br>$e_+, \sigma; e_-, -\sigma$ | $S = 0$    | $q = 0$        | gauge           |
| Triplet superconductor | electron–electron<br>$e_+, \sigma; e_-, \sigma$  | $S = 1$    | $q = 0$        | gauge           |
| Spin density wave      | electron–hole<br>$e_+, \sigma; h_-, -\sigma$     | $S = 1$    | $q = 2k_F$     | translational   |
| Charge density wave    | electron–hole<br>$e_+, \sigma; h_-, \sigma$      | $S = 0$    | $q = 2k_F$     | translational   |

**Figure 1.4:** Various broken symmetry ground states of one-dimensional metals. Figure is taken from [25].

The consequence of the electron-phonon interaction and of the divergent electronic response at  $q = 2k_F$  in one dimension is a strongly renormalized phonon spectrum generally referred to as the Kohn anomaly. This identifies a phase transition to a state where a periodic static lattice distortion and a periodically varying charge modulation with varying charge modulation with a wavelength  $\lambda_0 = \pi/k_F$  develops.

The ground states of different broken symmetries carry similar characteristics with superconducting state. One of these common properties is that for all of the condensates there is a complex order parameter which can be written as

$$\Delta = |\Delta|e^{i\phi} \quad (1.19)$$

Although the gauge symmetry is broken for superconducting ground states the broken symmetry for the density wave ground states is the translational symmetry. This difference between the superconducting and the density wave ground states is the one which makes them have different collective excitations and different coupling of the collective modes to applied electromagnetic fields. In Fig. 1.4 the different ground states of one-dimensional metals is given depending the total momentum, total spin, and broken symmetry.

The charge density waves' collective excitations occur below a single gap which has an amplitude of  $|\Delta|$ . This single particle gap occurs at  $\pm k_F$  and doesn't contribute to the DC conductivity due to the presence of impurities and lattice imperfections. Therefore, instead of causing a supercurrent as in the case of superconducting states the collective modes lead to semiconductor behavior below a transition temperature [23]. Fröhlich (1954) pointed out that the absence of these pinning and damping supercurrent of the condensate is lead by the collective modes [24].

### 1.1.3 Electrons in periodic potential

Although in simple free-electron models like Drude and Sommerfeld models the electrons are assumed to be in an empty box, to explore the properties of the metals we need to consider the crystalline structure of the ions since the conduction electrons move in the periodic potential formed by the ions.

The Fourier transform of the periodic potential felt by the electrons is [1]

$$V(r) = \sum_{\mathbf{K}} V_{\mathbf{K}} e^{i\mathbf{K}\cdot\mathbf{r}} , \quad (1.20)$$

where  $\mathbf{K}$  is the vectors of the reciprocal lattice. Using the relation  $\mathbf{K}\cdot\mathbf{R} = 2\pi \times \text{integer}$  between reciprocal vector  $\mathbf{K}$  and translation vector  $\mathbf{R}$  we can write

$$V(\mathbf{r} + \mathbf{R}) = \sum_{\mathbf{K}} V_{\mathbf{K}} e^{i\mathbf{K}\cdot(\mathbf{r}+\mathbf{R})} = \sum_{\mathbf{K}} V_{\mathbf{K}} e^{i\mathbf{K}\cdot\mathbf{r}} = V(\mathbf{r}) \quad (1.21)$$

due to the periodicity of the crystalline structure. The Bloch's theorem states that in a lattice-periodic the Hamiltonian is also periodic and the eigenfunctions can be written as

$$\psi_{\mathbf{k}}(\mathbf{r}) = e^{i\mathbf{k}\cdot\mathbf{r}} u(\mathbf{r}) = \sum_{\mathbf{K}} C_{\mathbf{K}} e^{i(\mathbf{k}+\mathbf{K})\cdot\mathbf{r}} \quad (1.22)$$

where  $u(\mathbf{r})$  are lattice-periodic functions and where we expanded the periodic part in Fourier series.

In Schrödinger equation

$$H(\mathbf{r})\psi(\mathbf{r}) = \left[ -\frac{\hbar^2}{2m}\nabla^2 + V(\mathbf{r}) \right] \psi(\mathbf{r}) = E\psi(\mathbf{r}) \quad (1.23)$$

we substitute the Fourier expansions and find

$$\sum_{\mathbf{K}'} \left[ \frac{\hbar^2}{2m}(\mathbf{k} + \mathbf{K}')^2 + \sum_{\mathbf{K}''} V_{\mathbf{K}''} e^{i\mathbf{K}'' \cdot \mathbf{r}} \right] C_{\mathbf{K}'} e^{i(\mathbf{k} + \mathbf{K}') \cdot \mathbf{r}} = E \sum_{\mathbf{K}'} C_{\mathbf{K}'} e^{i(\mathbf{k} + \mathbf{K}') \cdot \mathbf{r}} \quad (1.24)$$

Integrating over the volume and simplifying we obtain

$$\left[ E - V_0 - \frac{\hbar^2}{2m}(\mathbf{k} + \mathbf{K})^2 \right] C_{\mathbf{K}} = \sum_{\mathbf{H} \neq 0} V_{\mathbf{H}} C_{\mathbf{K} - \mathbf{H}} \quad (1.25)$$

The main goal is to obtain a good approximation to the potential  $V(r)$  by solving this infinite set of equations to understand the energy band structure. Solving these equations by assuming that  $V_{\mathbf{K}} = 0$  for  $\mathbf{K} \neq 0$  is called the free electron model then we can write

$$E_{\mathbf{K}} = V_0 + \varepsilon_{\mathbf{k} + \mathbf{K}} \quad (1.26)$$

and  $C_{\mathbf{K}}^{(0)} = 1$  for only band  $\mathbf{K}$  and zero otherwise. Then the energy band structure can be plotted as in Fig. 1.5.

Another way to solve these infinite set of equations is to use the perturbation theory in which  $V_{\mathbf{K}}$  for  $|\mathbf{K}| \neq 0$  is taken to be very small. This type of model is called the *nearly-free-electron model*. Let us start with the lowest band which has  $C_0^{(0)} = 1$ . Then we can write

$$E^{(0)} = V_0 + \frac{\hbar^2 k^2}{2m}, \quad C_0^{(0)} = 1 \quad \text{and} \quad C_{\mathbf{K}}^{(0)} = 0 \quad \text{for} \quad |\mathbf{K}| \neq 0. \quad (1.27)$$

The first order equation is then

$$\left[ E - V_0 - \frac{\hbar^2}{2m}(\mathbf{k} + \mathbf{K})^2 \right] C_{\mathbf{K}}^{(1)} = \sum_{\mathbf{H} \neq 0} C_{\mathbf{K} - \mathbf{H}} V_{|\mathbf{H}|} \quad (1.28)$$



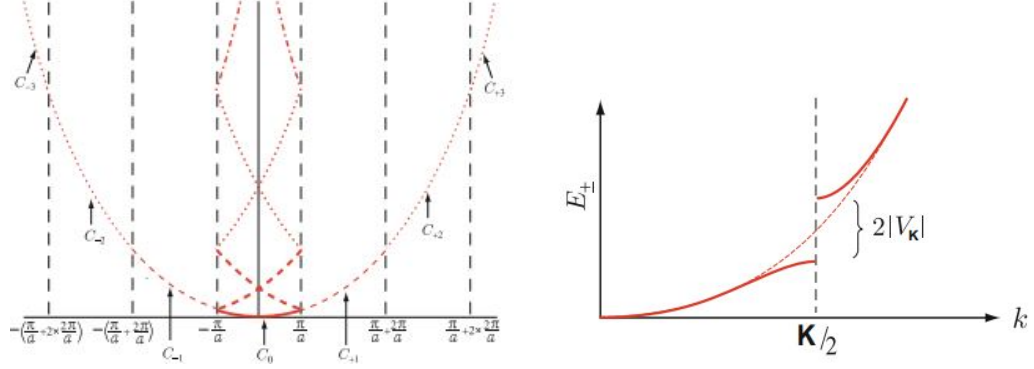


**Figure 1.5:** One dimensional energy band structure for free electron model on the left side. Band gap formation in the presence of periodic lattice on the right side. Figures are taken from [1].

and we can solve for  $C_{\mathbf{K}}^{(1)}$  and find

$$C_{\mathbf{K}}^{(1)} = \frac{V_{\mathbf{K}}}{\frac{\hbar^2}{2m} [\mathbf{k}^2 - (\mathbf{k} + \mathbf{K})^2]} \quad (1.29)$$

which gives the equation for the energy of the lowest band as following.

$$E = V_0 + \varepsilon_{\mathbf{k}} - \sum_{|\mathbf{K}| \neq 0} \frac{|V_{\mathbf{K}}|^2}{\varepsilon_{\mathbf{k}+\mathbf{K}} - \varepsilon_{\mathbf{k}}} \quad (1.30)$$

which is valid for  $|\varepsilon_{\mathbf{k}+\mathbf{K}} - \varepsilon_{\mathbf{k}}| \gg |V_{\mathbf{K}}|$  where we defined  $\varepsilon_{\mathbf{k}} = \frac{\hbar^2 \mathbf{k}^2}{2m}$ . The denominator goes to zero at  $\varepsilon_{\mathbf{k}+\mathbf{K}} = \varepsilon_{\mathbf{k}}$  or  $|\mathbf{k} + \mathbf{K}| = |\mathbf{k}|$ .

When the difference between two wave vectors is equal to the reciprocal lattice vector, i.e.  $\mathbf{k}' - \mathbf{k} = \mathbf{K}$ , they are said to obey the Bragg reflection condition. For the degenerate case where  $|\mathbf{k} + \mathbf{K}| \simeq |\mathbf{k}|$  denominator of Eq. (1.29) goes to zero and there is a degeneracy which can be lifted by the presence of the periodic potential. This degeneracy eliminates one of the basic assumptions of the perturbation theory of having small coefficients. To resolve this issue we assume that  $C_0$  and  $C_{\mathbf{K}}$  are not small but important at this particular point. The reason for these coefficients being large is the mixing of the degenerate states [2]. Then we obtain the following system

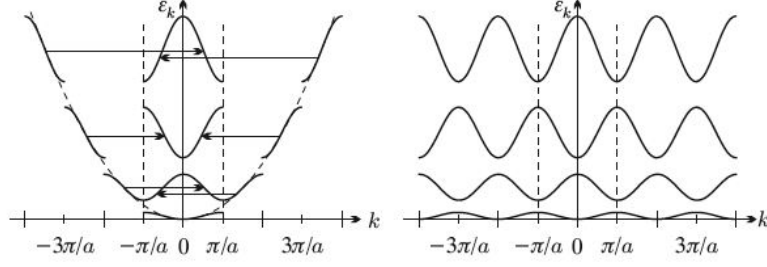


**Figure 1.6:** Nearly-free-electron model band structure for reduced and extended-zone scheme respectively. Figures are taken from [2].

of equations.

$$\begin{aligned}
 (E - V_0 - \varepsilon_{\mathbf{k}})C_0 &= C_{\mathbf{K}}V_{-\mathbf{K}} , \\
 (E - V_0 - \varepsilon_{\mathbf{k}+\mathbf{K}})C_{\mathbf{K}} &= C_0V_{\mathbf{K}} .
 \end{aligned}
 \tag{1.31}$$

The solution of this system of equations give two solutions for the band energy as

$$E_{\pm}(\mathbf{k}) = V_0 + \frac{1}{2} [\varepsilon_{\mathbf{k}} + \varepsilon_{\mathbf{k}+\mathbf{K}}] \pm \left[ |V_{\mathbf{K}}|^2 + \left( \frac{\varepsilon_{\mathbf{k}+\mathbf{K}} - \varepsilon_{\mathbf{k}}}{2} \right)^2 \right]^{1/2}
 \tag{1.32}$$

For the particular case of Bragg condition the band energy becomes

$$E_{\pm}(\mathbf{k}) = V_0 + \varepsilon_{\mathbf{k}} \pm |V_{\mathbf{K}}| .
 \tag{1.33}$$

The plot of this energy band structure can be seen in Fig.1.5. Looking at the Brillouin zone boundary one can see that the degeneracy is lifted and there is a gap between two bands. The magnitude of the band gap is proportional to the magnitude of the periodic lattice potential. In Fig. 1.6 the extended and repeated zone scheme is plotted where all degeneracies are lifted at the center and boundaries of the Brillouin zone. The difference between the free-electron model and the nearly-free-electron model is the lift of degeneracies at the center of the zone boundary. Another interesting point in the nearly-free-electron model is that the group velocity

and its perpendicular component are zero at the center and boundary of the zone respectively. As a result of this the dispersion curves are perpendicular to the zone boundary [2].

## 1.2 AdS/CFT Correspondence and Holography

In 1997 Maldacena proposed a conjecture which states that type IIB string theory compactified on  $\text{AdS}_5 \times \text{S}^5$  and four dimensional  $\mathcal{N} = 4$  supersymmetric Yang-Mills theory are equivalent to each other. This conjecture is then called the *AdS/CFT correspondence* where AdS stands for anti-de Sitter space and CFT stands for the conformal field theory. In other words, we can state the equivalence as a quantum gravity theory in an asymptotically anti-de Sitter spacetime is equivalent to a quantum field theory in a lower dimensional space. This is the reason why this correspondence is referred as *holographic principle*. Another reason is that the number of degrees of freedom in the bulk is equal to the number of degrees of freedom at the boundary.

The derivation of the AdS/CFT correspondence in the original conjecture that was proposed by Maldacena can be done by considering type IIB string theory in 9+1 dimensional spacetime with a stack of  $N$  D3-branes [26]. One of the ways to think of D-branes is that they are open string theory objects on which the open strings end on them. Another way is that low energy closed string theory equations of motion gives solitonic solutions which are D-branes. A stack of  $N$  D3 branes can be described in terms of both closed and open strings. At the low energy, which is below the string mass scale  $(\alpha')^{-1/2}$  or which is equivalent to taking  $l_s \rightarrow 0$ , the quantum gravity of closed strings are reduced to classical supergravity. On the other hand, open string theory in this limit corresponds to the planar limit  $N \rightarrow \infty$  of  $\text{SU}(N)$  gauge theory. Therefore, at this low energy limit the open and closed string descriptions reduce to  $\mathcal{N} = 4$  super Yang-Mills theory and string theory on  $\text{AdS}_5 \times \text{S}^5$ , respectively [27].

Since we do not have a full understanding of non-perturbative structure of the type IIB string theory on a curved space background there is no mathematical proof for the AdS/CFT correspondence. Although there is no mathematical proof for Maldacena's conjecture, recently published studies [31] and [32] test the duality by providing a numerical calculations which presents convincing evidence that the conjecture is true [33].

To test the accuracy of the proposal by Maldacena, Hanada *et. al.* did numerical calculations on the both sides. They compared the entropy of a black hole in the gauge theory and entropy with a gravity theory with the first quantum gravity correction included. As a result of their Monte Carlo simulations they found out an agreement between the two computations. This agreement presents an evidence that the gauge/gravity duality is valid and string theory is internally consistent as a quantum theory of gravity [34].

## Large $N$ Expansion

Although there are different forms of AdS/CFT correspondence conjecture the starting point of the Maldacena's conjecture was due to a paper of 't Hooft in 1973 in which 't Hooft proposed an interesting connection between  $SU(N_c)$  gauge theories in the large  $N_c$  limit, i.e.  $N_c \rightarrow \infty$ , and string theory [4]. A simple toy model in  $\mathcal{N} = 4$  Super-Yang Mills theory has the Lagrangian of the form

$$\mathcal{L} \propto \text{Tr} [\partial\Phi_i\partial\Phi_j + g_{\text{YM}}c^{ijk}\Phi_i\Phi_j\Phi_k + g_{\text{YM}}^2d^{ijkl}\Phi_i\Phi_j\Phi_k\Phi_l] \quad (1.34)$$

where the fields  $\Phi_i$  can either be any bosonic field  $X^i$  or  $g_{\text{YM}}A_\mu$ . After rescaling the fields by  $\tilde{\Phi}_i = g_{\text{YM}}\Phi_i$  and defining the fixed 't Hooft coupling,  $\lambda = g_{\text{YM}}^2N_c$  as  $N_c \rightarrow \infty$  it was found out that the expansion of Feynman diagrams in  $1/N_c$  is equivalent to a topological expansion of the corresponding surfaces. In the weak form of the correspondence the limit of  $N_c \rightarrow \infty$  and  $\lambda$  is very large case the  $\alpha'$  is assumed to

be small. Therefore, expanding supergravity in small  $\alpha'$  is dual to a field theory expansion around strong coupling limit.

The virtue of providing strong/weak coupling duality of AdS/CFT helps us to explore properties of strongly coupled quantum field theories from the calculations done in weakly coupled gravity. This is also what lets us to study the holographic lattice structure and holographic fermions and their zeros and poles in this thesis in the following chapters.

Now, let us summarize some properties of AdS space which are useful in constructing the correspondence.

### Anti-de Sitter (AdS) Space

One of the solutions to Einstein's equations with negative cosmological constant is anti-de Sitter space (AdS). It is a maximally symmetric Lorentzian manifold with negative curvature [6]. A  $d$ -dimensional hyperboloid

$$X_0^2 + X_d^2 - \sum_{i=1}^{d-1} X_i^2 = L^2 , \quad (1.35)$$

in  $(d+1)$ -dimensional embedding with AdS radius,  $L$ , which is a global constant and in which the metric is

$$ds^2 = -dX_0^2 - dX_d^2 + \sum_{i=1}^{d-1} dX_i^2 . \quad (1.36)$$

The construction of AdS space gives it an isometry group of  $SO(2, d-1)$ . Since the conformal group of the gauge theory is the same as the isometry group of AdS it is easier to establish the gauge/gravity duality.

In different coordinate systems the metric of the AdS space can be written in different forms. One of the forms that satisfy Eq.(1.35) is that

$$\begin{aligned} X_0 &= L \cosh \chi \cos \tau , \\ X_d &= L \cosh \chi \sin \tau , \\ X_i &= L \sinh \chi \Omega_i \end{aligned} \tag{1.37}$$

where  $i$  stands for  $i = 1, \dots, d-1$ ,  $\tau \in [0, 2\pi)$ ,  $\chi \geq 0$ , and  $\sum_i \Omega_i^2 = 1$  which gives the metric

$$ds^2 = L^2(-\cosh^2 \chi d\tau^2 + d\chi^2 + \sinh^2 \chi d\Omega_d^2) . \tag{1.38}$$

The coordinates  $(\tau, \chi, \Omega)$  covers the entire space therefore they are defined as the global coordinates. Due to violation of causality the coordinate  $\tau$  needs to be unwrapped so that it is between  $-\infty < \tau < \infty$ .

In a different form we can write the metric by using Poincaré coordinates as following. The local coordinates  $(u, t, \mathbf{x})$  with  $0 < u$ ,  $-\infty < t < \infty$ ,  $\mathbf{x} \in \mathbb{R}^d$  can be defined in terms of the global coordinates as

$$\begin{aligned} X_0 &= \frac{1}{2u} [1 + u^2(L^2 + \mathbf{x}^2 - t^2)] , & X_d &= Lut , \\ X_{d+1} &= \frac{1}{2u} [1 - u^2(L^2 + \mathbf{x}^2 - t^2)] , & X_i &= Lux_i \quad \text{for } i = 1, \dots, d . \end{aligned} \tag{1.39}$$

The reason why these coordinates are local is that they cover only half of the hyperboloid in Eq.(1.35). Then we obtain the metric with Poincaré coordinates as

$$ds^2 = L^2 \left[ \frac{du^2}{u^2} + u^2 dx_\mu dx^\mu \right] . \tag{1.40}$$

In addition to using the coordinate  $u$  it is more general to use the transformation  $z = u^{-1}$  then this transformation gives the metric

$$ds^2 = \frac{L^2}{z^2} (-dt^2 + d\vec{x}^2 + dz^2) \tag{1.41}$$

where the conformal boundary is located at  $z = 0$ . Another useful parametrization is given by  $r = L^2 u$  which leads to

$$ds^2 = \frac{r^2}{L^2} dx_\mu dx^\mu + \frac{L^2 dr^2}{r^2} . \quad (1.42)$$

Finally, another form of coordinates is the static coordinates  $(t, r, \theta, \phi)$  where the static coordinates are defined as  $t = L\tau$  and  $r = L \sinh \chi$ . For example, the asymptotically AdS metric for  $d = 1$  is

$$ds^2 = - \left(1 + \frac{r^2}{L^2}\right) dt^2 + \left(1 + \frac{r^2}{L^2}\right)^{-1} dr^2 + r^2 d\Omega^2 . \quad (1.43)$$

Due to the factor  $-g_{00} = 1 + \frac{r^2}{L^2}$  the temperature and the energy is red-shifted therefore, there is an infinite potential wall at the asymptotic infinity of AdS space. In AdS/CFT, the radial coordinate is interpreted as the energy scale of the gauge theory. Depending on how close an energy excitation to the AdS boundary the energy of the gauge theory changes from IR to UV as  $r \rightarrow 0$  to  $r \rightarrow \infty$  [29].

For Einstein-Hilbert action with a cosmological constant  $\Lambda$

$$S = \frac{1}{16\pi G_N} \int d^{d+1}x \sqrt{-g} [-2\Lambda + R] \quad (1.44)$$

where  $G_N$  is Newton's constant,  $g$  is the determinant of metric  $g_{\mu\nu}$ , and  $R$  is the scalar curvature the solution to Einstein's equations is the AdS metric. Then the cosmological constant and the scalar curvature are obtained as

$$\Lambda = -\frac{d(d+1)}{2L^2} , \quad R = -\frac{d(d+1)}{L^2} \quad (1.45)$$

respectively [30].

One of the properties of 5- $d$  AdS spaces is that their large symmetry group matches with the group of conformal symmetries of  $N = 4$  super Yang-Mills theory.

Hawking-Page and Witten discussed the thermodynamics of Schwarzschild-AdS black holes and found out that they go through a first order phase transition at a critical temperature. Above this critical temperature the large black hole has a smaller free energy than radiation and the small black hole. Since the temperature of this black hole is the temperature of the CFT side, Hawking-Page transition is the gravitational form of the thermal phase transition on the CFT side [28].

Although Maldacena proposed a correspondence between a conformal field theory in  $d$  dimensions and a theory on  $AdS_{d+1}$ , Witten was the one who included the precise way for computing observables of the conformal field theory in terms of supergravity on  $AdS_{d+1}$  in his paper in 1998 [5].

## Dictionary of the Correspondence

As stated in the earlier sections there is an equivalence between  $\mathcal{N} = 4$  Super-Yang-Mills theory which is a conformal theory, and type IIB supergravity on  $AdS_5 \times S^5$ . In order to understand this equivalence we need to form a dictionary between the operators  $\mathcal{O}$  in conformal field theory and the fields in  $\phi$  in supergravity. For the fields of the conformal theory let us use dilaton field  $\phi$  [6].

The string coupling  $g_s$  and the expectation value of the dilaton field are related to each other and the expectation value of the dilaton field is determined by the boundary condition for the dilaton field at the AdS boundary. Therefore, changing the boundary value of the field  $\phi$  leads to a deformation of the Lagrangian by an operator  $\mathcal{O}$  in the dual field theory. Because of the correspondence between couplings  $g_{YM}$  and  $g_s$ , a change in  $g_s$  formed by the variation of the expectation value of the dilaton field will induce a change in the gauge coupling  $g_{YM}$ . Therefore, the boundary value of the dilaton field acts as a source for the dual operator  $\mathcal{O}$ . The correspondence can be expressed in terms of the generating function for correlation functions of the super Yang-Mills theory and the boundary partition function of the string theory.

$$\langle e^{\int dx^4 \phi_{\text{bdy}}(x) \mathcal{O}(x)} \rangle_{\text{CFT}} = Z_{\text{AdS}} [\phi(z, x)|_z = 0 = \phi_{\text{bdy}}(x)] \quad (1.46)$$



This relation is called the *GKP-Witten relation* [35]. The large  $N_c$  limit it suffices to use classical gravitational theory and not evaluate the full partition function of the string theory in *GKP-Witten* relation [29]. As a result of this relation there should be an operator  $\mathcal{O}_i$  with conformal dimension  $\Delta_i$  in gauge theory for every field  $\phi_i$  in AdS.

Now, let us show that the scaling dimension  $\Delta$  of the operator  $\mathcal{O}$  which transforms under the superconformal group  $SU(2, 2|4)$  is given by the mass  $m$  of the dual free field  $\phi$  in AdS space. The field equation is then

$$(\square_g - m^2)\phi = 0 . \quad (1.47)$$

Then using the metric (1.36), we find two independent solutions of the radial equation

$$\left( \partial_z^2 - \frac{3}{z} \partial_z - \frac{R^2 m^2}{z^2} \right) \phi = 0 . \quad (1.48)$$

As  $z \rightarrow 0$  the solutions behave as  $z^{4-\Delta}$  (*non-normalizable* solution), and  $z^\Delta$  (*normalizable* solution) where  $\Delta = 2 + \sqrt{4 + R^2 m^2}$  or in general we can state this as  $\Delta = \frac{1}{2} (d + \sqrt{d^2 + 4R^2 m^2})$  in  $AdS_{d+1}$  spacetime. Thus, we need to regularize the boundary condition of the field  $\phi$  and in general we can write it as the following.

$$\phi(x, z) = z^{4-\Delta} \phi_{\text{bdy}}(x) \quad (1.49)$$

To make the scalar field  $\phi$  dimensionless  $\phi_{\text{bdy}}(x)$  has to have dimension  $[\text{length}]^{\Delta-4}$ . Then from equation (1.46) we can infer that the operator  $\mathcal{O}$  has dimension  $\Delta$ . We can also conclude that the normalizable solution  $z^\Delta$  has dimension  $[\text{length}]^\Delta$  is related to the vacuum expectation value (vev) of the dual operator  $\langle \mathcal{O} \rangle$ .

For the fields with different Lorentz quantum numbers conformal fields will have different dimensions. Let's consider the example of a massless  $p$ -form  $C$  on  $AdS$  space coupled with a  $d-p$ -form operator  $\mathcal{O}$  on the boundary via coupling  $\int_{M_d} C \wedge \mathcal{O}$  then due to the conformal invariance the dimension of  $\mathcal{O}$  becomes  $d-p$ . On the other hand,

| boundary: gauge (operator)          | bulk: gravity (field)                          |
|-------------------------------------|--|
| energy momentum tensor $T^{\mu\nu}$ | metric field $g_{ab}$                          |
| global current $J^\mu$              | Maxwell field $A_a$                            |
| scalar operator $\mathcal{O}_b$     | scalar field $\phi$                            |
| fermionic operator $\mathcal{O}_f$  | Dirac field $\psi$                             |
| global symmetry                     | local isometry                                 |
| spin/charge of the operator         | spin/charge of the field                       |
| conformal dimension of the operator | mass of the field                              |
| source of the operator              | boundary value of the field                    |
| VEV of the operator                 | boundary value of radial momentum of the field |
| temperature                         | Hawking temperature                            |
| chemical potential/charge density   | boundary values of the gauge potential         |
| phase transition                    | Instability of black holes                     |

**Figure 1.7:** The dictionary of AdS/CFT correspondence taken from [36].

for the massive field the  $C_{bdy}$  is a  $p$ -form on the boundary of conformal dimension  $p + \Delta$ , and an operator that couples to  $C_{bdy}$  has conformal dimension  $\Delta$  calculated from

$$(\Delta + p)(\Delta + p - d) = m^2 . \quad (1.50)$$

A general form of a dictionary table which gives the dual description of each parameter in the boundary theory and in the bulk was provided by Zaanen et. al. [36]. We also used this dictionary table (see Fig. 1.7) throughout this thesis in our calculations.

### 1.2.1 Holographic Superconductors

As stated in the earlier sections, due to the strongly correlated structure of the high  $T_c$  superconductors the microscopic theory behind them is not clear yet. There is an endeavour going on for high  $T_c$  superconductors to understand their pairing mechanism. Gauge/gravity duality is a recently developed tool to understand strongly coupled systems. Since condensed matter theorists do not have sufficient tools to make a contribution to the solution of this problem gauge/gravity duality might be an alternative tool to help condensed matter theorists. AdS/CFT correspondence can

be used as a way to work out the equation of state, real time correlation functions and transport properties such as diffusion constants, conductivities, and viscosities.

A holographic dual for a superconductor requires a notion of temperature which is provided by the black hole temperature on the gravity side and a condensate which is described by the some field coupled to gravity in the bulk. In gauge/gravity duality black holes whose spacetime asymptotically approaches to AdS space at infinity are used and these black holes have positive specific heat, i.e., their temperature increases with their mass. The other requirement of a superconductor, a condensate, is obtained by a static nonzero field outside this black hole which is called the black hole “hair”. More precisely, our goal is to find a Schwarzschild or Reissner-Nordström AdS black hole to be unstable to forming hair, *i.e.* at low temperature [37]. Gubser showed in his paper [38] that a *charged* scalar field around a *charged* black hole in AdS would have this instability to forming hair at low temperature. Then the action to be considered is

$$S = \int dx^4 \sqrt{-g} \left( R + \frac{6}{L^2} - \frac{1}{4} F_{\mu\nu} F^{\mu\nu} - |\nabla\Psi - iqA\Psi|^2 - m^2|\Psi|^2 \right) \quad (1.51)$$

where there is gravitation term with cosmological constant  $\Lambda = -\frac{3}{L^2}$  coupled with Maxwell field and charged scalar field of mass  $m$  and charge  $q$ . Let us define the effective mass of the charged scalar field  $\Psi$ ,  $m_{\text{eff}}^2 = m^2 + q^2 g^{tt} A_t^2$ . For this black hole to be unstable  $m_{\text{eff}}^2$  needs to become sufficiently negative near the horizon. Moreover, as the temperature of the charged black hole is lowered it becomes near extremal which means since  $g_{tt}$  is closer to developing a double zero at the horizon  $|g_{tt}|$  becomes larger and the possible instability becomes stronger.

The AdS black hole plays a crucial role in confining the created pairs of charged particles as a box due to the negative cosmological constant. Thus, these charged particles stay outside the horizon and form the hair of the black hole.

We will now discuss the system in the probe limit which means that there is no backreaction of the matter fields on the metric. The probe limit is obtained by first rescaling the fields  $A_\mu = \tilde{A}_\mu/q$  and  $\Psi_\mu = \tilde{\Psi}_\mu/q$  and then taking the limit  $q \rightarrow \infty$

while keeping  $qA$  and  $q\Psi$  fixed. This will drop out the matter sources from Einstein's equations while the scalar and the Maxwell equations remain essentially unchanged.

### Condensate

As we discussed earlier the planar Schwarzschild AdS metric ansatz for solving the Einstein's equations in 3+1 dimensions is

$$ds^2 = -f(r)dt^2 + \frac{dr^2}{f(r)} + r^2(dx^2 + dy^2) \quad (1.52)$$

with  $\Psi = \Psi(r)$  and  $A_t = \phi(r)$ . Solving the Einstein equations give

$$f(r) = \frac{r^2}{L^2} \left( 1 - \frac{r_0^3}{r^3} \right) \quad (1.53)$$

where  $L$  and  $r_0$  are AdS and Schwarzschild radii respectively. Then from the  $g_{tt}$  term the Hawking temperature of the black hole is calculated from

$$T_H = T = \frac{3r_0}{4\pi L^2} . \quad (1.54)$$

To analyze this system we need to solve the Maxwell- scalar field equations in this fixed background. From the Maxwell equations choosing  $A_r = A_x = A_y = 0$  shows that the phase of the scalar field  $\psi$  must be constant therefore we take  $\psi$  to be real. The Maxwell and scalar field equations are obtained as the following.

$$\psi'' + \left( \frac{f'}{f} + \frac{2}{r} \right) \psi' + \frac{\phi^2}{f^2} \psi - \frac{m^2}{f} \psi = 0 \quad (1.55)$$

$$\phi'' + \frac{2}{r} \phi' - \frac{2\psi^2}{f} \phi = 0 . \quad (1.56)$$

The term which will lead to the scalar hair at low temperature in eq.(1.55) is  $(\phi^2/f^2) \psi$  since it has the opposite sign with the mass term in scalar field equation.

We choose the mass to be  $m^2 = -2/L^2$  which seems to be tachyonic but this case is perfectly allowed in gauge/gravity duality. This type of mass describes instability. However, it was shown by Breitenlohner and Freedman [39] that the  $AdS_{d+1}$  spacetime is stable if  $m^2 \geq m_{\text{BF}}^2$  where

$$m_{\text{BF}}^2 = -\frac{d^2}{4L^2} . \quad (1.57)$$

Therefore, mass choice of  $m^2 = -2/L^2$  satisfies the BF bound. For large enough  $\mu/T$  or low enough temperature the scalar field becomes tachyonic and condensates.

We now need to consider the boundary conditions at the horizon and at the infinity to solve the Maxwell and scalar field equations. First of all,  $\phi = A_t$  needs to vanish at the horizon. The reason for that can be explained as the following. The source for Maxwell's equations in the bulk is, of course, gauge invariant. But in a gauge in which  $\psi$  is real, the current is just  $\psi^2 A_\mu$ . Since the current must remain finite at the horizon, we need  $A_\mu$  to remain finite, and hence  $\phi = A_t = 0$ . Second constraint at the horizon is coming from the requirement that the solution needs to be smooth at the horizon. From eq.(1.55) one can find that there is a two parameter family of solutions which is regular at the horizon, i.e.  $\psi(r_0)$  and  $\phi'(r_0)$ .

Now, let us look at the boundary conditions at infinity. The general asymptotic behavior of the scalar and the Maxwell field are

$$\psi = \frac{\psi^{(1)}}{r} + \frac{\psi^{(2)}}{r^2} + \dots \quad (1.58)$$

and

$$\phi = \mu - \frac{\rho}{r} + \dots . \quad (1.59)$$

Since our choice of mass value is close to BF bound both of these falloffs are normalizable so that we can choose the boundary condition in which either of them vanishes at the end we will have a one parameter family of solutions.

Gauge/gravity duality allows us to tell some properties of the dual field theory. The dual theory is a 2+1 dimensional conformal field theory (CFT) at temperature

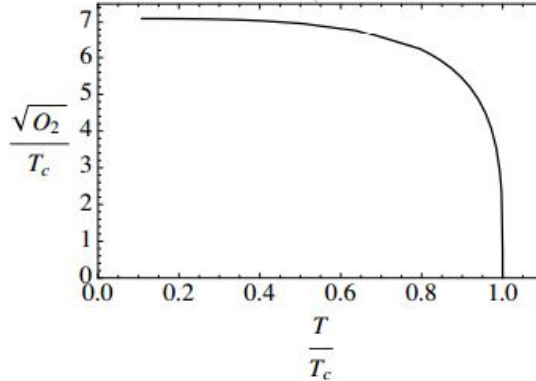


**Figure 1.8:** The condensate as a function of temperature. The critical temperature is proportional to the chemical potential. Figure is taken from [37].

$T$  given by (1.54). The local gauge symmetry in the bulk corresponds to a global  $U(1)$  symmetry in the CFT. Also from the asymptotic behavior of the bulk solution the chemical potential  $\mu$  and the charge density  $\rho$  can be found from eq (1.59). The condensate of the scalar operator  $\mathcal{O}$  in the field theory dual to the field  $\psi$  is given by

$$\langle \mathcal{O}_i \rangle = \sqrt{2} \psi^{(i)}, \quad i = 1, 2 \quad (1.60)$$

with the boundary condition  $\epsilon_{ij} \psi^j = 0$ . The normalization constant  $\sqrt{2}$  corresponds to taking the bulk-boundary coupling  $\frac{1}{2} \int d^3x (\bar{\mathcal{O}}\psi + \mathcal{O}\bar{\psi})$ .

The numerical solution of the Maxwell and scalar field equations exist. In Fig. 1.8 we can see the temperature dependence of the condensate. The qualitatively behavior of the graph obtained is similar to BCS theory. As seen in Fig. 1.8 the condensate rises as soon as  $T$  is decreased below the critical temperature,  $T_c$  and becomes zero at zero temperature. Near  $T_c$  behavior of the graph is  $O_2 = 100T_c^2 \left(1 - \frac{T}{T_c}\right)^{1/2}$  which is the standard behavior predicted by Landau-Ginzburg theory.

To discuss the continuity of the phase transition the free energy (Euclidean action) can be calculated. Remember that  $\psi = 0$ ,  $\phi = \rho(1/r_0 - 1/r)$  are also solutions for the equations but they do not develop a scalar hair in the black hole. After calculating the free energies of these two particular solutions it turns out that the free energy of

the hairy configuration is always lower and it becomes equal as  $T \rightarrow T_c$ . In addition to that the difference of free energies scales like  $(T - T_c)^2$  near the transition which tells us that there is a second order phase transition. This kind of finite temperature continuous symmetry breaking phase transitions are only possible in  $2+1$  dimensions in the large  $N$  limit, where fluctuations are suppressed.

For a general scalar field of mass  $m$  in  $AdS_4$  remember that the scalar field can be written as

$$\psi = \frac{\psi_-}{r^{\lambda_-}} + \frac{\psi_+}{r^{\lambda_+}} + \dots \quad (1.61)$$

Therefore, for a scalar field of mass

$$\lambda_{\pm} = \frac{1}{2} \left( 3 \pm \sqrt{9 + 4(mL)^2} \right) \quad (1.62)$$

There are again two boundary conditions to be considered. For  $m^2 \geq m_{BF}^2 + L^{-2}$ , the normalizable falloff is the one with  $\lambda_+$ . Therefore, the expectation value of the operator dual to the scalar field is  $\psi_+ = \langle \mathcal{O} \rangle$  which is dual to the response, and the source for this operator is  $\psi_- = 0$ . One can also consider the other boundary condition in which  $\psi_+ = 0$  for  $m_{BF}^2 \leq m^2 < m_{BF}^2 + L^{-2}$ .

In Fig.1.9 condensates for different mass and scaling dimension values are shown. The qualitative behavior is the same as before, i.e. the condensate is zero above a critical temperature  $T_c$  and there is a square root behavior near the critical temperature,  $\langle \mathcal{O} \rangle \propto (T - T_c)^{1/2}$ . There is one exceptional case at  $\lambda = 1$  in which the condensate grows up at low temperature. This kind of behavior is attributed to the neglected backreaction on the metric. Once the solution is done away from the probe limit the condensate at this particular  $\lambda$  approaches a finite limit at zero temperature. In conclusion, for this particular model for higher temperature superconductor one should lower the dimension of the condensate.

The holographic superconductors are GL theory type but adding fermions to the bulk one can also study Fermi liquid and non-Fermi liquid phases. The ultimate goal is

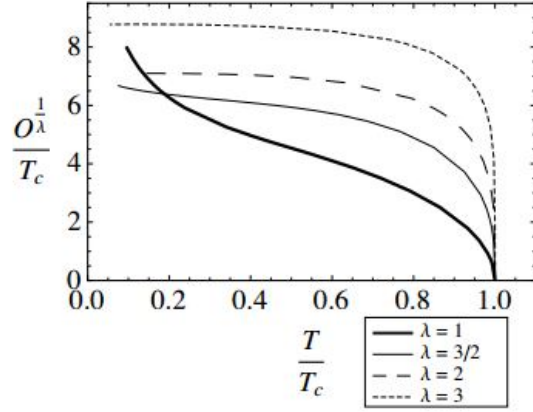


**Figure 1.9:** Condensates with different dimension,  $\lambda$ , as a function of temperature. The condensate tends to increase with  $\lambda$ . Figure is taken from [37].

to study all gravity dual of these phases to understand the high  $T_c$  superconductivity and other strongly coupled condensed matter systems [29].



# Chapter 2

## Spontaneously Generated Inhomogeneous Phases via Holography

### 2.1 Introduction

There has been considerable recent activity studying phenomena at strong coupling using a weakly coupled dual gravity description. The tool to carry out such a study is the gauge/gravity duality. This holographic principle [3] has many applications in string theory, where it is well founded, but it has also been applied to other physical systems encountered in condensed matter physics. One of the most extensively studied condensed matter systems using the gauge/gravity duality is the holographic superconductor (for a review see [37]).

The gravity dual of a homogeneous superconductor consists of a system with a black hole and a charged scalar field. The black hole admits scalar hair at temperatures lower than a critical temperature [38], while there is no scalar hair at higher temperatures. According to the holographic principle, this breaking of the abelian  $U(1)$  symmetry corresponds in the boundary theory to a scalar operator which

condenses at a critical temperature dependent on the charge density of the scalar potential. The fluctuations of the vector potential give the frequency dependent conductivity in the boundary theory [9]. Backreaction effects on the metric were studied in [10]. In [74] an exact gravity dual of a gapless superconductor was discussed in which the charged scalar field responsible for the condensation was an exact solution of the equations of motion, and below a critical temperature dressed a vacuum black hole with scalar hair.

Apart from holographic applications to conventional homogeneous superconductors, extensions to unconventional superconductors characterized by higher critical temperatures, such as cuprates and iron pnictides, have also been studied. Interesting new features of these systems include competing orders related to the breaking of lattice symmetries introducing inhomogeneities. A study of the effect on the pairing interaction in a weakly coupled BCS system was performed in [40]. Additionally, numerical studies of Hubbard models [41, 42] suggest that inhomogeneity might play a role in high-Tc superconductivity.

The recent discovery of transport anomalies in  $\text{La}_{2-x}\text{Ba}_x\text{CuO}_4$  might be explained under the assumption that the cuprate is a superconductor with a unidirectional charge density wave, i.e., a “striped” superconductor [43]. Other studies using mean-field theory have also shown that, unlike the homogeneous superconductor, the striped superconductor exhibits the existence of a Fermi surface in the ordered phase [44, 45] and possesses complex sensitivity to quenched disorder [43]. Holographic striped superconductors were discussed in [46] by introducing a modulated chemical potential producing superconducting stripes below a critical temperature. Properties of the striped superconductors and backreaction effects were studied in [47, 48]. Striped phases breaking parity and time-reversal invariance were found in electrically charged AdS-Reissner-Nordström black branes with neutral pseudo-scalars [49]. In [50], it was shown that similar phases could be generated in Einstein-Maxwell-dilaton theories that leave parity and time-reversal invariance intact.

Inhomogeneities also appear in condensed matter systems other than superconductors. These systems are characterized by additional ordered states which compete or coexist with superconductivity [51, 52]. The most important of these are charge and spin density waves (CDW and SDW, respectively) [53]. The development of these states corresponds to spontaneous modulation of the electronic charge and spin density, below a critical temperature  $T_c$ . Density waves are widely spread among different classes of materials. One may distinguish between types either orbitally [54], Zeeman driven [55], field-induced CDWs, confined [56], and even unconventional density waves [57].

The usual approach to study the effect of inhomogeneity at strong coupling is to introduce a modulated chemical potential. According to the holographic principle this is translated into a modulated boundary value for the electrostatic potential in the AdS black hole gravity background. The corresponding Einstein-Maxwell-scalar systems can be obtained which below a critical temperature undergoes a phase transition to a condensate with a non-vanishing modulation. Depending on what symmetries are broken, the modulated condensate gives rise to ordered states like CDW or SDW in the boundary theory [58, 46].

To explore the properties of spatial inhomogeneities in holographic superfluids, gravitational backgrounds which are not spatially homogeneous were introduced in [59, 60, 61]. In [62] the breaking of the translational invariance is sourced by a scalar field with a non-trivial profile in the  $x$ -direction. Upon perturbing the one-dimensional “lattice”, the Einstein-Maxwell-scalar field equations were numerically solved at first order and the optical conductivity was calculated. Further properties of this construction were studied in [63].

In this work, we study a holographic superfluid in which a spatially inhomogeneous phase is spontaneously generated. The gravity sector consists of a RN-AdS black hole, an electromagnetic field, and a scalar field. We introduce high-derivative interaction terms between the electromagnetic field and the scalar field. These higher-order terms are essential in spontaneously generating the inhomogeneous phase in the boundary

theory. Alternative approaches for spontaneously breaking translational symmetries have been found by use of an interaction with the Einstein tensor [64, 65], a Chern-Simons interaction [66, 67], and more recently with a dilaton [50].

We put the gravitational background on a one-dimensional “lattice” generated by an  $x$ -dependent profile of the scalar field. At the onset of the condensation of the scalar field, we calculate the transition temperature. We find that as the wavenumber of the scalar field increases starting from zero (homogeneous profile), the transition temperature increases, showing that inhomogeneous configurations dominate at higher temperatures. We find a maximum transition temperature corresponding to a certain finite wavenumber. This is the critical temperature ( $T_c$ ) of our system. Below  $T_c$  the system undergoes a second order phase transition to an inhomogeneous phase. This occurs in a range of parameters of the system that we discuss.

We then solve the equations of motion below the critical temperature. we use perturbation theory to expand the bulk fields right below  $T_c$ , thus obtaining an analytic solution to the coupled system of Einstein-Maxwell-scalar field equations at first order. We find that a spatially inhomogeneous charge density is spontaneously generated in the boundary theory.

The paper is organized as follows. In section 2.2, we present the basic setup of the holographic model, and introduce the higher-derivative couplings. In section 2.3, we discuss the instability to a spatially inhomogeneous phase. We calculate numerically the critical temperature of the system, and analyze its dependence on the various parameters of the system. In section 2.4, we use perturbation theory to obtain an analytic solution below the critical temperature, and show that the charge density in the boundary theory is spatially inhomogeneous. Finally, in section 2.5, we present our conclusions.

## 2.2 The setup

In this section we introduce a holographic model whose main feature is the spontaneous generation of spatially inhomogeneous phases in the boundary theory. This cures the main deficiency of an earlier proposal [58]. This is achieved by introducing higher-derivative coupling of the electromagnetic field to the scalar field.

Consider a system consisting of a  $U(1)$  gauge field,  $A_\mu$ , with corresponding field strength  $F_{\mu\nu} = \partial_\mu A_\nu - \partial_\nu A_\mu$ , and a scalar field  $\phi$  with charge  $q$  under the  $U(1)$  group. The fields live in a spacetime of negative cosmological constant  $\Lambda = -6/L^2$ .

The action is given by

$$S = \int d^4x \sqrt{-g} \mathcal{L} \quad , \quad \mathcal{L} = \frac{R + 6/L^2}{16\pi G} - \frac{1}{4} F_{\mu\nu} F^{\mu\nu} - (D_\mu \phi)^* D^\mu \phi - m^2 |\phi|^2 \quad . \quad (2.1)$$

where  $D_\mu \phi = \partial_\mu \phi - iqA_\mu \phi$ . For simplicity, we shall set  $16\pi G = L = 1$ .

Our main concern is to generate spatially inhomogeneous phases in the boundary theory. To this end, we may introduce higher-derivative interaction terms of the form

$$\mathcal{L}_{\text{int}} = \phi^* [\eta \mathcal{G}^{\mu\nu} D_\mu D_\nu + \eta' \mathcal{H}^{\mu\nu\rho\sigma} D_\mu D_\nu D_\rho D_\sigma + \dots] \phi + \text{c.c.} \quad , \quad (2.2)$$

which may arise from quantum corrections. The possible operators in the above expression and their emergence from string theory are worth exploring. Candidates for  $\mathcal{G}_{\mu\nu}$  include contributions to the stress-energy tensor from the electromagnetic field and the scalar field, the Einstein tensor [64, 65], etc., and similarly for  $\mathcal{H}_{\mu\nu\rho\sigma}$ , etc. Here we shall be content with a special choice which leads to inhomogeneities,

$$\mathcal{L}_{\text{int}} = \eta \mathcal{G}^{\mu\nu} (D_\mu \phi)^* D_\nu \phi - \eta' |D_\mu \mathcal{G}^{\mu\nu} D_\nu \phi|^2 \quad , \quad (2.3)$$

where

$$\mathcal{G}_{\mu\nu} = T_{\mu\nu}^{(\text{EM})} + g_{\mu\nu} \mathcal{L}^{(\text{EM})} = F_{\mu\rho} F_\nu{}^\rho - \frac{1}{2} g_{\mu\nu} F^{\rho\sigma} F_{\rho\sigma} \quad , \quad (2.4)$$

coupling the scalar field  $\phi$  to the gauge field. This coupling is the essential tool for the generation of spatial inhomogeneities.

From the action (2.1), together with the interaction term (4.3), we obtain the Einstein equations

$$R_{\mu\nu} - \frac{1}{2}Rg_{\mu\nu} - 3g_{\mu\nu} = \frac{1}{2}T_{\mu\nu} , \quad (2.5)$$

where  $T_{\mu\nu}$  is the stress-energy tensor,

$$T_{\mu\nu} = T_{\mu\nu}^{(EM)} + T_{\mu\nu}^{(\phi)} + \eta\Theta_{\mu\nu} + \eta'\Theta'_{\mu\nu} , \quad (2.6)$$

containing a gauge, scalar, and interaction term contributions, respectively,

$$\begin{aligned} T_{\mu\nu}^{(EM)} &= F_{\mu\rho}F_{\nu}{}^{\rho} - \frac{1}{4}g_{\mu\nu}F^{\rho\sigma}F_{\rho\sigma} , \\ T_{\mu\nu}^{(\phi)} &= (D_{\mu}\phi)^*D_{\nu}\phi + D_{\mu}\phi(D_{\nu}\phi)^* - g_{\mu\nu}(D_{\alpha}\phi)^*D^{\alpha}\phi - m^2g_{\mu\nu}|\phi|^2 , \\ \Theta_{\mu\nu} &= \frac{2}{\sqrt{-g}}\frac{\delta}{\delta g^{\mu\nu}} \int d^4x\sqrt{-g}\mathcal{G}^{\mu\nu}(D_{\mu}\phi)^*D_{\nu}\phi , \\ \Theta'_{\mu\nu} &= -\frac{2}{\sqrt{-g}}\frac{\delta}{\delta g^{\mu\nu}} \int d^4x\sqrt{-g}|D_{\mu}\mathcal{G}^{\mu\nu}D_{\nu}\phi|^2 . \end{aligned} \quad (2.7)$$

Varying the Lagrangian with respect to  $A_{\mu}$  we find the Maxwell equations

$$\nabla_{\mu}F^{\mu\nu} = J^{\nu} , \quad (2.8)$$

where  $J_{\mu}$  is the current,

$$J_{\mu} = qJ_{\mu}^{(\phi)} + \eta\mathcal{J}_{\mu} + \eta'\mathcal{J}'_{\mu} , \quad (2.9)$$

containing scalar and interaction term contributions, respectively,

$$\begin{aligned} J_{\mu} &= i[\phi^*D_{\mu}\phi - (D_{\mu}\phi)^*\phi] , \\ \mathcal{J}_{\mu} &= \frac{1}{\sqrt{-g}}\frac{\delta}{\delta A^{\mu}} \int d^4x\sqrt{-g}\mathcal{G}^{\mu\nu}(D_{\mu}\phi)^*D_{\nu}\phi , \\ \mathcal{J}'_{\mu} &= -\frac{1}{\sqrt{-g}}\frac{\delta}{\delta A^{\mu}} \int d^4x\sqrt{-g}|D_{\mu}\mathcal{G}^{\mu\nu}D_{\nu}\phi|^2 . \end{aligned} \quad (2.10)$$

Finally, the equation of motion for the scalar field is

$$D_\mu D^\mu \phi - m^2 \phi = \eta D_\mu (\mathcal{G}^{\mu\nu} D_\nu \phi) + \eta' D_\rho (\mathcal{G}^{\mu\rho} D_\mu (D_\nu (\mathcal{G}^{\nu\sigma} D_\sigma \phi))). \quad (2.11)$$

Our aim is to study the Einstein-Maxwell-scalar system of equations first at the critical temperature, and then below the critical temperature using perturbation theory.

## 2.3 The critical temperature

At the critical temperature, we have  $\phi = 0$ . The Einstein-Maxwell system has a static solution with metric of the form

$$ds^2 = \frac{1}{z^2} \left[ -h(z) dt^2 + \frac{dz^2}{h(z)} + dx^2 + dy^2 \right]. \quad (2.12)$$

The system possesses a scaling symmetry. The arbitrary scale is often taken to be the radius of the horizon. It is convenient to fix the scale by using a radial coordinate  $z$  so the horizon is at  $z = 1$ . Since the scale has been fixed, we should only be reporting on scale-invariant quantities.

The Maxwell equations admit the solution

$$A_t = \mu(1 - z), \quad (2.13)$$

so that the  $U(1)$  gauge field has an electric field in the  $z$ -direction equal to the chemical potential,  $E_z = \mu$ .

The Einstein equations are then solved by

$$h(z) = 1 - \left(1 + \frac{\mu^2}{4}\right) z^3 + \frac{\mu^2}{4} z^4. \quad (2.14)$$

The temperature is given as

$$\frac{T_c}{\mu} = -\frac{h'(1)}{4\pi\mu} = \frac{3}{4\pi\mu} \left(1 - \frac{\mu^2}{12}\right) , \quad (2.15)$$

where we divided by  $\mu$  to create a scale-invariant quantity.

Additionally, at the critical temperature the scalar field satisfies the wave equation,

$$\partial_z^2 \phi + \left[ \frac{h'}{h} - \frac{2}{z} \right] \partial_z \phi + \frac{1}{h} (1 - \eta\mu^2 z^4 - \eta'\mu^4 z^{10} \nabla_2^2) \nabla_2^2 \phi - \frac{1}{h} \left[ \frac{m^2}{z^2} - q^2 \frac{A_t^2}{h} \right] \phi = 0 , \quad (2.16)$$

where  $\nabla_2^2 = \partial_x^2 + \partial_y^2$ , and we fixed the gauge so that  $\phi$  is real.

The wave equation (2.16) can be solved by separating variables,

$$\phi(z, x, y) = \Phi(z)Y(x, y) , \quad (2.17)$$

where  $Y$  is an eigenfunction of the two-dimensional Laplacian,

$$\nabla_2^2 Y = -\tau Y . \quad (2.18)$$

We will keep translation invariance in the  $y$ -direction, and concentrate on the one-dimensional "lattice" defined by

$$Y = \cos(kx) , \quad (2.19)$$

with  $\tau = k^2$ , and leave the two-dimensional lattices for future study.

The radial function  $\Phi(z)$  satisfies the wave equation

$$\Phi'' + \left[ \frac{h'}{h} - \frac{2}{z} \right] \Phi' + \frac{\tau}{h} [1 - \eta\mu^2 z^4 - \eta'\tau\mu^4 z^{10}] \Phi - \frac{1}{h} \left[ \frac{m^2}{z^2} - q^2 \frac{A_t^2}{h} \right] \Phi = 0 . \quad (2.20)$$



The asymptotic behavior (as  $z \rightarrow 0$ ) is  $\Phi \sim z^\Delta$ , where  $\Delta(\Delta-3) = m^2$ . It is convenient to write

$$\Phi(z) = \frac{\langle \mathcal{O}_\Delta \rangle}{\sqrt{2}} z^\Delta F(z) \quad , \quad F(0) = 1 \quad . \quad (2.21)$$

For general  $\Delta$ , we obtain

$$F'' + \left[ \frac{2(\Delta-1)}{z} + \frac{h'}{h} \right] F' + \left[ -\frac{\tau(1 - \eta\mu^2 z^4 - \eta'\tau\mu^4 z^{10})}{h} + \frac{q^2 A_t^2}{h^2} + \frac{m^2}{z^2} \left( 1 - \frac{1}{h} \right) + \frac{\Delta h'}{zh} \right] F = 0 \quad . \quad (2.22)$$

The maximum transition temperature of the system can be calculated by solving (2.22) numerically, and using the expression (2.15) for the temperature. The maximum transition temperature is the critical temperature  $T_c$  of the system. Figure 2.1 shows the numerically calculated transition temperature without the higher-derivative couplings ( $\frac{\eta}{\mu^2} = \frac{\eta'}{\mu^4} = 0$ ) dependent on the wavenumber  $k$ . Both quantities are divided by the chemical potential  $\mu$  to render them dimensionless. The maximum value is found at  $k = 0$ , which shows that the homogeneous solution is dominant. When the higher-derivative interaction terms are turned on, the critical temperature  $T_c$  of the system also depends on the coupling constants  $\eta, \eta'$ , and the homogeneous solution no longer dominates.

In the limit of vanishing second higher-derivative coupling,  $\eta' \rightarrow 0$ , we may analytically calculate the asymptotic critical temperature. The latter is found in the limit in which the wavenumber diverges ( $\tau \rightarrow \infty$ ). In this limit, the wave equation (2.22) is dominated by the term proportional to  $\tau$  near the horizon ( $z \rightarrow 1$ ), thus giving the critical value for the chemical potential as  $\mu_c^4 = \frac{\mu^2}{\eta}$ , and corresponding temperature (2.15)

$$\lim_{\tau/\mu^2 \rightarrow \infty} \frac{T_0}{\mu} = \frac{3}{4\pi} \left( \frac{\eta}{\mu^2} \right)^{1/4} \left( 1 - \frac{1}{12\sqrt{\frac{\eta}{\mu^2}}} \right) \quad . \quad (2.23)$$

The critical temperature for a standard Einstein-Maxwell-scalar system, i.e.,  $\frac{\eta}{\mu^2} = \frac{\eta'}{\mu^4} = 0$ , with a neutral scalar was calculated in [68]. For  $\Delta = 2$ , it was found

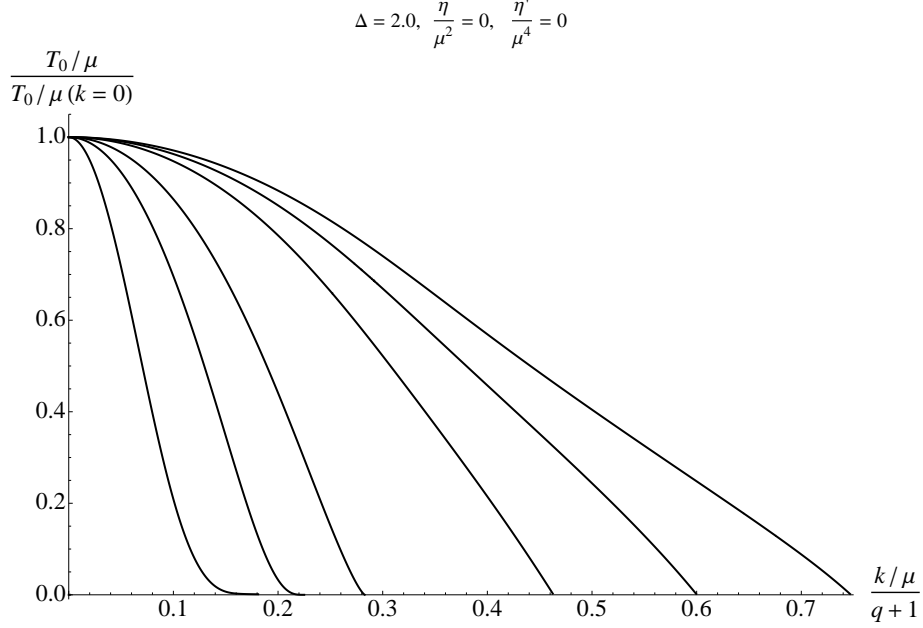


**Figure 2.1:** Dependence of the transition temperature  $T_0/\mu$  on the wavenumber  $k/\mu$  for  $\Delta = 2$  in the absence of higher-derivative interactions ( $\frac{\eta}{\mu^2} = \frac{\eta'}{\mu^4} = 0$ ). From left-to-right the lines correspond to  $q = 0, 1, 1.5, 3, 5, 10$ . The maximum transition temperature (i.e., the critical temperature) occurs at  $k = 0$  and the homogeneous configuration is dominant.

that  $\frac{T_c}{\mu} \approx .00009$ . For  $\eta$  large enough, the asymptotic ( $\tau/\mu^2 \rightarrow \infty$ ) transition temperature will be higher than that of the homogeneous solution. In this case, the transition temperature monotonically increases as we increase the wavenumber  $k$  and asymptotes to (2.23). Hence the higher-derivative coupling's encoding of the electric field's back reaction near the horizon is the cause of spontaneous generation of spatial modulation.

As we switch on  $\eta' > 0$ , the transition temperature is bounded from above by (2.23). It attains a maximum value at a finite  $k$ . Thus the second higher-derivative coupling acts as a UV cutoff on the wavenumber, which in turn determines the size of the "lattice" through  $k = \frac{2\pi}{a}$ , where  $a$  is the lattice spacing. As  $\eta' \rightarrow 0$ , the lattice spacing also vanishes ( $a \rightarrow 0$ ) and the wavenumber diverges ( $k \rightarrow \infty$ ). We will focus on small-to-zero charge, realizing a transition temperature at zero wavenumber *below*

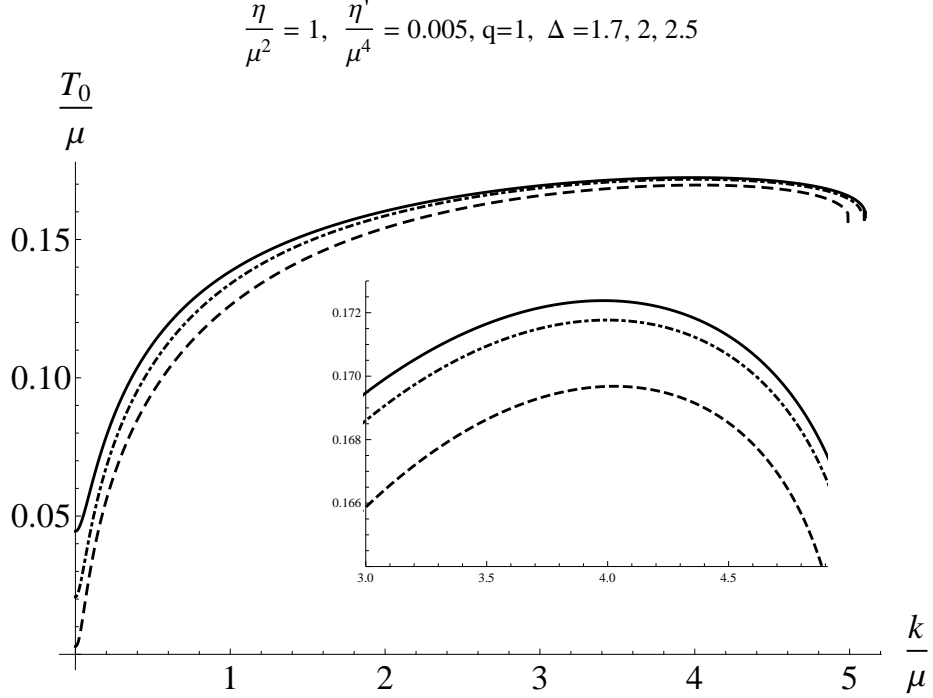


**Figure 2.2:** Dependence of the transition temperature  $\frac{T_0}{\mu}$  on the wavenumber  $\frac{k}{\mu}$  for  $\frac{\eta}{\mu^2} = 1$ ,  $\frac{\eta'}{\mu^4} = 0.005$ ,  $q = 1$ , and  $\Delta = 1.7$  (solid line), 2 (dash-dotted line), and 2.5 (dotted line).

(2.23), which guaranties that  $k \neq 0$  at the maximum transition temperature, hence the dominance of inhomogeneous modes. For our purposes, we do not expect any quantitative differences between small and zero charge, even with a neutral scalar leaving the boundary  $U(1)$  symmetry intact.

In Figure 2.2, we show the transition temperature  $T_0$  as a function of the wavenumber  $k$  with  $q = 1$ ,  $\frac{\eta}{\mu^2} = 1$ ,  $\frac{\eta'}{\mu^4} = 0.005$ , for various values of the conformal dimension of the scalar field  $\Delta$ . The critical temperature of the system is the maximum transition temperature which occurs at finite  $k/\mu \approx 3.98$ . The effect of the charge  $q$  is shown in Fig. 2.3. It can be seen that for finite coupling constants  $\eta$  and  $\eta'$ , and small enough charge  $q$ , the system produces a *critical* temperature at non-vanishing finite values of  $k/\mu$ . For large enough  $q$ , the homogeneous solution ( $k = 0$ ) remains the dominant solution.

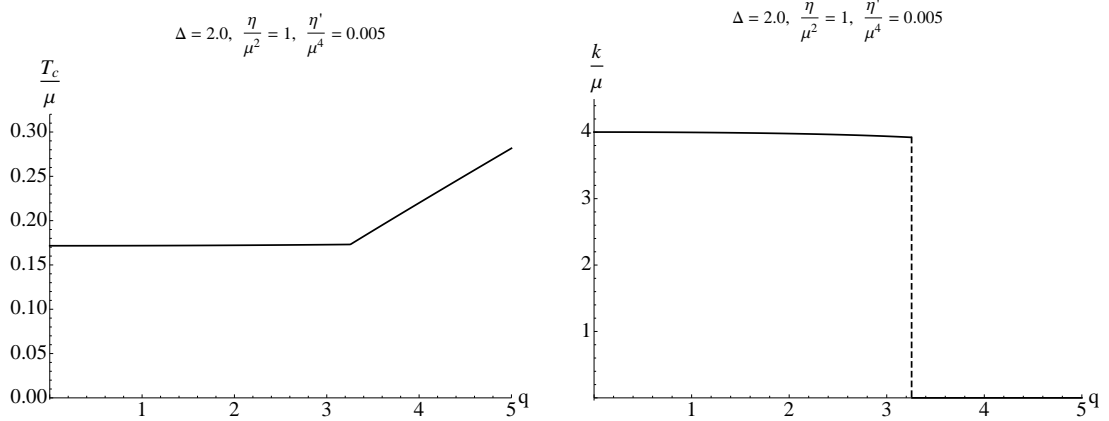


**Figure 2.3:** The critical temperature  $\frac{T_c}{\mu}$  (left panel) and corresponding wavenumber  $\frac{k}{\mu}$  (right panel) as functions of  $q$  with  $\frac{\eta}{\mu^2} = 1$ ,  $\frac{\eta'}{\mu^4} = 0.005$ , and  $\Delta = 2$ . When  $q \lesssim 3.2$ , the charge is small enough that the higher-derivative couplings spontaneously generate inhomogeneity. Above that range, the homogeneous scalar is dominant.

Figure 2.4 shows the dependence of the critical temperature  $T_c$  and wavenumber  $k$  on the second higher-derivative coupling constant  $\frac{\eta'}{\mu^4}$ . There is little to no dependence of  $T_c$  on the conformal dimension  $\Delta$ . We see numerical confirmation that in the absence of the second coupling ( $\eta' = 0$ ), the maximum transition temperature corresponds to  $k \rightarrow \infty$ . Thus  $\eta'$  acts as an effective UV cutoff, determining the wavenumber  $k$  at the critical temperature, and therefore the size of the “lattice” of the system (if  $k = \frac{2\pi}{a}$ , where  $a$  is the lattice spacing). The value of the wavenumber decreases with increasing coupling  $\eta'$ , as shown on the right panel of Fig. 2.4. The UV cutoff  $\eta'$ , or effective lattice spacing, can be understood as stabilizing the inhomogeneous modes introduced by the first higher-derivative coupling  $\eta$ . Looking forward, we trust our linearization below the critical temperature because it will not rely on a gradient expansion but on an order parameter proportional to  $(T - T_c)^{1/2}$ .

Summarizing, at the critical temperature the electric field backreacts on the system, the Einstein-Maxwell field equations admit solutions with a spatially dependent scalar field while the electric field attains a constant value equal to the chemical potential. In the next section we will perturb around the critical temperature

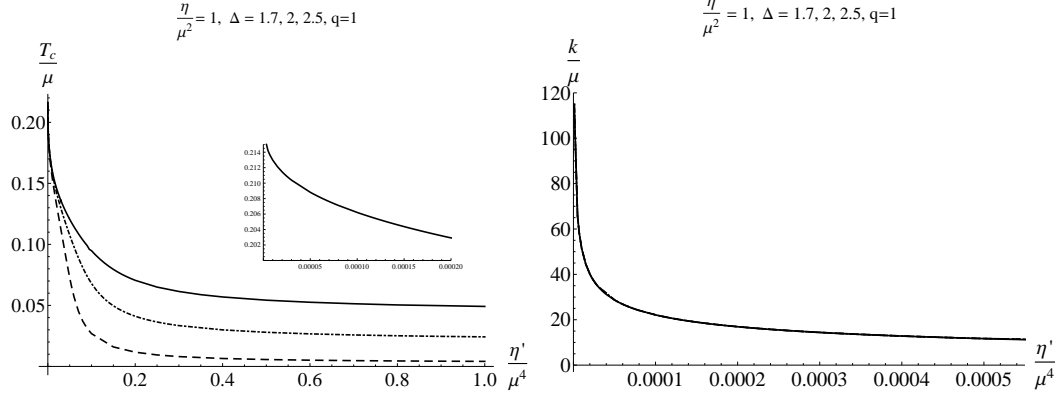


**Figure 2.4:** Dependence of the critical temperature  $\frac{T_c}{\mu}$  (left panel) and corresponding wavenumber  $\frac{k}{\mu}$  (right panel) on the second higher-derivative coupling constant  $\frac{\eta'}{\mu^4}$ , for  $\frac{\eta}{\mu^2} = 1$ ,  $q = 1$ ,  $\Delta = 1.7$  (solid), 2 (dash-dotted), and 2.5 (dashed). The inset is shown only for  $\Delta = 2$  because, at the scale shown, no difference can be seen between the three different conformal dimensions of the full graph.

and show the system develops a spatially inhomogeneous phase in the boundary theory.

## 2.4 Below the critical temperature

In this section we study the system below the critical temperature. The equations of motion resulting from the considered action (2.1) together with (4.3) may be perturbed near the critical temperature with spatially dependent solutions. We will study the behavior of the system analytically, leaving a full numerical study for the future. To simplify the discussion somewhat, we shall assume that the effects of the cutoff are negligible near the critical temperature ( $T \approx T_c$ ), and set  $\eta' = 0$ . We will build a perturbative expansion on the departure below  $T_c$  and not in terms of gradients or momentum of the scalar mode. It is straightforward, albeit tedious, to include the effects of the cutoff below  $T_c$ .

Below the critical temperature the scalar field backreacts on the metric. Consider the following *ansatz*

$$ds^2 = \frac{1}{z^2} \left[ -h(z, x) e^{-\alpha(z, x)} dt^2 + \frac{dz^2}{h(z, x)} + e^{\beta(z, x)} dx^2 + e^{-\beta(z, x)} dy^2 \right]. \quad (2.24)$$

To solve the equations of motion (4.5), (4.8), and (4.11) below the critical temperature  $T_c$ , we expand in the order parameter

$$\xi = \frac{\langle \mathcal{O}_\Delta \rangle}{\sqrt{2}}, \quad (2.25)$$

and write

$$\begin{aligned} h(z, x) &= h_0(z) + \xi^2 h_1(z, x) + \mathcal{O}(\xi^4), \\ \alpha(z, x) &= \xi^2 \alpha_1(z, x) + \mathcal{O}(\xi^4), \\ \beta(z, x) &= \xi^2 \beta_1(z, x) + \mathcal{O}(\xi^4), \\ \phi(z, x) &= \xi \phi_0(z, x) + \xi^3 \phi_1(z, x) + \mathcal{O}(\xi^5), \\ A_t(z, x) &= A_{t0}(z) + \xi^2 A_{t1}(z, x) + \mathcal{O}(\xi^4), \end{aligned} \quad (2.26)$$

where  $A_{t0}$ ,  $h_0$ , and  $\xi \phi_0$  are defined at the critical temperature  $T_c$  by eqs. (2.13), (2.14), and (2.16), respectively. The chemical potential is given as

$$\mu \equiv A_t(0, x) = \mu_0 + \xi^2 \mu_1 + \mathcal{O}(\xi^2), \quad \mu_0 = A_{t0}(0), \quad \mu_1 = A_{t1}(0, x). \quad (2.27)$$

It should be noted that we are working with an ensemble of fixed chemical potential, which seems to contradict eq. (4.19) in which the chemical potential appears to receive corrections below the critical temperature. However, the reported chemical potential is measured in units in which the radius of the horizon is 1 and a change in  $\mu$ , in these units, is due to a change in our scale as we lower the temperature.

At each given order of the parameter  $\xi$ , only a finite number of modes of the various fields are generated. At  $\mathcal{O}(\xi^2)$ , we have only 0 and  $2k$  Fourier modes,

$$\begin{aligned}
h_1(z, x) &= z^3 (h_{10}(z) + h_0^2(z)h_{11}(z) \cos 2kx) , \\
\alpha_1(z, x) &= \alpha_{10}(z) + z^3 h_0(z)\alpha_{11}(z) \cos 2kx , \\
\beta_1(z, x) &= \beta_{10}(z) + z^3 \beta_{11}(z) \cos 2kx , \\
A_{t1}(z, x) &= A_{t10}(z) + zh_0(z)A_{t11}(z) \cos 2kx , 
\end{aligned} \tag{2.28}$$

where we included explicit factors of  $z$  and  $h_0(z)$  for convenience. From (4.19), we obtain the boundary condition

$$A_{t10}(0) = \mu_1 . \tag{2.29}$$

Then from the Maxwell equation (4.8), and the boundary condition (2.29), we find

$$A_{t10}(z) = C(1 - z) + \frac{\mu_0}{4} \int_1^z dw \int_1^w dw' w'^{2\Delta-2} h_0(w') \mathcal{A}(w') , \tag{2.30}$$

where

$$\begin{aligned}
C &= \mu_1 + \frac{\mu_0}{4} \int_0^1 dz \int_1^z dw w^{2\Delta-2} h_0(w) \mathcal{A}(w) , \\
\mathcal{A}(z) &= \left[ q^2 \frac{\mu_0^2 (1-z)^2 z^3 + 4q^2 (1-z) h_0(z)}{h_0^2(z)} + z (\Delta^2 + 8k^2 \eta (1 + \Delta) z^2) \right] F^2(z) \\
&\quad + 2z^2 [\Delta + 4k^2 \eta z^2] F(z) F'(z) + z^3 [F'(z)]^2 . 
\end{aligned} \tag{2.31}$$

Thus the integration constant  $\mathcal{C}$  is expressed in terms of the chemical potential parameters  $\mu_0$  and  $\mu_1$ . While  $\mu_0$  is determined at the critical temperature,  $\mu_1$  still needs to be determined. Subsequently, we will determine  $\mathcal{C}$  using the scalar equation and use that value in eq. (2.30) to find  $\mu_1$ .

After some algebra, from the Einstein equations we deduce that the mode function  $\alpha_{10}(z)$  is given by

$$\alpha_{10}(z) = \frac{1}{2} \int_0^z dw w^{2\Delta-1} \left[ \left( q^2 \mu_0^2 \frac{(1-w)^2 w^2}{h_0^2(w)} + \Delta^2 \right) F^2(w) + 2\Delta w F(w) F'(w) + w^2 [F'(w)]^2 \right]. \quad (2.32)$$

Notice that the mode function  $\alpha_{10}$  contributes to  $\alpha_1$  at an order higher than  $\mathcal{O}(z^3)$  near the boundary for  $\Delta > \frac{3}{2}$ .

The mode function  $\beta_{10}(z)$  is given by

$$\beta_{10}(z) = \frac{k^2}{2} \int_0^z \frac{dw w^2}{h_0(w)} \int_w^1 dw' w'^{2\Delta-2} (1 - \eta \mu_0^2 w'^4) F^2(w'), \quad (2.33)$$

The mode function  $\beta_{10}$  also contributes at  $\mathcal{O}(z^3)$  near the boundary, because  $\beta_{10} \sim z^3$  at the boundary.

Finally, the mode function  $h_{10}(z)$  is given by

$$h_{10}(z) = -\frac{\mu_0[2C + \mu_0\alpha_{10}(1)]}{4} (1-z) - \frac{1}{4} \int_z^1 dw w^{2\Delta-4} \mathcal{H}(w), \quad (2.34)$$

where

$$\begin{aligned} \mathcal{H}(z) = & \left[ m^2 + \frac{q^2 \mu_0^2 z^2 (1-z)^2}{h_0(z)} + k^2 z^2 (1 + \eta z^4 \mu_0^2) + \Delta^2 h_0(z) \right] F^2(z) \\ & + 2z \Delta h_0(z) F(z) F'(z) + z^2 h_0(z) [F'(z)]^2 \\ & - z^{4-2\Delta} \mu_0^2 \int_1^z dw w^{2\Delta} F(w) \left[ \left( \frac{2q^2(1-w)}{w^2 h_0(w)} + 4\tau\eta(\Delta+1)w \right) F(w) + 4\tau\eta w^2 F'(w) \right]. \end{aligned} \quad (2.35)$$

The mode function  $h_{10}$  contributes at  $\mathcal{O}(z^3)$  to the metric (2.24) near the boundary because  $h_{10}(0)$  is finite, and we removed a factor of  $z^3$  in the definition (4.21). We fix one of the integration constants by setting  $h_{10}(1) = 0$ , so that the horizon remains at  $z = 1$ .  $C$  (eq. (2.31)) is the remaining integration constant to be determined.



The remaining first-order modes  $\alpha_{11}, \beta_{11}, h_{11}, A_{t11}$  are determined by a system of coupled linear ordinary differential equations,

$$\begin{aligned}
& \alpha'_{11} + \frac{zh'_0 + 3h_0 + 2k^2z^2}{zh_0} \alpha_{11} - \frac{4k^2z}{h_0} h_{11} - \frac{z^{2\Delta-4}}{2h_0} \mathcal{A}_1 = 0, \\
& \beta'_{11} - \frac{3}{2} z \mu_0 A'_{t11} - 4h_0 h'_{11} + 3 \frac{2k^2z^2 + h_0}{zh_0} \beta_{11} - \frac{\mu_0 (5h_0 + 3zh'_0)}{2h_0} A_{t11} \\
& + \frac{1}{4} (-8k^2z + 3\mu_0^2 z^3 + 2h'_0) \alpha_{11} + \frac{(10k^2z^2 - h_0 - 8zh'_0)}{z} h_{11} + \frac{z^{2\Delta-4}}{4h_0^2} \mathcal{A}_2 = 0, \\
& h'_{11} - \alpha'_{11} - \frac{\beta'_{11}}{h_0} + \left[ \frac{1}{z} + \frac{2h'_0}{h_0} \right] h_{11} + \frac{\mu_0 A_{t11}}{h_0} - \frac{3}{2} \left[ \frac{2}{z} + \frac{h'_0}{h_0} \right] \alpha_{11} - \frac{3\beta_{11}}{zh_0} + \frac{z^{2\Delta-4}}{2h_0} \mathcal{A}_3 = 0, \\
& A''_{t11} + 2 \left[ \frac{1}{z} + \frac{h'_0}{h_0} \right] A'_{t11} + \frac{2h'_0 + z(-4k^2 + h''_0)}{zh_0} A_{t11} - \frac{\mu_0}{2} z^2 \alpha'_{11} \\
& - \frac{\mu_0}{2} z^2 \left[ \frac{3}{z} + \frac{h'_0}{h_0} \right] \alpha_{11} - \frac{z^{2\Delta-3} \mu_0 F^2 [q^2(1-z) - 2\tau\eta z^3 h_0]}{h_0^2} = 0, \tag{2.36}
\end{aligned}$$

where

$$\begin{aligned}
\mathcal{A}_1(z) &= z^2 h_0^2 F'^2 + 2z \Delta h_0^2 F F' + [q^2(1-z)^2 \mu_0^2 + \Delta^2 h_0^2] F^2, \\
\mathcal{A}_2(z) &= 5z^2 h_0^2 F'^2 + 2z(5\Delta - 1) h_0^2 F F' \\
&+ [5q^2 \mu_0^2 (1-z)^2 z^2 + 3(m^2 - k^2 z^2 (1 + 2\eta z^4 \mu_0^2)) h_0 + \Delta(5\Delta - 2) h_0^2] F^2, \\
\mathcal{A}_3(z) &= F(\Delta F + z F'), \tag{2.37}
\end{aligned}$$

with  $F$  defined as in (2.21). The system of equations (2.36) can be seen to possess a unique solution by requiring finiteness of all functions in the entire domain  $z \in [0, 1]$ . Notice that the unknown parameter  $\mathcal{C}$  is absent, which is due to the fact that at first-order the 10 modes decouple from the 11 modes (see eq.(4.21) for the definition of the Fourier modes). However, explicit solutions can only be obtained numerically. A complete numerical analysis will be presented elsewhere.

To complete the determination of the first order modes, we need to calculate the integration constant  $C$  (or, equivalently, the chemical potential parameter  $\mu_1$  - see eq. (2.31)). To this end, we turn to the scalar wave equation. At zeroth order, the

chemical potential parameter  $\mu_0$  was obtained as an eigenvalue of the scalar wave equation. The first-order correction,  $\mu_1$ , is determined by the first-order equation of the scalar wave equation.

Considering (4.11) below the critical temperature, the scalar field at first order has two Fourier modes,

$$\phi_1(z, x) = \Phi_{10}(z) \cos kx + \Phi_{11}(z) \cos 3kx . \quad (2.38)$$

The first ( $\Phi_{10}$ ) mode satisfies the equation

$$\Phi_{10}'' + \left[ \frac{h_0'}{h_0} - \frac{2}{z} \right] \Phi_{10}' + \frac{\tau}{h_0} (1 - \eta \mu_0^2 z^4) \Phi_{10} - \frac{1}{h_0} \left[ \frac{m^2}{z^2} - q^2 \frac{A_{t0}}{h_0} \right] \Phi_{10} + z^{\Delta+1} \mathcal{B} + C z^{\Delta+2} \mathcal{C} = 0 , \quad (2.39)$$

where

$$\mathcal{B} = \mathcal{B}_2 F'' + \mathcal{B}_1 F' + \mathcal{B}_0 F , \quad \mathcal{C} = \mathcal{C}_2 F'' + \mathcal{C}_1 F' + \mathcal{C}_0 F , \quad (2.40)$$

and the coefficients  $\mathcal{B}_i$  and  $\mathcal{C}_i$  ( $i = 0, 1, 2$ ) are

$$\begin{aligned} \mathcal{B}_0 &= \frac{z \mu_0^2 [q^2(1-z)^2 + k^2 z^4 \eta h_0]}{h_0} \alpha_{10} - \frac{1}{2} \Delta h_0 \alpha'_{10} + \tau z (1 - \eta z^4 \mu_0^2) \beta_{10} \\ &+ \frac{z^2 [-q^2(1-z)^2 z^2 \mu_0^2 + \Delta^2 h_0^2]}{h_0^2} \mathbf{h} + z^3 \Delta \mathbf{h}' - \frac{2q^2(-1+z)z\mu_0}{h_0} \mathbf{A} \\ &- 2\tau \eta \mu_0 z^5 \mathbf{A}' + \frac{1}{4} z^2 (2q^2(1-z)^2 z^2 \mu_0^2 - 3\Delta h_0^2 - z h_0 (2k^2 z + \Delta h_0')) \alpha_{11} \\ &- \frac{1}{4} z^3 \Delta h_0^2 \alpha'_{11} - \frac{1}{2} \tau z^4 (1 - \eta z^4 \mu_0^2) \beta_{11} - z^2 \mu_0 (q^2(-1+z) + 2k^2 z^3 \eta h_0) A_{t11} \\ &+ \frac{1}{2} z^2 (-q^2(1-z)^2 z^2 \mu_0^2 + \Delta^2 h_0^2 + 2z \Delta h_0 h_0') h_{11} + \frac{1}{2} z^3 \Delta h_0^2 h'_{11} , \\ \mathcal{B}_1 &= z^3 (1 + 2\Delta) \mathbf{h} + z^4 \mathbf{h}' - \frac{1}{2} z h_0 \alpha'_{10} - \frac{1}{4} z^3 h_0 (3h_0 + z h_0') \alpha_{11} - \frac{1}{4} z^4 h_0^2 \alpha'_{11} \\ &+ \frac{1}{2} z^3 h_0 (h_0 + 2\Delta h_0 + 2z h_0') h_{11} + \frac{1}{2} z^4 h_0^2 h'_{11} , \\ \mathcal{B}_2 &= z^4 \mathbf{h} + \frac{1}{2} z^4 h_0^2 h_{11} , \end{aligned} \quad (2.41)$$

$$\begin{aligned}
\mathcal{C}_0 &= \frac{\mu_0}{2h_0^2} [q^2(1-z)^2 ((z-1)z^3\mu_0^2 + 4h_0) + z(-\Delta^2 + \Delta(\Delta+1)z + 4\tau\eta z^3) h_0^2] , \\
\mathcal{C}_1 &= \frac{\mu_0}{2} z^2 [-1 - 2\Delta + 2z(1 + \Delta)] , \\
\mathcal{C}_2 &= \frac{\mu_0}{2} (z-1)z^3 .
\end{aligned} \tag{2.42}$$

We defined (see eqs. (2.31) and (2.35))

$$\begin{aligned}
\mathbf{h}(z) &= -\frac{1}{4} \int_z^1 dw w^{2\Delta-4} \mathcal{H}(w) , \\
\mathbf{A}(z) &= \frac{\mu_0}{4} \int_1^z dw \int_1^w dw' w'^{2\Delta-2} h_0(w') \mathcal{A}(w') .
\end{aligned} \tag{2.43}$$

By using the zeroth order wave equation (2.16), we obtain

$$C = -\frac{\int_0^1 dz z^{2\Delta+1} F [\mathcal{B}_2 F'' + \mathcal{B}_1 F' + \mathcal{B}_0 F]}{\int_0^1 dz z^{2\Delta+2} F [\mathcal{C}_2 F'' + \mathcal{C}_1 F' + \mathcal{C}_0 F]} . \tag{2.44}$$

Having obtained the integration constant  $C$ , the remaining unknown parameter  $\mu_1$  is calculated using eq. (2.30).

The temperature of our system below the critical temperature  $T_c$  can be calculated using

$$\frac{T}{\mu} = -\frac{h'(1)e^{-\alpha(1)}}{4\pi\mu} . \tag{2.45}$$

We obtain

$$\frac{T}{T_c} = 1 - \xi^2 \left( \alpha_{10}(1) + \frac{\mu_1}{\mu_0} \right) - \frac{\xi^2}{3 - \frac{\mu_0^2}{4}} h'_{10}(1) , \tag{2.46}$$

where  $\xi$  is given by eq. (2.25).

Eq. (2.46) can be inverted to find the energy gap (2.25) as a function of temperature near the critical temperature,

$$\frac{\langle \mathcal{O}_\Delta \rangle^{1/\Delta}}{T_c} \approx \gamma \left( 1 - \frac{T}{T_c} \right)^{\frac{1}{2\Delta}} , \quad \gamma = \frac{4\pi}{3 - \frac{\mu_0^2}{4}} \left( \frac{\alpha_{10}(1)}{2} + \frac{\mu_1}{2\mu_0} + \frac{h'_{10}(1)}{2(3 - \frac{\mu_0^2}{4})} \right)^{-\frac{1}{2\Delta}} . \tag{2.47}$$

Thus, as the temperature of the system is lowered below the critical temperature  $T_c$  the condensate is spontaneously generated. The dependence of the condensate on the temperature is of the same form as in conventional holographic superconductors.

Finally, the charge density of the system is determined by using

$$\frac{\rho}{\mu^2} = -\frac{\partial_z A_t(0, x)}{[A_t(0, x)]^2} = \frac{\rho_0 + \xi^2 \rho_1(x)}{\mu_0^2}, \quad (2.48)$$

where  $\rho_0 = \mu_0$  is the charge density at or above the critical temperature, and

$$\rho_1(x) = -2\mu_1 - A'_{t10}(0) - A_{t11}(0) \cos 2kx, \quad (2.49)$$

from eq. (A.10). This is an important result showing the generation of a spatially inhomogeneous charge density below the critical temperature in the presence of a *spatially homogeneous* (constant) chemical potential. This is the case provided  $A_{t11}(0) \neq 0$ , which is guaranteed analytically from the system of equations (2.36) for the 11 modes. Indeed, from the last equation in (2.36), we obtain  $A'_{t11}(0) = 0$ . Moreover, there is a boundary condition at the horizon  $z = 1$  where we demand finiteness of  $A_{t11}$  ( $A_{t11}(1) < \infty$ ). If additionally  $A_{t11}(0) = 0$ , then the second-order differential equation is overdetermined and has no solution. Thus, a general solution has  $A_{t11}(0) \neq 0$ .

## 2.5 Conclusions

We have discussed a holographic model in which the gravity sector consists of a  $U(1)$  gauge field and a scalar field coupled to an AdS charged black hole under a *constant* chemical potential. We introduced higher-derivative interaction terms between the  $U(1)$  gauge field and the scalar field. A gravitational lattice was generated spontaneously by a spatially dependent profile of the scalar field. The transition temperature was calculated as a function of the wavenumber. The critical

temperature was determined as the maximum transition temperature. This occurred at finite non-vanishing wavenumber, showing that the inhomogeneous solution was dominant over a range of the parameters of the system which we discussed.

The system was then studied below the critical temperature. We obtained analytic expressions for the various fields using perturbation theory in the (small) order parameter. It was found that a spatial inhomogeneous phase is generated at the boundary. In particular, we showed analytically that a spatially inhomogeneous charge density is spontaneously generated in the system while it is held at constant chemical potential.

It will be illuminating to compare features between different mechanisms for generating spontaneous translation symmetry breaking seen with the Einstein tensor-scalar coupling [64], Chern-Simons interaction [66, 67], and dilaton [50]. Additionally, this work only considered a uni-directional lattice. It would be interesting to extend our discussion to a more general two-dimensional lattice and determine which configuration is energetically favorable. Finally, one would like to understand the origin of the higher-derivative couplings we introduced in terms of quantum corrections within string theory. Work in these directions is in progress.

# Chapter 3

## Duality between zeroes and poles in holographic systems with massless fermions and a dipole coupling

### 3.1 Introduction

The AdS/CFT correspondence is a principle that connects a strongly coupled  $d$ -dimensional conformal field theory with a weakly coupled  $(d+1)$ -dimensional gravity theory [3]. This principle, also known as the gauge/gravity duality, is well-founded in string theory, and has been applied to many field theories having gravity duals with the most noticeable application in condensed matter physics. One of the earliest applications of the gauge/gravity duality to condensed matter systems was the holographic description of a superconductor [69]. It is described by an Einstein-Maxwell-scalar field theory in which the breaking of a gauge symmetry in the gravity sector corresponds, in the boundary theory, to an operator (the order parameter) which condenses below a critical temperature signaling the onset of superconductivity.

The gauge/gravity duality has also been used as a framework for Fermi liquid behavior [70], non-linear hydrodynamics [71], quantum phase transitions [72] and

transport [73]. Thus, classical gravity theories have been transformed into a laboratory for exploring condensed matter physics from a different point of view [74]. In this way the holographic principle is a powerful tool for studying strongly-correlated systems.

Recently, there has been considerable activity using the holographic principle to describe metallic states of matter outside of Landau's Fermi liquid theory [75, 76]. Experiments provide evidence for the existence of materials whose electronic structure cannot be described by Fermi liquid theory, nor by any other known effective theory. While Fermi liquids are characterized by stable quasi-particles, these exotic materials possess well-defined Fermi surfaces but lack long-lived quasi-particles. A quantitative discussion of signatures of different excitations is presented in detail below. To describe such metallic systems, one needs to introduce charged fermions in the gravity sector of the holographic system. However, in general, fermions cannot be treated classically as in the case of charged scalar fields of holographic superfluids or superconductors. The coupled system of Einstein-Maxwell-Dirac field equations become tractable only in the limit in which the fermions may be treated locally in the bulk as a charged ideal fluid of zero temperature. The solutions of these systems are known as an electron star [77, 78, 79], Dirac hair [80] or confined Fermi liquid [81].

In another approach to describe the various phases of a metallic state at low temperatures, a dipole coupling for massless charged fermions is introduced [82, 83]. The modified Dirac equation in the background of an AdS-Reissner-Nordström black hole produces a boundary fermionic spectrum with vanishing spectral weight for a range of energies around  $\omega = 0$  without the breaking of any symmetry. As the dipole coupling strength is varied, the fluid has Fermi, marginal Fermi, non-Fermi liquid phases and also an additional insulating phase. The insulating phase possesses the characteristics representative of Mott insulators, namely the dynamic formation of a gap and spectral weight transfer. Similar behavior was found in other constructions [84, 85, 86, 87, 88]. The dependence of the Fermi surface and selection of (non-) Fermi liquid type are discussed in [89].

For a Fermi liquid, the characteristic signature of a quasi-particle is a pole in the retarded Green Function  $G_R$ . The location of the pole

$$G_R^{-1}(\omega = 0, k = k_F) = 0 , \quad (3.1)$$

in momentum space at zero frequency dictates the Fermi surface and dispersion. Additionally, the real component of the Green function,  $\Re G_R$ , must change signs. In a normal, weakly-coupled metal, this is only possible through the pole, and via Luttinger's theorem, integrating over the positive region of  $G_R$  one obtains the particle density [90].

Apart from Fermi liquids, one of the principal examples of a strongly correlated condensed matter system is the Mott insulator, parent state of high-temperature copper-oxide superconductors in which a gap is dynamically generated. An explanation for the insulating nature [91] is that a Mott gap manifests as a surface of zeroes in the Green function. The Green function of interest,  $G_R$ , may be expressed in terms of the non-interacting theory Green function,  $G_0$ , and the self-energy  $\Sigma$ ,

$$G_R^{-1}(\omega, k) = G_0^{-1}(\omega, k) + \Sigma(\omega, k) , \quad (3.2)$$

of which a zero is indicative of a divergent self-energy. It is the divergent self-energy that restricts the band from crossing the Fermi energy leading to Motttness. The full condition for Motttness is specifically on the eigenvalues of the matrix  $G_R$  and represented with the determinant as,

$$\det G_R(\omega = 0, k = k_L) = 0 . \quad (3.3)$$

For our purposes, we are interested in the spinor space but the statement may be extended to multiple bands [92]. A mean-field theory approach such as conventional BCS theory as calculated with the Nambu propagator, is unable to produce such a



result. The location of poles and zeroes in  $G_R$  provides a path to uncover a system's behavior.

The interplay between poles and zeros is a characteristic feature of QCD. The renormalization from high (UV) to low (IR) energy of couplings and masses in QCD involves free quarks at UV scales, which exhibit poles in the propagator, while at IR scales the poles are converted to zeros [93] signaling the formation of bound states. The zero of the single quark propagator in the IR is due to an orthogonal configuration between the (UV) single quark description and the composite mesons in the IR.

In condensed matter physics the competition of poles ( $k = k_F$ ) and zeroes ( $k = k_L$ ) in the Green function provides an illuminating criterion for characterizing the different phases found in strongly-coupled fermion systems [92]. Exploring the Hubbard model in this context has led to a variety of features present in doped Mott insulators, including spectral weight transfer, Fermi arcs found in the pseudo-gap state, and Fermi pockets [91, 94]. The Fermi arcs may be seen as a general consequence of a composite state of UV fields, and hence zeroes, existing at low energies within the Hubbard model [95]. In [96], a “pole-zero mechanism” for the two-dimensional Hubbard model was used to characterize the transition from metal to Mott insulator in terms of interfering pole and zero surfaces. The formalism is comprehensive enough to accommodate arcs, hole pockets, in-gap states, Lifshitz transitions and non-Fermi liquids. The work was furthered in [97] to address several anomalies in connection to (non) d-wave symmetries seen in the pseudo-gap and to suggest a topological quantum phase transition responsible for a non-Fermi liquid phase.

A holographic description of the structure of poles and zeros and their interconnection addresses central issues in strongly-coupled fermionic systems. A Fermi surface in the Green function for holographic fermions was discovered in [98, 75] with the discussion further expanded in [76, 70]. Near the Fermi surface, the structure of the poles is expanded similarly to eq. (3.2) as

$$G_R^{-1}(\omega, k) \sim k - k_F - \omega/v_F - \Sigma(\omega, k) \tag{3.4}$$

with self-energy  $\Sigma(\omega, k)$  [99] given as

$$\Sigma(\omega, k) \sim c\omega^{2\nu_k^\pm} \quad , \quad 6\nu_k^2 = k^2 - \frac{q^2}{2} \quad , \quad (3.5)$$

with fermion charge  $q$  and numerically calculated constant  $c$ . It is this scaling dimension  $\nu_k$  that selects the leading term in (3.4) dictating the dispersion relation at the Fermi surface, and hence the type of fluid. For scaling dimension  $\nu_k < 1/2$ , the pole of  $G_R$  corresponds to an unstable quasi-particle. This is identified as a non-Fermi fluid. With the value  $\nu_k = 1/2$ , the excitations are of marginal Fermi fluid type. For  $\nu_k > 1/2$  the dispersion relation is linear. This is the Fermi (non-Landau) fluid. Lastly, imaginary  $\nu_k$  corresponds to “log oscillatory” solutions.

Since the discovery of Fermi surfaces within the strongly coupled field theories analyzed via holography, an exploration of fermions has taken place. Mechanisms underlying different p-wave [100] and d-wave [101] symmetries for spectral functions have been offered. An effective lattice was added in [102] by using a modulated chemical potential. The spatial dependence alters the energy scaling and offers identifying signs for a holographic realization of a pseudo-gap state.

More fundamental (top-down) holographic theories from truncations of string/M-theory have produced viable models describing superfluidity and superconductivity [103, 104, 105, 106, 107]. In higher dimensions, fermions are typically coupled to gravity and gauge fields with high-order derivatives. There are consistent truncations to lower dimensions in the fermionic sector giving interesting fermionic couplings [108, 109]. Dipole (Pauli) couplings are found to be a common feature of the theories with the coupling constant realized as scalar-dependent [110]. It would be interesting to explore their effect on fermion spectral functions at the boundary.

In this work, we aim at studying the zeroes and poles of the Green function  $G_R$  in a holographic system with a gravity sector consisting of an AdS-Reissner-Nordström black hole and a dipole coupling of massless charged fermions to an electromagnetic field. By exploring a duality between the zeroes and poles of this holographic system

we show that by varying the dipole coupling strength,  $G_R$  may possess only poles, only zeroes, or both poles and zeroes.

This behavior suggests that the dipole coupling strength plays the role of an order parameter in the Mott physics. By studying a simple model in which a fermion is coupled to a gauge field through a dipole interaction in the bulk, we find that on the field theory side as the strength of this interaction is varied, a new band in the density of states emerges and spectral density is transferred between bands. In the language of Green functions only poles is the signature of the Fermi and non-Fermi liquids, only zeroes corresponds to the Mott insulating phase, and the coexistence of both poles and zeroes is the pseudo-gap phase.

This duality between zeroes and poles also suggests that within the holographic system, the properties of the Green function  $G_R$  signifying the Mott phase can be inferred by mapping to the well understood Green function of a Fermi liquid by simply changing the sign of the dipole coupling constant  $p \rightarrow -p$ .

The discussion is organized as follows. In Section (3.2) we set up the theory and derive the Einstein-Maxwell-Dirac equations. In Section (3.3) we solve the Dirac equation. In Section (3.4) we discuss the duality of poles and zeros, and finally, Section (3.5) contains our conclusions.

## 3.2 Gravitational Bulk

The bulk dynamics in an asymptotically Anti-de Sitter (AdS) space is described by the Einstein-Maxwell action with cosmological constant  $\Lambda = -3/L^2$ ,

$$S = \int d^4x \sqrt{-g} \left[ \frac{R + 6/L^2}{16\pi G} - \frac{1}{4} F_{MN} F^{MN} \right], \quad (3.6)$$

where  $F_{MN} = \partial_M A_N - \partial_N A_M$  is the field strength of the  $U(1)$  vector potential  $A_M$ . For convenience, we set  $L = 4\pi G = 1$ .

The Einstein-Maxwell equations admit a charged four-dimensional AdS black hole solution,

$$ds^2 = \frac{1}{z^2} \left[ -h(z)dt^2 + \frac{dz^2}{h(z)} + dx^2 + dy^2 \right] . \quad (3.7)$$

The metric function is given by

$$h(z) = 1 - (1 + \mu^2) z^3 + \mu^2 z^4 , \quad (3.8)$$

with the horizon radius set at  $z = 1$ , and the  $U(1)$  potential is

$$A_t = \mu(1 - z) , \quad A_z = A_x = A_y = 0 , \quad (3.9)$$

corresponding to a non-vanishing electric field in the radial  $z$  direction,

$$F_{tz} = -F_{zt} = \mu . \quad (3.10)$$

The Hawking temperature is given by

$$T = -\frac{h'(1)}{4\pi} = \frac{3 - \mu^2}{4\pi} , \quad (3.11)$$

with  $\mu^2 = 3$  providing the zero temperature limit. There is a scaling symmetry of the solutions found as

$$z \rightarrow \lambda z , \quad x \rightarrow \lambda x , \quad \mu \rightarrow \mu/\lambda , \quad T \rightarrow T/\lambda , \quad (3.12)$$

and we should only report on scale-invariant quantities, such as  $T/\mu$ , etc.

In this gravitational background we add a massless fermion with charge  $q$  and we include a dipole coupling to the  $U(1)$  field [82, 83]. The action is

$$S_{\text{fermion}} = i \int d^4x \sqrt{-g} \bar{\Psi} [\not{D} - p \Sigma^{MN} F_{MN}] \Psi . \quad (3.13)$$

The various terms in the action are

$$\begin{aligned}
\mathcal{D} &= e_a^M \Gamma^a (\partial_M + \Omega_M - iqA_M) , \\
\Omega_M &= \frac{1}{8} \omega_{abM} [\Gamma^a, \Gamma^b] , \\
\omega_{abM} &= \eta_{ac} \omega_{bM}^c , \\
\omega_{bI}^a &= e_M^a \partial_I e_b^M + e_M^a e_b^N \Gamma_{NI}^M , \\
\Sigma^{MN} &= \frac{i}{4} [\Gamma^a, \Gamma^b] e_a^M e_b^N , 
\end{aligned} \tag{3.14}$$

with spin connection  $\omega_{abM}$  and vierbein  $e_a^M$ , and lower-case indices  $a, b$  belong to the tangent space.

In the conventional case,  $p = 0$ , the system is of two non-interacting Weyl fermions of opposite chiralities. With  $p \neq 0$ , the dipole term introduces an interaction between the two Weyl fermions. The system corresponds to an order parameter in the dual gauge theory of conformal dimension  $\Delta = \frac{3}{2}$ .

To analyze the Dirac equations of the bulk fermion we find it more convenient to go to momentum space by Fourier transforming

$$\Psi = e^{-i\omega t - ikx} \sqrt{\frac{z^3}{h}} \begin{pmatrix} \psi_- \\ \psi_+ \end{pmatrix} , \quad \psi_{\pm} = \begin{pmatrix} \psi_{\pm 1} \\ \psi_{\pm 2} \end{pmatrix} , \tag{3.15}$$

and choosing a basis for the  $\Gamma$  matrices

$$\begin{aligned}
\Gamma^1 &= \begin{pmatrix} i\sigma_1 & 0 \\ 0 & i\sigma_1 \end{pmatrix} , & \Gamma^2 &= \begin{pmatrix} -\sigma_2 & 0 \\ 0 & -\sigma_2 \end{pmatrix} , \\
\Gamma^3 &= \begin{pmatrix} 0 & -i\sigma_2 \\ i\sigma_2 & 0 \end{pmatrix} , & \Gamma^4 &= \begin{pmatrix} -\sigma_3 & 0 \\ 0 & -\sigma_3 \end{pmatrix} .
\end{aligned} \tag{3.16}$$

The Dirac equation decomposes into decoupled equations

$$\begin{aligned}\pm h\psi'_{-,12} + \left(\mu q(1-z) + \omega \pm k\sqrt{h} \mp p\mu\sqrt{h}\right)\psi_{-,21} &= 0, \\ \pm h\psi'_{+,12} + \left(\mu q(1-z) + \omega \mp k\sqrt{h} \mp p\mu\sqrt{h}\right)\psi_{+,21} &= 0.\end{aligned}$$

The presence of the dipole coupling  $p$  modifies the Dirac equation. The effects of the coupling will be seen more clearly in the solutions of the Dirac equations.

### 3.3 Solutions of the Dirac Equations

To solve the Dirac equations we choose in-going boundary conditions at the horizon,

$$\psi_{\pm,12} = (1-z)^{-i\omega/(4\pi T)} \mathcal{F}_{\pm,12}. \quad (3.17)$$

The ratios

$$\xi_{\pm} = \frac{\mathcal{F}_{\pm 1}}{\mathcal{F}_{\pm 2}}, \quad (3.18)$$

satisfy the non-linear flow equations [76]

$$h\xi'_{\pm} + \left[\omega + \mu q(1-z) + \sqrt{h}(\pm k + \mu pz)\right]\xi_{\pm}^2 + \omega + \mu q(1-z) + \sqrt{h}(\mp k - \mu pz) = 0, \quad (3.19)$$

together with the in-going boundary conditions,

$$\xi_{\pm} = \begin{cases} i & , \quad \omega \neq 0, \\ i\sqrt{\frac{q/\sqrt{2} + \sqrt{3}p \pm k}{q/\sqrt{2} - \sqrt{3}p \mp k}} & , \quad \omega = 0. \end{cases} \quad (3.20)$$

The solution to the flow equations determines the retarded Green function as

$$G_R(\omega, k) = \begin{pmatrix} G_+ & 0 \\ 0 & G_- \end{pmatrix}, \quad G_{\pm}(\omega, k) = \xi_{\pm}|_{z \rightarrow 0}. \quad (3.21)$$

From the symmetries of the Dirac equation (3.15), we deduce the relation between the Green functions

$$G_{\pm}(\omega, k) = G_{\mp}(\omega, -k) . \quad (3.22)$$

The Fermi momentum is found as the pole

$$G_{\pm}^{-1}(\omega = 0, k = k_F) = 0 . \quad (3.23)$$

Since both solutions  $\psi_{\pm}$  are normalizable, there is an alternative quantization in which  $G_+$  and  $G_-$  are interchanged.\* This leads to physically equivalent results.

To identify the type of (non-) Fermi fluid, we look at the near-horizon region,  $z \rightarrow 1$ . Employing the limiting procedure [76], we obtain the scaling dimension  $\nu_k^{\pm}$  given by

$$6 (\nu_k^{\pm})^2 = \left( \sqrt{3}p \pm k \right)^2 - \frac{q^2}{2} , \quad (3.24)$$

to be compared with (3.5). The self energy  $\Sigma(\omega, k)$  at the Fermi surface remains

$$\Sigma(\omega, k) \sim c\omega^{2\nu_k} . \quad (3.25)$$

For our system with fixed fermion charge and mass,  $\nu_k$  and the fluid character is determined by the strength of the dipole interaction  $p$ .

To study explicit solutions, we set the fermion charge to  $q = 1$ , and numerically solve the flow equation (3.19) to determine where the system possesses a Fermi surface and the type of excitations. Figure 3.1 displays our results for  $\nu_k^{\pm}$  evaluated at the Fermi momentum  $k_F$ . We recover the results of [82, 83] and classify the excitations as Fermi liquid ( $p \lesssim -.53$ ), marginal Fermi liquid ( $p \sim -.53$ ), non-Fermi liquid ( $-.53 \lesssim p \lesssim .41$ ) and log-oscillatory ( $p \gtrsim .41$ ). The system has a Fermi surface with  $p \lesssim .41$  but no Fermi surface for larger values of  $p$ .

---

\*Since the appearance of this work, the duality between poles and zeroes has subsequently been shown as a consequence of the two possible quantizations [111].

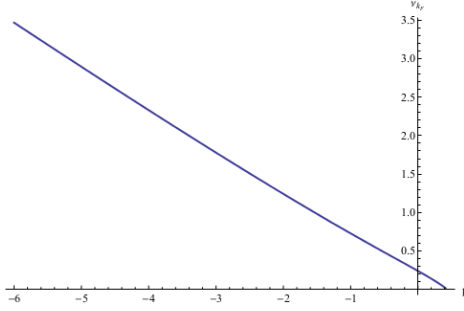


**Figure 3.1:** Scaling dimension  $\nu_{k_F}$  vs.  $p$  for  $q = 1$ .

### 3.4 Duality of poles and zeroes

Using the properties of the solutions (3.21) of the flow equation (3.19) we will show that there is a duality between poles and zeroes. We first emphasize that a pole of  $G_{\pm}$  at  $\omega = 0$  (eq. (3.23)) is not necessarily a pole of the determinant

$$\det G_R = G_+ G_- . \quad (3.26)$$

It is known [99] that in the conventional case,  $p = 0$ ,

$$\det G_R(\omega = 0, k; p = 0) = 1 , \quad (3.27)$$

therefore it possesses neither poles nor zeroes. This is because poles (zeroes) of  $G_+$  are cancelled by zeroes (poles) of  $G_-$  at the same momentum. We shall see that this coincidence of poles and zeroes is lifted when the dipole coupling is turned on, resulting in poles and zeroes of  $\det G_R$ .

It is easily deduced from the flow equation (3.19), that the reciprocal of  $\xi_{\pm}$ ,

$$\zeta_{\pm} = \frac{1}{\xi_{\pm}} , \quad (3.28)$$



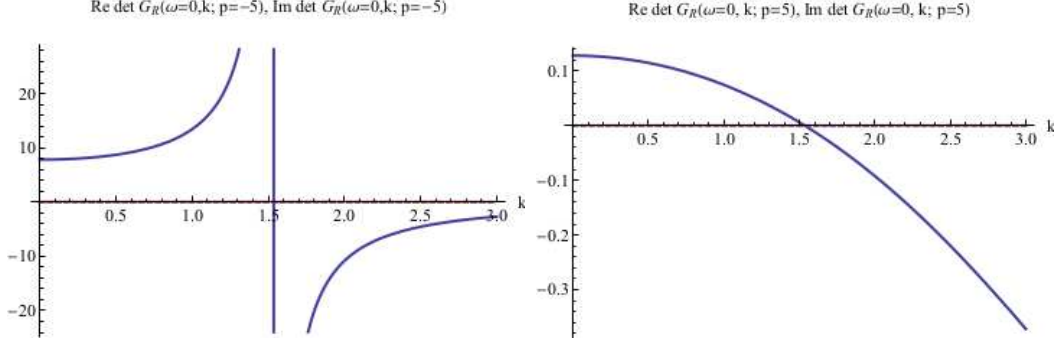


**Figure 3.2:** Plots of  $\Re \det G_R$  ( $\Im \det G_R = 0$ ) with  $q = 1$  for  $p = -5$  (first panel) showing a pole at  $k = k_F \approx 1.5$ , and  $p = 5$  (second panel) showing a zero at  $k = k_L \approx 1.5$ .

satisfies the flow equation

$$h\zeta'_\pm + \left[ -\omega - \mu q(1 - z) + \sqrt{h}(\pm k + \mu p z) \right] \zeta_\pm^2 - \mu q(1 - z) + \sqrt{h}(\mp k - \mu p z) - \omega = 0. \quad (3.29)$$

Upon comparison of the two flow equations, we see that  $\zeta_\pm$  solves the same equation as  $-\xi_\pm$  under the change of parameters  $k \rightarrow -k$  and  $p \rightarrow -p$ . It follows that the inverse Green function  $G_\pm^{-1}(0, k)$  at  $p$  is identified with  $-G_\pm(0, -k)$  at opposite dipole coupling  $-p$ . Using the relation between the two Green functions (3.22), we arrive at

$$\det G_R(\omega = 0, k; p) = \frac{1}{\det G_R(\omega = 0, k; -p)}. \quad (3.30)$$

This is the central result of our work and its importance relies on the fact that it establishes a relation between poles and zeroes of the determinant of the Green function at zero frequency between systems of opposite dipole coupling. For  $p = 0$ , we recover eq. (3.27). For  $p \neq 0$ , the poles found for  $p < 0$  (Fermi liquid) correspond to zeroes for  $p > 0$  (Mott insulator).

For large negative dipole coupling strength, i.e.,  $p \lesssim -53$ , we are in the Fermi liquid phase, since  $\nu_k > 1/2$  (figure 3.1). In this regime, we obtain poles of  $\det G_R$  and no zeroes. A typical example is shown in figure 3.2 (first panel) for  $p = -5$ . In this case,  $\Im \det G_R$  vanishes and the graph has two poles at  $k = k_F \approx \pm 1.5$ , and no

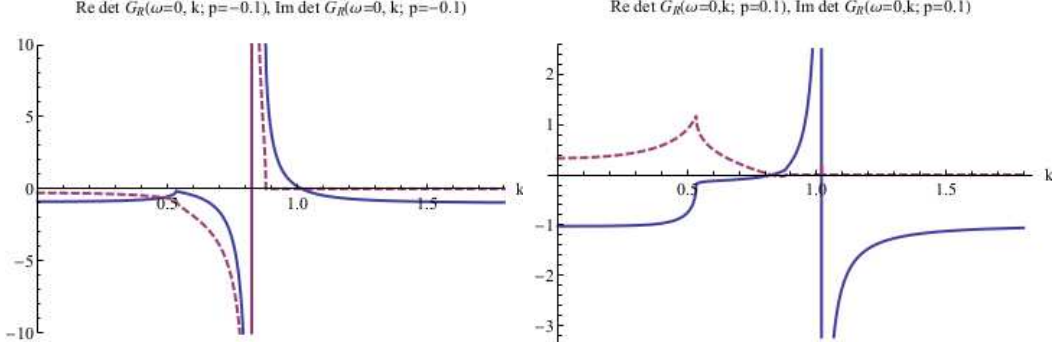


**Figure 3.3:** Plots of  $\Re \det G_R$  (solid lines) and  $\Im \det G_R$  (dashed lines) with  $q = 1$  for  $p = -0.1$  (first panel) showing a pole at  $k = k_F \approx 0.8$  and a zero at  $k = k_L \approx 1.0$ , and  $p = 0.1$  (second panel) showing a pole at  $k = k_F \approx 1.0$  and a zero at  $k = k_L \approx 0.8$ .

zeroes. According to the duality (3.30), we expect to see two zeroes at  $k = k_L \approx \pm 1.5$  and no poles for a system with  $p = 5$ . This is indeed what we obtain by a numerical calculation of  $\det G_R$  (second panel of figure 3.2). This is in the Mott insulator regime and no Fermi surface is found.

For small values of the dipole coupling strength ( $|p| \lesssim .41$ ), we expect both zeroes and poles. Again, using the duality (3.30), the zeroes can be deduced from the poles at opposite  $p$  (and vice versa). An example is shown in figure 3.3 for  $p = \pm 1$ . Unlike in the case of large  $p$ ,  $\Im \det G_R$  does not vanish. Instead, the zeroes for  $p = .1$  found at  $k = k_L \approx \pm .8$  are isolated zeroes of both  $\Re \det G_R$  and  $\Im \det G_R$ . Correspondingly, the same is true for the poles at  $k = k_F \approx \pm .8$  for  $p = -.1$ . At the other set of zeroes at  $k = k_L \approx \pm 1.0$  for  $p = -.1$  (and correspondingly poles at  $k = k_F \approx \pm 1.0$  for  $p = .1$ ),  $\Im \det G_R$  vanishes over a range containing the zeroes (poles).

Finally, figure 3.4 shows the location of poles ( $k = k_F$ ) and zeroes ( $k = k_L$ ) as the dipole coupling strength  $p$  varies. Notice the symmetry under  $k \rightarrow -k$ , as well as the interchange  $k_L \leftrightarrow k_F$  under the mapping  $p \rightarrow -p$ .

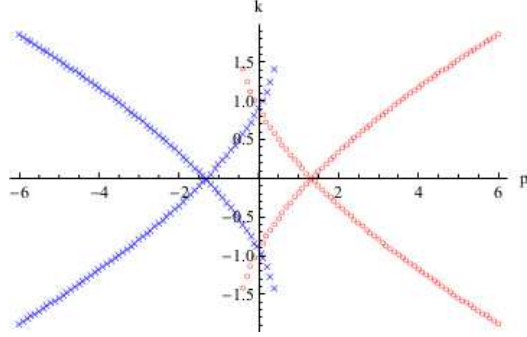


**Figure 3.4:** Poles at  $k = k_F$  (blue lines) and zeroes at  $k = k_L$  (red lines) *vs.*  $p$  with  $q = 1$ . Notice the symmetry under  $k \rightarrow -k$ , and the duality of poles and zeroes under  $p \rightarrow -p$ .

### 3.5 Conclusions and discussion

We have shown that a holographic theory with a bulk dipole interaction between a massless fermion and gauge field possesses a robust phase diagram including Fermi and non-Fermi liquids, insulating Mott state and pseudo-gap state. The various phases are identified by the structure of the poles and zeroes found in  $G_R$ . The selection of the phase is controlled by the strength of the dipole coupling which plays the role of an order parameter in the holographic system [82, 83].

A pole of  $G_R$  is indicative of a Fermi or non-Fermi fluid while a zero is responsible for an insulating phase. It is the coexistence of both that underlies the identification of a holographic pseudo-gap state. We showed that a duality exists relating systems of opposite dipole coupling strength  $p$ . This duality maps zeroes to poles and vice versa, pointing to the interesting possibility of understanding the properties of a system with zeroes (insulating phase) by mapping the system to one with poles (Fermi liquid).

It will be interesting to explore further the pseudo-gap state and other aspects that may be recovered by the evolution of the Fermi and Luttinger surfaces. Of particular significance will be the response of the system with  $\vec{k}$  dependence. Also, it might be worth exploring further the physical significance of the behavior of  $\Im \det G_R$  near zeroes and poles.

As we discussed in the introduction, the interplay between the state of matter and the appearance of poles and zeroes is also observed in QCD. The difference with QCD is that the appearance of free quarks or bound states depends on the dynamics of the strong gauge theory while in our case there is a variation of a simple coupling that gives the various phases of matter. It would be intriguing to find other dynamical systems exhibiting this behavior.

One may wonder if this analysis can be applied to holographic superconductors. In BCS superconductivity the role of the order parameter is played by the condensate of a scalar field. The formation of a condensate corresponds to a critical temperature below which the system enters the superconductivity phase. In this phase, the electrons are combined to form Cooper pairs which are electronic bound states and therefore correspond to zeroes. On the contrary, the electrons in the normal phase are free corresponding to poles.

In spite of the similarities with superconductivity, our analysis does not explicitly break a gauge symmetry that could have defined an order parameter for the various phases. Instead the metallic phases are controlled by an explicit coupling of charged fermions to a gauge field. Nevertheless, it will be enlightening to consider how a bulk scalar responsible for superconductivity or the coupling will influence the system. Also worth exploring is if a description with additional fields could explain the Green function zeroes in terms of a composite excitation.

Another way to better understand our results is to calculate the holographic entanglement entropy in our theory. The entanglement entropy [112, 113] has proven to be a powerful tool in counting the degrees of freedom available in a holographic system. In [114] it was found that the holographic entanglement entropy of a superconducting phase is less than that of the normal phase due to the formation of Cooper pairs reducing the degrees of freedom available (see also [115]). Near the contact interface, the normal phase entanglement entropy possesses a higher value compared to the superconducting phase due to the proximity effect: the leakage of Cooper pairs to the normal phase so more free electrons were available. Similarly we

expect that the entanglement entropy in a holographic fermionic system with a dipole coupling will vary, as the degrees of freedom change from the Fermi liquid phase to the Mott insulating phase providing important information on the various phases of the system. However, such a study has to overcome the basic difficulty of working with a probe fermionic system. The boundary theory will see the effect of the dipole coupling only with a fully back-reacted solution. Once a full solution is obtained the dipole coupling could leave some trace on the metric. Work in this direction is in progress.

# Chapter 4

## Holographic Fermions with Spontaneously Generated Inhomogeneous Phases

### 4.1 Introduction

The study of the Cu-O high-temperature superconductors shows that in the normal state the electrical resistivity, the thermal conductivity and the optical conductivity are anomalous. An explanation of this behaviour was put forward in [116]. In these high-temperature superconductors over a wide range of momentum, there exist excitations which make a contribution to both the charge and spin polarizability. Calculating the retarded one-particle self-energy due to exchange of these charge and spin fluctuations they found a quite different behaviour from the one-particle self-energy in a conventional Fermi liquid. This behaviour was referred in [116] as representing a marginal Fermi liquid. Calculating the spectral function  $A(k, \omega)$  they found that it has some distinct features from the Fermi liquid case. It is much broader (a normal Fermi liquid, for example, has a  $\delta$ -function peak when  $\epsilon_k = 0$ , and carries substantially more weight in the wings because of the  $\omega^{-1}$  tail).

The formation of marginal Fermi liquid in the normal phase of the superconductor implies that the formed quasiparticles are unstable. A way to stabilize the quasiparticles of the marginal Fermi liquid was proposed in [119]. It was shown that with a suitable coupling between the fermion and the condensate which is formed in the superconducting phase below a critical temperature  $T_c$ , there are stable quasiparticles with a gap.

In this work we will propose another way to stabilize the quasiparticles. We will show that without having a direct coupling of a fermion field to a scalar field that it condenses below  $T_c$ , a Fermi surface is formed with a gap below  $T_c$  because of lattice effects. To simulate the lattice effects we introduce a spontaneously generated inhomogeneity and we analyze the behaviour of a fermionic system at the boundary. The inhomogeneity is introduced by a higher order derivative coupling between electromagnetic term and the scalar field [12]. The band gap behaviour of the fermions is analyzed due to this backreacted geometry in the bulk by using the Green's function behaviour of the Dirac field.

This work is organized as follows. In Section 4.2 we study the numerical and analytical solutions of a holographic system with a spontaneously generated inhomogeneous phases introduced by higher derivative couplings by using perturbation theory. In Section 4.3 we introduce Dirac field into this holographic model which includes holographic lattice structure in one dimension to analyze the holographic lattice effects on Fermi surface by studying the spectral function of the system. To this end, we solve the Dirac equations in periodic background both numerically and analytically at each perturbation order at small but finite temperature in Section 4.4. The numerical results of the spectral function at zeroth and second order of perturbation where the band gap is observable are given in Sections 4.4.3 and 4.4.5 respectively. Finally, in Section 4.5 we discuss the results of the study and present and outlook for future studies.

## 4.2 The Holographic Setup

The holographic system includes a  $U(1)$  gauge field  $A_\mu$ , with field strength  $F_{\mu\nu} = \partial_\mu A_\nu - \partial_\nu A_\mu$ , and a scalar field  $\phi$  with charge  $q$  under  $U(1)$  group of the gauge field. In addition a Dirac field with mass  $m_f$  and charge  $q_f$  is added to the system. The  $AdS$  spacetime geometry of the bulk where these fields live has negative cosmological constant of  $\Lambda = -6/L^2$ .

We consider the following action

$$S = \int d^4x \sqrt{-g} \mathcal{L} , \quad \mathcal{L} = \frac{R + 6/L^2}{16\pi G} - \frac{1}{4} F_{\mu\nu} F^{\mu\nu} - (D_\mu \phi)^* D^\mu \phi - m^2 |\phi|^2 , \quad (4.1)$$

with  $D_\mu \phi = \partial_\mu \phi - iqA_\mu \phi$ . In the rest of this paper, we shall set  $16\pi G = L = 1$  for simplicity and without loss of generality.

Following [12] introducing a higher derivative term leads to spatial inhomogeneity in the boundary theory. A general form of higher-derivative interaction term is

$$\mathcal{L}_{\text{int}} = \phi^* [\eta \mathcal{G}^{\mu\nu} D_\mu D_\nu + \eta' \mathcal{H}^{\mu\nu\rho\sigma} D_\mu D_\nu D_\rho D_\sigma + \dots] \phi + \text{c.c.} \quad (4.2)$$

In [12] to produce the ‘holographic lattice’ structure at the boundary, a special choice of the interaction term was made

$$\mathcal{L}_{\text{int}} = \eta \mathcal{G}^{\mu\nu} (D_\mu \phi)^* D_\nu \phi - \eta' |D_\mu \mathcal{G}^{\mu\nu} D_\nu \phi|^2 , \quad (4.3)$$

where

$$\mathcal{G}_{\mu\nu} = T_{\mu\nu}^{(\text{EM})} + g_{\mu\nu} \mathcal{L}^{(\text{EM})} = F_{\mu\rho} F_\nu{}^\rho - \frac{1}{2} g_{\mu\nu} F^{\rho\sigma} F_{\rho\sigma} . \quad (4.4)$$

The action (4.1) with the interaction term 4.3 is added gives the Einstein equations

$$R_{\mu\nu} - \frac{1}{2} R g_{\mu\nu} - 3g_{\mu\nu} = \frac{1}{2} T_{\mu\nu} , \quad (4.5)$$



where  $T_{\mu\nu}$  is the stress-energy tensor,

$$T_{\mu\nu} = T_{\mu\nu}^{(EM)} + T_{\mu\nu}^{(\phi)} + \eta\Theta_{\mu\nu} + \eta'\Theta'_{\mu\nu} , \quad (4.6)$$

where gauge, scalar, and interaction term contributions can be written as

$$\begin{aligned} T_{\mu\nu}^{(EM)} &= F_{\mu\rho}F_{\nu}{}^{\rho} - \frac{1}{4}g_{\mu\nu}F^{\rho\sigma}F_{\rho\sigma} , \\ T_{\mu\nu}^{(\phi)} &= (D_{\mu}\phi)^*D_{\nu}\phi + D_{\mu}\phi(D_{\nu}\phi)^* - g_{\mu\nu}(D_{\alpha}\phi)^*D^{\alpha}\phi - m^2g_{\mu\nu}|\phi|^2 , \\ \Theta_{\mu\nu} &= \frac{2}{\sqrt{-g}}\frac{\delta}{\delta g^{\mu\nu}} \int d^4x\sqrt{-g}\mathcal{G}^{\mu\nu}(D_{\mu}\phi)^*D_{\nu}\phi , \\ \Theta'_{\mu\nu} &= -\frac{2}{\sqrt{-g}}\frac{\delta}{\delta g^{\mu\nu}} \int d^4x\sqrt{-g}|D_{\mu}\mathcal{G}^{\mu\nu}D_{\nu}\phi|^2 , \end{aligned} \quad (4.7)$$

respectively. The Maxwell equations are obtained by varying the total Lagrangian with interaction term included with respect to  $A_{\mu}$  as

$$\nabla_{\mu}F^{\mu\nu} = J^{\nu} , \quad (4.8)$$

where  $J_{\mu}$  is the current,

$$J_{\mu} = qJ_{\mu}^{(\phi)} + \eta\mathcal{J}_{\mu} + \eta'\mathcal{J}'_{\mu} , \quad (4.9)$$

containing scalar and interaction term contributions, respectively,

$$\begin{aligned} J_{\mu} &= i[\phi^*D_{\mu}\phi - (D_{\mu}\phi)^*\phi] , \\ \mathcal{J}_{\mu} &= \frac{1}{\sqrt{-g}}\frac{\delta}{\delta A^{\mu}} \int d^4x\sqrt{-g}\mathcal{G}^{\mu\nu}(D_{\mu}\phi)^*D_{\nu}\phi , \\ \mathcal{J}'_{\mu} &= -\frac{1}{\sqrt{-g}}\frac{\delta}{\delta A^{\mu}} \int d^4x\sqrt{-g}|D_{\mu}\mathcal{G}^{\mu\nu}D_{\nu}\phi|^2 . \end{aligned} \quad (4.10)$$

Finally, varying the Lagrangian with respect to the scalar field the equation of motion for the scalar field is found as

$$D_{\mu}D^{\mu}\phi - m^2\phi = \eta D_{\mu}(\mathcal{G}^{\mu\nu}D_{\nu}\phi) + \eta'D_{\rho}(\mathcal{G}^{\mu\rho}D_{\mu}(D_{\nu}(\mathcal{G}^{\nu\sigma}D_{\sigma}\phi))) . \quad (4.11)$$

To capture the lattice effects we consider the following metric *ansatz*

$$ds^2 = \frac{1}{z^2} \left[ - (1-z)P(z)Q_{tt}(x,z)dt^2 + \frac{Q_{zz}(x,z)dz^2}{P(z)(1-z)} + Q_{xx}(x,z)(dx + z^2Q_{xz}(x,z)dz)^2 + Q_{yy}(x,z)dy^2 \right], \quad (4.12)$$

where  $P(z)$  is defined as

$$P(z) = 1 + z + z^2 - \frac{\mu_0^2}{4}z^3. \quad (4.13)$$

Then the temperature is given by

$$\frac{T}{\mu} = \frac{12 - \mu_0^2}{16\pi\mu}. \quad (4.14)$$

The required boundary conditions at the horizon and the boundary are respectively

$$Q_{tt}(x,1) = Q_{zz}(x,1), \quad (4.15)$$

and

$$Q_{tt}(x,0) = Q_{zz}(x,0) = Q_{xx}(x,0) = Q_{yy}(x,0) = 1, \quad Q_{xz}(x,0) = 0, \quad A_t(x,0) = \mu(x). \quad (4.16)$$

The critical temperature solutions of this system has the same form as in Section III of our previous paper [12]. Now, we will solve the below critical temperature equations with a slightly different *ansatz* (4.12) in the following section.

### 4.2.1 Below the critical temperature

We will solve the coupled Einstein-Maxwell-scalar field equations perturbatively below the critical temperature. For this we expand all the field in the order parameter

$$\xi = \frac{\langle \mathcal{O} \rangle}{\sqrt{2}} , \quad (4.17)$$

and write

$$\begin{aligned} Q_{tt}(z, x) &= 1 + \xi^2 Q_{tt1}(z, x) + \mathcal{O}(\xi^4) , \\ Q_{zz}(z, x) &= 1 + \xi^2 Q_{zz1}(z, x) + \mathcal{O}(\xi^4) , \\ Q_{xx}(z, x) &= 1 + \xi^2 Q_{xx1}(z, x) + \mathcal{O}(\xi^4) , \\ Q_{xz}(z, x) &= \xi^2 Q_{xz1}(z, x) + \mathcal{O}(\xi^4) , \\ Q_{yy}(z, x) &= 1 + \xi^2 Q_{yy1}(z, x) + \mathcal{O}(\xi^4) , \\ \phi(z, x) &= \xi \phi_0(z, x) + \xi^3 \phi_1(z, x) + \mathcal{O}(\xi^5) , \\ A_t(z, x) &= (1 - z) [A_{t0}(z) + \xi^2 A_{t1}(z, x) + \mathcal{O}(\xi^4)] , \end{aligned} \quad (4.18)$$

where  $\xi \phi_0$ , and  $A_{t0}$  are defined at the critical temperature  $T_c$ . The chemical potential is given by

$$\mu \equiv A_t(0, x) = \mu_0 + \xi^2 \mu_1 + \mathcal{O}(\xi^2) , \quad \mu_0 = A_{t0}(0) , \quad \mu_1 = A_{t1}(0, x) . \quad (4.19)$$

Going to the Fourier modes on the boundary the fields (4.18) become

$$\begin{aligned}
Q_{tt}(z, x) &= 1 + \xi^2(Q_{tt10}(z) + Q_{tt11}(z) \cos 2kx) + \mathcal{O}(\xi^4) , \\
Q_{zz}(z, x) &= 1 + \xi^2(Q_{zz10}(z) + Q_{zz11}(z) \cos 2kx) + \mathcal{O}(\xi^4) , \\
Q_{xx}(z, x) &= 1 + \xi^2(Q_{xx10}(z) + Q_{xx11}(z) \cos 2kx) + \mathcal{O}(\xi^4) , \\
Q_{xz}(z, x) &= \xi^2 Q_{xz1}(z, x) + \mathcal{O}(\xi^4) , \\
Q_{yy}(z, x) &= 1 + \xi^2(Q_{yy10}(z) + Q_{yy11}(z) \cos 2kx) + \mathcal{O}(\xi^4) , \\
\phi(z, x) &= \xi \phi_0(z, x) + \xi^3 \phi_1(z, x) + \mathcal{O}(\xi^5) , \\
A_t(z, x) &= (1 - z) [A_{t0}(z) + \xi^2(A_{t10}(z) + A_{t11}(z) \cos 2kx) + \mathcal{O}(\xi^4)] ,
\end{aligned} \tag{4.20}$$

At each given order of the parameter  $\xi$ , only a finite number of modes of the various fields are generated. At the first order, i.e.  $\mathcal{O}(\xi^2)$ , we have only 0 and  $2k$  Fourier modes,

$$\begin{aligned}
Q_{tt1}(z, x) &= Q_{tt10}(z) + Q_{tt11}(z) \cos 2kx , \\
Q_{zz1}(z, x) &= Q_{zz10}(z) + Q_{zz11}(z) \cos 2kx , \\
Q_{xx1}(z, x) &= Q_{xx10}(z) + Q_{xx11}(z) \cos 2kx , \\
Q_{xz1}(z, x) &= Q_{xz10}(z) + Q_{xz11}(z) \sin 2kx , \\
Q_{yy1}(z, x) &= Q_{yy10}(z) + Q_{yy11}(z) \cos 2kx , \\
A_{t1}(z, x) &= A_{t10}(z) + A_{t11}(z) \cos 2kx .
\end{aligned} \tag{4.21}$$

Solving the Maxwell's equations at second order we get

$$A_{t10}(z) = C + \int_1^z dw' \frac{1}{(w' - 1)^2} \int_1^{w'} \frac{1}{4P^2(w)} (1 - w) w^{2\Delta - 2} \mu_0 \mathcal{A}(w) dw , \tag{4.22}$$

where

$$\begin{aligned} \mathcal{A}(z) = & F^2(z) [q^2(z^3\mu_0^2 + 4P(z)) + z(\Delta^2 + 8k^2z^2\eta(1 + \Delta))P^2(z)] \\ & + 2z^2(\Delta + 4k^2z^2\eta)P^2(z)F(z)F'(z) + z^3P^2(z)[F'(z)]^2 . \end{aligned} \quad (4.23)$$

In the above expression of the first order gauge field  $A_{t10}(z)$  the only unknown is the integration constant  $C$ .

Having  $A_{t10}(z)$  from (??) we can solve Einstein equations to find  $Q_{tt10}, Q_{zz10}, Q_{xx10}, Q_{yy10}$ , as can be seen in the Appendix A ((A.1), (A.4), (A.7), (A.8) respectively). We find that  $Q_{xz10}$  does not appear at first order equations. So we can set  $Q_{xz10}(z) = 0$ . Then to find the other modes in the Appendix A we give the Einstein and Maxwell equations they satisfied. These are six equations with six unknown functions. Two equations are first order. We can solve (A.10) for  $Q_{xz11}(z)$  and (A.11) for  $Q_{zz11}(z)$ . Without loss of generality we can also set  $Q_{xz11} = 0$  as well. Then we can solve the remaining equations by using the boundary conditions specified.

To find this integration constant,  $C$  we will use the first order scalar field by expanding it in Fourier modes.

$$\phi_1(x, z) = \Phi_{10}(z) \cos(kx) + \Phi_{11}(z) \cos 3kx. \quad (4.24)$$

Then the scalar field equation at first order for  $\Phi_{10}(z)$  is

$$\begin{aligned} \Phi_{10}'' + \frac{(z-1)zP' - (z-2)P}{(z-1)zP} \Phi_{10}' + \frac{P(m^2 + k^2z^2(1 - \eta\mu_0^2z^4)) + \mu_0^2q^2(z-1)z^2}{(z-1)z^2P^2} \Phi_{10} \\ + Cz^\Delta \mathcal{C} + z^\Delta \mathcal{D} = 0 , \end{aligned} \quad (4.25)$$

where

$$\mathcal{C} = \mathcal{C}_2 F'' + \mathcal{C}_1 F' + \mathcal{C}_0 F , \quad \mathcal{D} = \mathcal{D}_2 F'' + \mathcal{D}_1 F' + \mathcal{D}_0 F , \quad (4.26)$$

where the coefficients  $\mathcal{C}_2, \mathcal{C}_1, \mathcal{C}_0$  and  $\mathcal{D}_2, \mathcal{D}_1, \mathcal{D}_0$  are given in Appendix B from (B.1) to (B.6).

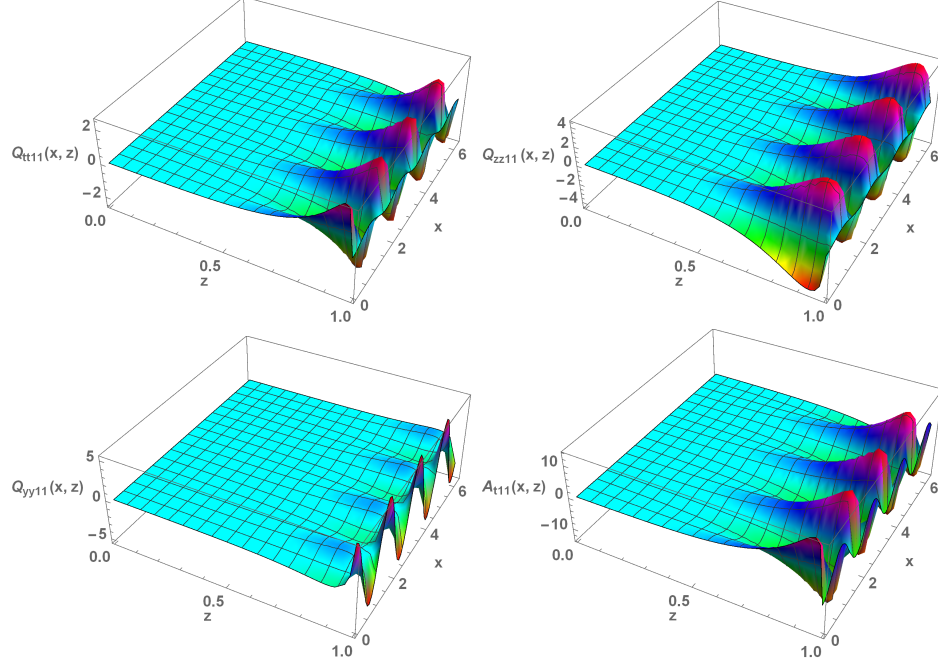


**Figure 4.1:** Numerical solutions for  $Q_{tt11}(x, z)$ ,  $Q_{zz11}(x, z)$ ,  $Q_{yy11}(x, z)$ , and  $A_{t11}(x, z)$  for  $\frac{\eta}{\mu_0^2} = 0.41$ ,  $\frac{\eta'}{\mu_0^4} = 0.005$ ,  $q = 0$ ,  $\Delta = 1$ .

Finally, we can calculate the integration constant from first order scalar field equation (4.25) and we find

$$C = - \frac{\int_0^1 dz z^{2\Delta} F [\mathcal{C}_2 F'' + \mathcal{C}_1 F' + \mathcal{C}_0 F]}{\int_0^1 dz z^{2\Delta} F [\mathcal{D}_2 F'' + \mathcal{D}_1 F' + \mathcal{D}_0 F]} . \quad (4.27)$$

The charge density of the system can also be determined by

$$\frac{\rho}{\mu^2} = - \frac{\partial_z [(1-z)A_t(z, x)]|_{z=0}}{[A_t(0, x)]^2} = \frac{\rho_0 + \xi^2 \rho_1(x)}{\mu_0^2} . \quad (4.28)$$

In Figure 4.1 we show the solutions for the metric functions  $Q_{tt11}(x, z)$ ,  $Q_{zz11}(x, z)$ ,  $Q_{yy11}(x, z)$ , and  $A_{t11}(x, z)$ , while the charge density of the system is shown in Fig. 4.2. As seen in Fig. 4.2 the charge density is spatially modulated which is an indicator of the holographic lattice structure. We observed that keeping the  $\xi$  value fixed when

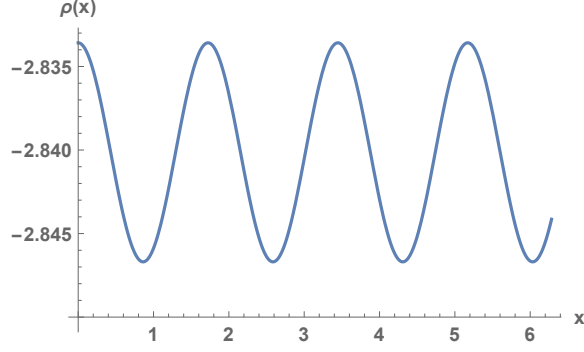


**Figure 4.2:** The charge density of the system for  $\frac{\eta}{\mu_0^2} = 0.41$ ,  $\frac{\eta'}{\mu_0^4} = 0.005$ ,  $q = 0$ ,  $\Delta = 1$ , and  $\xi = 0.1$ .

the parameters are changed such that the critical temperature,  $T_c$ , is lower than the magnitude of the spatial modulation decreases.

In summary, we have a fully-backreacted perturbative solution up to second order in  $\xi$  of the Einstein-Maxwell-scalar equations. In the next section we will introduce a Dirac field.

### 4.3 The Dirac Equation

In this section we will introduce a Dirac spinor field  $\Psi(z, t, \vec{x})$  with mass  $m_f$  and charge  $q_f$  in addition to the scalar and gauge field. The bulk action for Dirac field is

$$S_D = i \int d^4x \sqrt{-g} \bar{\Psi} (\Gamma^a \mathcal{D}_a - m_f) \Psi , \quad (4.29)$$

where  $\Gamma^a = (e_\mu)^a \Gamma^\mu$  with  $(e_\mu)^a$  a set of orthogonal normal vector bases and  $\Gamma^\mu$  Gamma matrices. The covariant derivative  $\mathcal{D}_a$  is defined as

$$\mathcal{D}_a = \partial_a + \frac{1}{4} (\omega_{\mu\nu})_a \Gamma^{\mu\nu} - iq_f A_a , \quad (4.30)$$

with  $\Gamma^{\mu\nu} = \frac{1}{2} [\Gamma^\mu, \Gamma^\nu]$ , and  $(\omega_{\mu\nu})_a = (e_\mu)_b \nabla_a (e_\nu)^b$  are the spin connection 1-forms. Here indices  $a, b$  denote tangent space and indices  $\mu, \nu, \dots$  denote indices along

boundary directions. Gamma matrices with tangent space indices satisfy Clifford algebra  $\{\Gamma^a, \Gamma^b\} = 2\eta^{ab}$  and  $\Gamma_{ab} = \frac{1}{2}[\Gamma_a, \Gamma_b]$ .

From the action (4.29) the most general form of the Dirac equation is

$$\begin{aligned}
& -\frac{1}{\sqrt{g_{zz}}}\Gamma^3\partial_z\Psi + \frac{1}{\sqrt{g_{tt}}}\Gamma^0(\partial_t - iq_f A_t)\Psi + \frac{1}{\sqrt{g_{xx}}}\Gamma^1\partial_x\Psi + \frac{1}{\sqrt{g_{yy}}}\Gamma^2\partial_y\Psi - m_f\Psi \\
& + \left(\frac{\partial_x g_{tt}}{4g_{tt}\sqrt{g_{xx}}} + \frac{\partial_x g_{yy}}{4g_{yy}\sqrt{g_{xx}}} + \frac{\partial_x g_{zz}}{4g_{zz}\sqrt{g_{xx}}}\right)\Gamma^1\Psi \\
& - \frac{1}{4g_{xx}\sqrt{g_{zz}}}\left(\partial_z g_{xx} + \frac{g_{xx}\partial_z g_{tt}}{g_{tt}} + \frac{g_{xx}\partial_z g_{yy}}{g_{yy}}\right)\Gamma^3\Psi = 0.
\end{aligned} \tag{4.31}$$

Following [13] we choose the basis

$$\Gamma^1 = \begin{pmatrix} i\sigma^1 & 0 \\ 0 & i\sigma^1 \end{pmatrix}, \quad \Gamma^2 = \begin{pmatrix} -\sigma^2 & 0 \\ 0 & \sigma^2 \end{pmatrix}, \quad \Gamma^3 = \begin{pmatrix} 0 & \sigma^2 \\ \sigma^2 & 0 \end{pmatrix}, \quad \Gamma^4 = \begin{pmatrix} -\sigma^3 & 0 \\ 0 & -\sigma^3 \end{pmatrix} \tag{4.32}$$

for the Gamma matrices of the (2+1)-dimensional boundary theory and the following *ansatz* for the spinor fields

$$\Psi = (g_{tt}g_{xx}g_{yy})^{-\frac{1}{4}}e^{-i\omega t + i(k_x x + k_y y)} \begin{pmatrix} \psi_+ \\ \psi_- \end{pmatrix}, \quad \psi_{\pm} = \begin{pmatrix} \psi_{\pm 1} \\ \psi_{\pm 2} \end{pmatrix}, \tag{4.33}$$

with two-component spinors  $\psi_{\pm}$ .

We have the holographic lattice structure in  $x$ -dimension only. Therefore, we can expand the spinor fields according to the Bloch theorem

$$\begin{pmatrix} \psi_{\pm 1}(x, z) \\ \psi_{\pm 2}(x, z) \end{pmatrix} = \sum_{l=0, \pm 1, \pm 2, \dots} \begin{pmatrix} \psi_{\pm 1}^{(l)}(z) \\ \psi_{\pm 2}^{(l)}(z) \end{pmatrix} e^{ilKx}. \tag{4.34}$$

If we substitute (4.34) to the Dirac equation (4.31) we get a set of infinite coupled equations with an infinite many fields to be solved, corresponding to the full range of  $l = 0, \pm 1, \pm 2, \dots, \pm\infty$ . In our holographic fermionic system we will use the retarded Green's function and the spectral function to get some information out of



it. This is equivalent to measuring the spectral function by using Angular Resolved Photoemission Spectroscopy (ARPES) in an experimental setup [99]. To this end, we will both numerically and analytically solve these equations using perturbation theory at small but finite temperature.

## 4.4 Perturbation Theory for Dirac Equations

### 4.4.1 Numerical Solution to Dirac Equation at Finite Temperature

The most general form of the Dirac equations are as follows.

$$-m_f \psi^{(l)} + \frac{1}{\sqrt{g_{\zeta\zeta}}} \Gamma^4 \partial_\zeta \psi^{(l)} + \frac{1}{\sqrt{g_{tt}}} \Gamma^1 (\omega + q_f A_t) \psi^{(l)} - i \frac{k_y}{\sqrt{g_{yy}}} \Gamma^3 \psi^{(l)} + \mathcal{A} \Gamma^2 \psi^{(l)} = 0 \quad (4.35)$$

where

$$\mathcal{A} = \frac{-g_{zz} \partial_x g_{xx} + g_{xx} [4i(k_x + Kl)g_{zz} + \partial_x g_{zz}]}{4(g_{xx})^{3/2} g_{zz}} \quad (4.36)$$

and

$$\psi^{(l)} = \begin{pmatrix} \psi_{+1}^{(l)} \\ \psi_{+2}^{(l)} \\ \psi_{-1}^{(l)} \\ \psi_{-2}^{(l)} \end{pmatrix}. \quad (4.37)$$

The retarded Green's function on the boundary can be found by considering the ingoing boundary conditions at the horizon. Therefore, we write

$$\begin{pmatrix} \psi_{\pm 1}^{(l)}(z) \\ \psi_{\pm 2}^{(l)}(z) \end{pmatrix} = \begin{pmatrix} 1 \\ -i \end{pmatrix} (1-z)^{-\frac{i\omega}{4\pi T}} \quad (4.38)$$

for each spinor mode and for each  $l$  when others are turned off. Another boundary condition is near AdS boundary. As  $z \rightarrow 0$  the solution to Dirac equation asymptotes

to

$$\psi_{\alpha l, \beta l'}^{(l)} = A_{\alpha l, \beta l'} z^{-m} \begin{pmatrix} 0 \\ 1 \end{pmatrix} + B_{\alpha l, \beta l'} z^m \begin{pmatrix} 1 \\ 0 \end{pmatrix}. \quad (4.39)$$

where  $\beta l'$  indicates the ingoing horizon boundary conditions. The retarded Green's function can be found from the expression

$$G_{\alpha l, \beta l'} = B_{\alpha l, \beta l'} A_{\alpha l, \beta l'}^{-1} \quad (4.40)$$

of the asymptotic expansion coefficients where  $\alpha, \beta = +, -$ .

To be able to solve the Dirac equations we need some simplifications. To this end, we will rotate Dirac spinors. After rotating the equations, we find the general expression for the Dirac equation as

$$-m_f \tilde{\psi}^{(l)} + \frac{1}{\sqrt{g_{zz}}} \Gamma^4 \partial_z \tilde{\psi}^{(l)} + \frac{1}{\sqrt{g_{tt}}} \Gamma^1 (\partial_t - iq_f A_t) \tilde{\psi}^{(l)} + \tilde{\mathcal{A}} \Gamma^2 \tilde{\psi}^{(l)} + \tilde{\mathcal{B}} \Gamma^3 \tilde{\psi}^{(l)} = 0 \quad (4.41)$$

where

$$\tilde{\mathcal{A}} = \frac{i(k_l^2 - (k_x + Kl)^2)}{k_l \sqrt{g_{yy}}} - i \frac{k_x + Kl}{4k_l g_{xx}^{3/2}} \left[ - (4(k_x + Kl)g_{xx} + i\partial_x g_{xx}) + \frac{ig_{xx}\partial_x g_{zz}}{g_{zz}} \right] \quad (4.42)$$

$$\tilde{\mathcal{B}} = \frac{(-1)^\alpha (k_x + Kl) - k_l}{4k_l g_{zz} g_{xx}^{3/2}} \left[ g_{xx} [4i(k_x + Kl)g_{zz} + \partial_x g_{zz}] - g_{zz} \left( 4i(k_x + Kl) \frac{g_{xx}^{3/2}}{\sqrt{g_{yy}}} + \partial_x g_{xx} \right) \right] \quad (4.43)$$

after expanding  $\tilde{\psi} \rightarrow \tilde{\psi}(x, z) e^{-i\omega t + ik_x x + ik_y y}$  and rotating the equations such that  $k_y \rightarrow 0$ . where

$$\tilde{\psi}_1^{(l)} = \psi_{+1}^{(l)} + \lambda \psi_{-1}^{(l)}, \quad \tilde{\psi}_2^{(l)} = \psi_{+2}^{(l)} + \lambda \psi_{-2}^{(l)}, \quad (4.44)$$

$$\tilde{\psi}_3^{(l)} = \psi_{+1}^{(l)} + \delta \psi_{-1}^{(l)}, \quad \tilde{\psi}_4^{(l)} = \psi_{+2}^{(l)} + \delta \psi_{-2}^{(l)}. \quad (4.45)$$

and  $k_l = \sqrt{(k_x + Kl)^2 + k_y^2}$ . We will explain the details of this rotation in Appendix C.

Having the Green's function we can calculate the spectral function  $A(\omega, k_x, k_y) = \Im(G_{\alpha l, \alpha l} + G_{\beta l, \beta l})$  which is imaginary part of the diagonal terms of the retarded Green function and from which the Fermi surface can be found. Although the Fermi surface is defined at zero temperature, as indicated in [118] and [101] Fermi surface can be located by searching a peak at spectral function  $A(\omega, k_x, k_y)$  with tiny frequency  $\omega$  at lower temperature.

Backreaction contribution of the scalar field and gauge field is small in higher orders therefore, we have expanded scalar field, gauge field, and metric functions in small  $\xi$  up to first order in (4.18). To solve the Dirac equation for the Dirac spinor field we will expand it in  $\xi$  up to second order for reasons which will be explained later. Therefore, we write

$$\begin{aligned}
\psi_{+,1}^{(l)}(z) &= \psi_{+,1}^{(0,l)} + \xi^2 \psi_{+,1}^{(1,l)} + \xi^4 \psi_{+,1}^{(2,l)} + \mathcal{O}(\xi^6) , \\
\psi_{+,2}^{(l)}(z) &= \psi_{+,2}^{(0,l)} + \xi^2 \psi_{+,2}^{(1,l)} + \xi^4 \psi_{+,2}^{(2,l)} + \mathcal{O}(\xi^6) , \\
\psi_{-,1}^{(l)}(z) &= \psi_{-,1}^{(0,l)} + \xi^2 \psi_{-,1}^{(1,l)} + \xi^4 \psi_{-,1}^{(2,l)} + \mathcal{O}(\xi^6) , \\
\psi_{-,2}^{(l)}(z) &= \psi_{-,2}^{(0,l)} + \xi^2 \psi_{-,2}^{(1,l)} + \xi^4 \psi_{-,2}^{(2,l)} + \mathcal{O}(\xi^6) .
\end{aligned} \tag{4.46}$$

Applying ingoing boundary conditions at the horizon we can write

$$\begin{aligned}
\psi_{+,1}^{(s,l)}(z) &= (1-z)^{-\frac{i\omega}{4\pi T}} F_1^{(s,l)}(z) , \\
\psi_{+,2}^{(s,l)}(z) &= (1-z)^{-\frac{i\omega}{4\pi T}} F_2^{(s,l)}(z) , \\
\psi_{-,1}^{(s,l)}(z) &= (1-z)^{-\frac{i\omega}{4\pi T}} F_3^{(s,l)}(z) , \\
\psi_{-,2}^{(s,l)}(z) &= (1-z)^{-\frac{i\omega}{4\pi T}} F_4^{(s,l)}(z) .
\end{aligned} \tag{4.47}$$

Similarly, below the critical temperature,  $T_c$ , boundary condition at the boundary can be written as

$$\psi_{\alpha l, \beta l'} = \sum_{s=0,1,\dots} A_{\alpha l, \beta l'}^{(s)} z^{-m} \begin{pmatrix} 0 \\ 1 \end{pmatrix} + \sum_{s=0,1,\dots} B_{\alpha l, \beta l'}^{(s)} z^m \begin{pmatrix} 1 \\ 0 \end{pmatrix}, \quad (4.48)$$

where  $s$  is the order of perturbation and  $l$  indicates the Brillouin zone. We will only solve the equations up to second order. To find the retarded Green's function we need to find the inverse of the matrix  $A$  which includes both diagonal and off-diagonal terms. The elements of matrices  $A$  and  $B$  are formed based on the two assumptions. The first assumption is that the diagonal elements of matrix  $A$  are in order of 1 and  $\xi^4$  and the second assumption is that the off-diagonal elements are in order of  $\xi^2$ . Taking these assumptions into consideration and using the inverse of a matrix  $A^{-1} = \frac{1}{\det A}(\text{cofactors of matrix } A)^T$  the retarded Green's function was found in [117] as

$$G_{Ret, \alpha l} = \frac{1}{\det A} \left( \sum_{\beta=+,-} (B_{\alpha l, \beta l-1} \Delta_{\alpha l, \beta l-1} + B_{\alpha l, \beta l+1} \Delta_{\alpha l, \beta l+1}) + B_{\alpha l, \alpha l} \Delta_{\alpha l, \alpha l} \right) \quad (4.49)$$

where  $\Delta_{\alpha l, \alpha l}$  are cofactors of matrix  $A$  and the cofactors and  $\det A$  up to second order are given in [117].

#### 4.4.2 Analytical Solution to Dirac Equation at Finite Temperature

Below the critical temperature at finite temperature near horizon metric can be written as

$$ds^2 = \frac{R_2^2}{\zeta^2} \left( -\left(1 - \frac{\zeta^2}{\zeta_0^2}\right) Q_{tt}(\zeta, x) dt^2 + \frac{Q_{\zeta\zeta}(\zeta, x) d\zeta^2}{1 - \frac{\zeta^2}{\zeta_0^2}} \right) + \mu_*^2 R^2 Q_{xx}(\zeta, x) dx^2 + \mu_*^2 R^2 Q_{yy}(\zeta, x) dy^2. \quad (4.50)$$

The gauge potential then becomes

$$A_t(\zeta, x) = \frac{e_d}{\zeta} \left( 1 - \frac{\zeta}{\zeta_0} \right) + A_{t1}(\zeta, x) \quad (4.51)$$

where

$$\begin{aligned} \zeta &\equiv \frac{z_*^2}{d(d-1)(z_* - z)}, & \zeta_0 &\equiv \frac{z_*^2}{d(d-1)(z_* - z_0)}, & e_d &\equiv \frac{g_F}{\sqrt{2d(d-1)}}, \\ \mu_* &\equiv \frac{1}{z_*} = 2(d-2)e_d \frac{\mu}{g_F^2}. \end{aligned} \quad (4.52)$$

where  $g_F$  is the bulk gauge coupling and in our system we choose it to be  $g_F = 2$ . We are also working in  $d + 1 = 4$  spacetime in the bulk, therefore  $d = 3$ . Using these we can write the parameters as

$$\zeta_0 = \frac{z_*^2}{6(z_* - z_0)}, \quad e_d = \frac{1}{\sqrt{3}}, \quad \mu_* = \frac{\mu}{2\sqrt{3}}. \quad (4.53)$$

The metric functions and gauge field can be expanded as

$$\begin{aligned} Q_{tt} &= 1 + \xi^2 [Q_{tt10} + Q_{tt11} \cos(2kx)] + \mathcal{O}(\zeta^4), \\ Q_{\zeta\zeta} &= 1 + \xi^2 [Q_{\zeta\zeta10} + Q_{\zeta\zeta11} \cos(2kx)] + \mathcal{O}(\zeta^4), \\ Q_{xx} &= 1 + \xi^2 [Q_{xx10} + Q_{xx11} \cos(2kx)] + \mathcal{O}(\zeta^4), \\ Q_{yy} &= 1 + \xi^2 [Q_{yy10} + Q_{yy11} \cos(2kx)] + \mathcal{O}(\zeta^4), \\ A_t(\zeta, x) &= \frac{e_d}{\zeta} \left( 1 - \frac{\zeta}{\zeta_0} \right) + \xi^2 \left( 1 - \frac{\zeta}{\zeta_0} \right) [A_{t10}(\zeta) + A_{t11}(\zeta) \cos(2kx)] + \mathcal{O}(\zeta^4). \end{aligned} \quad (4.54)$$

To be able to solve the Dirac equations we again rotate Dirac spinors. After rotating the equations we find the general expression for the Dirac equation with metric (4.50) as

$$-m_f \tilde{\psi}^{(l)} + \frac{1}{\sqrt{g_{\zeta\zeta}}} \Gamma^4 \partial_\zeta \tilde{\psi}^{(l)} + \frac{1}{\sqrt{g_{tt}}} \Gamma^1 (\partial_t - iq_f A_t) \tilde{\psi}^{(l)} + \tilde{\mathbf{A}} \Gamma^2 \tilde{\psi}^{(l)} + \tilde{\mathbf{B}} \Gamma^3 \tilde{\psi}^{(l)} = 0 \quad (4.55)$$

where

$$\tilde{\mathcal{A}} = \frac{i(k_l^2 - (k_x + Kl)^2)}{k_l \sqrt{g_{yy}}} - i \frac{k_x + Kl}{4k_l g_{xx}^{3/2}} \left[ - (4(k_x + Kl)g_{xx} + i\partial_x g_{xx}) + \frac{ig_{xx}\partial_x g_{\zeta\zeta}}{g_{\zeta\zeta}} \right] \quad (4.56)$$

$$\tilde{\mathcal{B}} = \frac{(-1)^\alpha (k_x + Kl) - k_l}{4k_l g_{\zeta\zeta} g_{xx}^{3/2}} \left[ g_{xx} [4i(k_x + Kl)g_{\zeta\zeta} + \partial_x g_{\zeta\zeta}] - g_{\zeta\zeta} \left( 4i(k_x + Kl) \frac{g_{xx}^{3/2}}{\sqrt{g_{yy}}} \partial_x g_{xx} \right) \right] \quad (4.57)$$

after expanding  $\tilde{\psi} \rightarrow \tilde{\psi}(x, z)e^{-i\omega t + ik_x x + ik_y y}$  and rotating the equations such that  $k_y \rightarrow 0$ . Using the Gamma matrices we can write

$$-m_f \tilde{\psi}_\alpha - \sigma^3 \frac{1}{\sqrt{g_{zz}}} \partial_\zeta \tilde{\psi}_\alpha + \frac{1}{\sqrt{g_{tt}}} \sigma^1 (\omega + qA_t) \tilde{\psi}_\alpha + \tilde{\mathcal{A}} (-1)^\alpha \sigma^2 \tilde{\psi}_\alpha + \tilde{\mathcal{B}} \sigma^2 \tilde{\psi}_\beta = 0 \quad (4.58)$$

where  $\alpha = 1, 2$  and  $\beta = 3 - \alpha$ .

To simplify the Dirac equations we will make another rotation here. Let us define  $\Phi = (-gg^{\zeta\zeta})^{-1/4} \tilde{\psi} = \frac{1}{\sqrt{2}} (1 - i\sigma^1) \tilde{\Phi}$ . We multiply (4.58) by  $\frac{1}{\sqrt{2}} (1 + i\sigma^1) \sigma^3$  from left after substituting  $\Phi = \frac{1}{\sqrt{2}} (1 - i\sigma^1) \tilde{\Phi}$  and find

$$m_f \sigma^2 \tilde{\Phi}^{(l)} - \frac{1}{\sqrt{g_{\zeta\zeta}}} \partial_\zeta \tilde{\Phi}_\alpha^{(l)} + \frac{i}{\sqrt{g_{tt}}} \sigma^3 (\omega + q_f A_t) \tilde{\Phi}_\alpha^{(l)} - \tilde{\mathcal{A}} (-1)^\alpha i \sigma^1 \tilde{\Phi}_\alpha^{(l)} - \tilde{\mathcal{B}} i \sigma^1 \tilde{\Phi}_\beta^{(l)} = 0. \quad (4.59)$$

At zeroth order we find

$$-m_f \sigma^2 \tilde{\Phi}_\alpha^{(0,l)} + \frac{\zeta \sqrt{f}}{R_2} \partial_\zeta \tilde{\Phi}_\alpha^{(0,l)} - \frac{i\zeta}{R_2 \sqrt{f}} \sigma^3 (\omega + q_f A_{t0}) \tilde{\Phi}_\alpha^{(0,l)} + \frac{k_l}{\mu_* R} (-1)^\alpha \sigma^1 \tilde{\Phi}_\alpha^{(0,l)} = 0 \quad (4.60)$$

where  $A_{t0} = \frac{e_d}{\zeta} \left(1 - \frac{\zeta}{\zeta_0}\right)$ . At higher orders the equations can be written as

$$\begin{aligned}
& -m_f \sigma^2 \tilde{\Phi}_\alpha^{(s,l)} + \frac{\zeta \sqrt{f}}{R_2} \partial_\zeta \tilde{\Phi}_\alpha^{(s,l)} - \frac{i\zeta}{R_2 \sqrt{f}} \sigma^3 (\omega + q_f A_{t0}) \tilde{\Phi}_\alpha^{(s,l)} + \frac{k_l}{\mu_* R} (-1)^\alpha \sigma^1 \tilde{\Phi}_\alpha^{(s,l)} \\
& - (-1)^\alpha i \sigma^1 \tilde{\mathcal{A}}^{(s-1,l')} - i \sigma^1 \tilde{\mathcal{B}}^{(s-1,l')} - i \sigma^3 \tilde{\mathcal{C}}^{(s-1,l')} = 0
\end{aligned} \tag{4.61}$$

where  $s$  is the order of perturbation.

### 4.4.3 Zeroth Order Solution to Dirac Equations

#### Zeroth Order Numerical Solution to Dirac Equations

After Bloch expansion the Dirac equation at zeroth order for the different spinor modes can be written as the follows

$$\partial_z \psi_{\alpha j}^{(0,l)} - i \frac{q_f \mu_0 (1-z) + \omega}{h} \sigma^2 \psi_{\alpha j}^{(0,l)} + \frac{k_x + Kl}{\sqrt{h}} \sigma^3 \psi_{\alpha j}^{(0,l)} - \frac{k_y}{\sqrt{h}} \sigma^1 \psi_{\beta m}^{(0,l)} = 0 \tag{4.62}$$

where  $\alpha = +, -, j = 1, 2$  and  $\beta = -\alpha, m = 3 - j, h(z) = (1-z)P(z)$  and where we set  $m_f = 0$ . We want to plot the spectral function with respect to  $k_y$  for a fixed  $k_x$  value therefore we take the transformation one step further to get Dirac equations to  $k_x + Kl \rightarrow 0$  form. Following that (A.10) can be combined with (A.11) to obtain

$$\begin{aligned}
& \sqrt{h} (\psi_{+1} + \lambda \psi_{-1} + \psi_{+1} + \delta \psi_{-1})' + \frac{m_f}{z} (\psi_{+1} + \lambda \psi_{-1} + \psi_{+1} + \delta \psi_{-1}) \\
& - \left[ \frac{\mu_0 q_f (1-z) + \omega}{\sqrt{h}} \right] (\psi_{+2} + \lambda \psi_{-2} + \psi_{+2} + \delta \psi_{-2}) - k_l (\psi_{+2} + \delta \psi_{-2} - \psi_{+2} - \lambda \psi_{-2}) = 0
\end{aligned} \tag{4.63}$$

which is identical to the first equation with  $k_x = 0$ . Similarly, by combining other equations we obtain

$$\begin{aligned} & \sqrt{h}(\psi_{+2} + \lambda\psi_{-2} + \psi_{+2} + \delta\psi_{-2})' - \frac{m_f}{z}(\psi_{+2} + \lambda\psi_{-2} + \psi_{+2} + \delta\psi_{-2}) \\ & + \left[ \frac{\mu_0 q_f(1-z) + \omega}{\sqrt{h}} \right] (\psi_{+1} + \lambda\psi_{-1} + \psi_{+1} + \delta\psi_{-1}) - k_l(\psi_{+1} + \delta\psi_{-1} - \psi_{+1} - \lambda\psi_{-1}) = 0 , \end{aligned} \quad (4.64)$$

$$\begin{aligned} & \sqrt{h}(\psi_{+1} + \delta\psi_{-1} - \psi_{+1} - \lambda\psi_{-1})' + \frac{m_f}{z}(\psi_{+1} + \delta\psi_{-1} - \psi_{+1} - \lambda\psi_{-1}) \\ & - \left[ \frac{\mu_0 q_f(1-z) + \omega}{\sqrt{h}} \right] (\psi_{+2} + \delta\psi_{-2} - \psi_{+2} - \lambda\psi_{-2}) - k_l(\psi_{+2} + \lambda\psi_{-2} + \psi_{+2} + \delta\psi_{-2}) = 0 , \end{aligned} \quad (4.65)$$

$$\begin{aligned} & \sqrt{h}(\psi_{+2} + \delta\psi_{-2} - \psi_{+2} - \lambda\psi_{-2})' - \frac{m_f}{z}(\psi_{+2} + \delta\psi_{-2} - \psi_{+2} - \lambda\psi_{-2}) \\ & + \left[ \frac{\mu_0 q_f(1-z) + \omega}{\sqrt{h}} \right] (\psi_{+1} + \delta\psi_{-1} - \psi_{+1} + \lambda\psi_{-1}) - k_l(\psi_{+1} + \lambda\psi_{-1} + \psi_{+1} + \delta\psi_{-1}) = 0 . \end{aligned} \quad (4.66)$$

These equations tell us that the modes decouple and the equations are the same as with  $k_x + Kl = 0$ . The modes corresponding to  $k_x + Kl = 0$  are as following.

$$\begin{aligned} \bar{\psi}_1^{(s,l)} &= \psi_{+1}^{(s,l)} + \lambda\psi_{-1}^{(s,l)} + \psi_{+1}^{(s,l)} + \delta\psi_{-1}^{(s,l)} , \\ \bar{\psi}_2^{(s,l)} &= \psi_{+2}^{(s,l)} + \lambda\psi_{-2}^{(s,l)} + \psi_{+2}^{(s,l)} + \delta\psi_{-2}^{(s,l)} , \\ \bar{\psi}_3^{(s,l)} &= \psi_{+1}^{(s,l)} + \delta\psi_{-1}^{(s,l)} - \psi_{+1}^{(s,l)} - \lambda\psi_{-1}^{(s,l)} , \\ \bar{\psi}_4^{(s,l)} &= \psi_{+2}^{(s,l)} + \delta\psi_{-2}^{(s,l)} - \psi_{+2}^{(s,l)} - \lambda\psi_{-2}^{(s,l)} . \end{aligned} \quad (4.67)$$



where  $s$  is the perturbation order. We can also write  $k_x + Kl \neq 0, k_y \neq 0$  modes in terms of  $k_x + Kl = 0$  modes as

$$\begin{aligned}
\psi_{+1}^{(s,l)} &= \frac{(\lambda - \delta)\bar{\psi}_1^{(s,l)} + (\lambda + \delta)\bar{\psi}_3^{(s,l)}}{2(\lambda - \delta)}, \\
\psi_{+2}^{(s,l)} &= \frac{(\lambda - \delta)\bar{\psi}_2^{(s,l)} + (\lambda + \delta)\bar{\psi}_4^{(s,l)}}{2(\lambda - \delta)}, \\
\psi_{-1}^{(s,l)} &= -\frac{\bar{\psi}_3^{(s,l)}}{\lambda - \delta}, \\
\psi_{-2}^{(s,l)} &= -\frac{\bar{\psi}_4^{(s,l)}}{\lambda - \delta}.
\end{aligned} \tag{4.68}$$

Applying the ingoing boundary conditions at zeroth order,

i.e.  $\psi_{\pm 1,2}^{(0,l)} = (1 - z)^{-\frac{i\omega}{4\pi T}} F_{\pm 1,2}^{(0,l)}$ , eq.s (C.1) in Appendix C are transformed into

$$\begin{aligned}
&F_{+1}'^{(0,l)} + \frac{m(z-1)(\mu_0^2 - 12) + 4iz\omega\sqrt{h}}{(z-1)z(\mu_0^2 - 12)\sqrt{h}} F_{+1}^{(0,l)} + \frac{\sqrt{h}(k_x + Kl) - q\mu_0(1-z) - \omega}{h} F_{+2}^{(0,l)} \\
&- \frac{k_y}{\sqrt{h}} F_{-2}^{(0,l)} = 0, \\
&F_{+2}'^{(0,l)} - \frac{m(z-1)(\mu_0^2 - 12) - 4iz\omega\sqrt{h}}{(z-1)z(\mu_0^2 - 12)\sqrt{h}} F_{+2}^{(0,l)} + \frac{\sqrt{h}(k_x + Kl) + q\mu_0(1-z) + \omega}{h} F_{+1}^{(0,l)} \\
&- \frac{k_y}{\sqrt{h}} F_{-1}^{(0,l)} = 0, \\
&F_{-1}'^{(0,l)} + \frac{m(z-1)(\mu_0^2 - 12) + 4iz\omega\sqrt{h}}{(z-1)z(\mu_0^2 - 12)\sqrt{h}} F_{-1}^{(0,l)} - \frac{\sqrt{h}(k_x + Kl) + q\mu_0(1-z) + \omega}{h} F_{-2}^{(0,l)} \\
&- \frac{k_y}{\sqrt{h}} F_{+2}^{(0,l)} = 0, \\
&F_{-2}'^{(0,l)} - \frac{m(z-1)(\mu_0^2 - 12) - 4iz\omega\sqrt{h}}{(z-1)z(\mu_0^2 - 12)\sqrt{h}} F_{-2}^{(0,l)} - \frac{\sqrt{h}(k_x + Kl) - q\mu_0(1-z) - \omega}{h} F_{-1}^{(0,l)} \\
&- \frac{k_y}{\sqrt{h}} F_{+1}^{(0,l)} = 0.
\end{aligned} \tag{4.69}$$

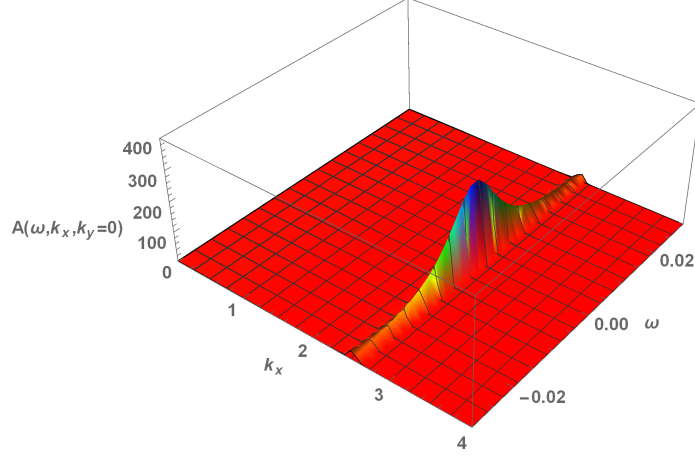


**Figure 4.3:** The plot of the peak of spectral function  $A(\omega, k_x, k_y = 0)$  at  $k_F = 2.573$  for  $q_f = 1.7$ ,  $\mu = 2.35$ ,  $\Delta = 1$  above the critical temperature,  $T_c$ .

Spectral function is found by solving differential equations at the boundary and it can be expressed as

$$A(\omega, k_x, k_y) = \Im \left[ \frac{F_{+1}^{(0,l)}(\epsilon)}{F_{+2}^{(0,l)}(\epsilon)} + \frac{F_{-1}^{(0,l)}(\epsilon)}{F_{-2}^{(0,l)}(\epsilon)} \right]. \quad (4.70)$$

The spectral function above the critical temperature,  $T_c$  is plotted in Fig. 4.3 for different  $k_x$  values at  $k_y = 0$  with tiny frequencies. The plot shows the peak of the spectral function at  $k_F = 2.653$  which is an indicator of Fermi surface. However, the peak is quite broad indicating an instability of the quasiparticles.

We can do a similar transformation for  $k_x + Kl = 0$  case, i.e.

$\bar{\psi}_{1,2,3,4}^{(0,l)} = (1-z)^{-\frac{i\omega}{4\pi T}} \bar{F}_{1,2,3,4}^{(0,l)}$ , eq.s (4.63)-(4.66) are transformed into

$$\begin{aligned}
\bar{F}_1'^{(0,l)} + \frac{m_f(z-1)(\mu_0^2 - 12) + 4iz\omega\sqrt{h}}{(z-1)z(\mu_0^2 - 12)\sqrt{h}} \bar{F}_1^{(0,l)} + \frac{-q_f\mu_0(1-z) - \omega}{h} \bar{F}_2^{(0,l)} - \frac{k_l}{\sqrt{h}} \bar{F}_4^{(0,l)} &= 0, \\
\bar{F}_2'^{(0,l)} + \frac{-m_f(z-1)(\mu_0^2 - 12) + 4iz\omega\sqrt{h}}{(z-1)z(\mu_0^2 - 12)\sqrt{h}} \bar{F}_2^{(0,l)} + \frac{q_f\mu_0(1-z) + \omega}{h} \bar{F}_1^{(0,l)} - \frac{k_l}{\sqrt{h}} \bar{F}_3^{(0,l)} &= 0, \\
\bar{F}_3'^{(0,l)} + \frac{m_f(z-1)(\mu_0^2 - 12) + 4iz\omega\sqrt{h}}{(z-1)z(\mu_0^2 - 12)\sqrt{h}} \bar{F}_3^{(0,l)} - \frac{q_f\mu_0(1-z) + \omega}{h} \bar{F}_4^{(0,l)} - \frac{k_l}{\sqrt{h}} \bar{F}_2^{(0,l)} &= 0, \\
\bar{F}_4'^{(0,l)} + \frac{-m_f(z-1)(\mu_0^2 - 12) + 4iz\omega\sqrt{h}}{(z-1)z(\mu_0^2 - 12)\sqrt{h}} \bar{F}_4^{(0,l)} + \frac{q_f\mu_0(1-z) + \omega}{h} \bar{F}_3^{(0,l)} - \frac{k_l}{\sqrt{h}} \bar{F}_1^{(0,l)} &= 0.
\end{aligned} \tag{4.71}$$

Then the spectral function is calculated from

$$\bar{A}(\omega, k_x + Kl, k_y) = \Im \left[ \frac{\bar{F}_1^{(0,l)}(\epsilon)}{\bar{F}_2^{(0,l)}(\epsilon)} + \frac{\bar{F}_3^{(0,l)}(\epsilon)}{\bar{F}_4^{(0,l)}(\epsilon)} \right]. \tag{4.72}$$

After the transformation above we can state wavefunctions  $F_{\pm 1,2}^{(s,l)}$  in terms of  $\bar{F}_{1,2,3,4}^{(s,l)}$  as following

$$\begin{aligned}
F_{+1}^{(s,l)} &= \frac{(\lambda - \delta)\bar{F}_1^{(s,l)} + (\lambda + \delta)\bar{F}_3^{(s,l)}}{2(\lambda - \delta)}, \\
F_{+2}^{(s,l)} &= \frac{(\lambda - \delta)\bar{F}_2^{(s,l)} + (\lambda + \delta)\bar{F}_4^{(s,l)}}{2(\lambda - \delta)}, \\
F_{-1}^{(s,l)} &= -\frac{\bar{F}_3^{(s,l)}}{\lambda - \delta}, \\
F_{-2}^{(s,l)} &= -\frac{\bar{F}_4^{(s,l)}}{\lambda - \delta}.
\end{aligned} \tag{4.73}$$

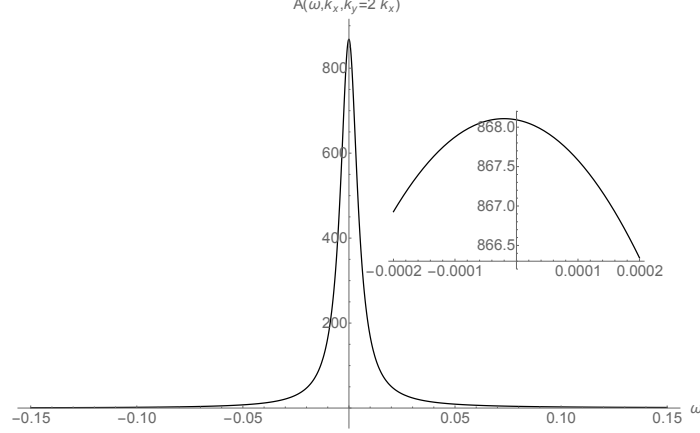


**Figure 4.4:** The plot of the peak of spectral function  $A(\omega, k_x, k_y = 2k_x)$  at  $k_F = 2.4548$  for  $q_f = 1.7$ ,  $\mu_0 = 2.257$ ,  $\Delta = 1$  above the critical temperature,  $T_c$ , as a function of  $\omega$  calculated from (4.72).

Therefore, we can state the spectral function  $A(\omega, k_x + Kl, k_y)$  in (4.70) at zeroth order as

$$\begin{aligned}
 A(\omega, k_x + Kl, k_y) &= \Im \left[ \frac{\frac{(\lambda - \delta)\bar{F}_1^{(0,l)}(\epsilon) + (\lambda + \delta)\bar{F}_3^{(0,l)}(\epsilon)}{2(\lambda - \delta)} - \frac{\bar{F}_3^{(0,l)}(\epsilon)}{\lambda - \delta}}{\frac{(\lambda - \delta)\bar{F}_2^{(0,l)}(\epsilon) + (\lambda + \delta)\bar{F}_4^{(0,l)}(\epsilon)}{2(\lambda - \delta)} - \frac{\bar{F}_4^{(0,l)}(\epsilon)}{\lambda - \delta}} \right] \\
 &= \Im \left[ \frac{(\lambda - \delta)\bar{F}_1^{(0,l)}(\epsilon) + (\lambda + \delta)\bar{F}_3^{(0,l)}(\epsilon)}{(\lambda - \delta)\bar{F}_2^{(0,l)}(\epsilon) + (\lambda + \delta)\bar{F}_4^{(0,l)}(\epsilon)} + \frac{\bar{F}_3^{(0,l)}(\epsilon)}{\bar{F}_4^{(0,l)}(\epsilon)} \right].
 \end{aligned} \tag{4.74}$$

After SO(2) rotation we can also plot the spectral function for non-zero  $k_x$  and  $k_y$  values as seen in Figs 4.4, 4.5, 4.6 . Fig. 4.4 is the plot of the spectral function  $A(\omega, k_x, k_y = 2k_x)$  as a function of  $\omega$ . There is a peak at small frequency such that  $k_F = 2.4548$  for parameters  $q_f = 1.7$ ,  $\mu_0 = 2.257$ ,  $\Delta = 1$  above and at the critical temperature. Similarly, we plotted the spectral function as a function of  $k_y$  as seen Fig. 4.5 for the same parameters and at tiny frequency. The plot shows a peak at  $k_y = 2.195$  such that  $k_F = \sqrt{k_x^2 + k_y^2} = 2.4548$ . Finally, Fig. 4.6 show the Fermi surface at tiny frequency for  $l = 1, 0, -1$  from left to right respectively.

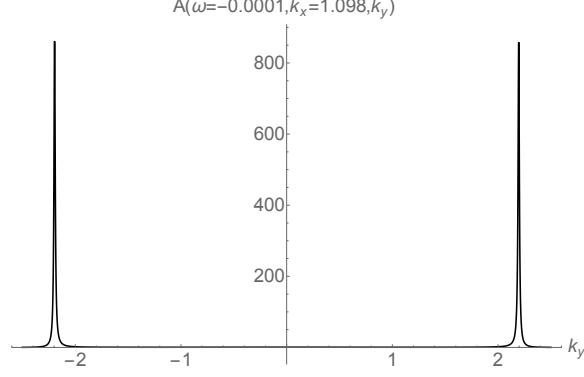


**Figure 4.5:** The plot of the peak of spectral function  $A(\omega = -0.0001, k_x = 1.098, k_y)$  at  $k_F = 2.4548$  for  $q_f = 1.7$ ,  $\mu_0 = 2.257$ ,  $\Delta = 1$  above the critical temperature,  $T_c$ , calculated from (4.72).

### Zerth Order Analytical Solution to Dirac Equations

At finite temperature, in  $T/\mu \ll 1$  limit the near horizon region spacetime is  $\text{AdS}_2 \times \mathbb{R}^{d-1}$  and the metric can be written as [76]

$$ds^2 = \frac{R_2^2}{\zeta^2} \left( -\left(1 - \frac{\zeta^2}{\zeta_0^2}\right) dt^2 + \frac{d\zeta^2}{1 - \frac{\zeta^2}{\zeta_0^2}} \right) + \mu_*^2 R^2 dx^2 + \mu_*^2 R^2 dy^2 \quad (4.75)$$

and the U(1) gauge field is

$$A_t = \frac{e_d}{\zeta} \left( 1 - \frac{\zeta}{\zeta_0} \right). \quad (4.76)$$

From this metric the temperature can also be calculated and found as

$$T = \frac{1}{2\pi\zeta_0}. \quad (4.77)$$

Varying action (4.29) we obtain Dirac equation

$$\left( \partial_\zeta - i\sigma^3 \frac{\omega + q_f A_t}{f} \right) \tilde{\Phi}^{(0,l)} = \frac{R_2}{\zeta\sqrt{f}} (m_f \sigma^2 + \tilde{m} \sigma^1) \tilde{\Phi}^{(0,l)} \quad (4.78)$$

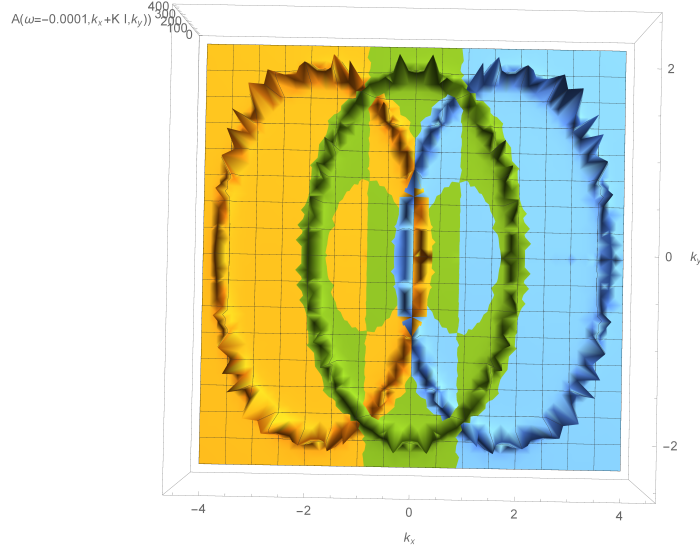


**Figure 4.6:** The plot of the peak of spectral function  $A(\omega = -0.0001, k_x + Kl, k_y)$  for  $q_f = 1.56$ ,  $\mu_0 = 2.257$ ,  $\Delta = 1$  above the critical temperature,  $T_c$ , calculated from (4.72).

where  $f(\zeta) = 1 - \frac{\zeta^2}{\zeta_0^2}$ ,  $R_2 = \frac{1}{\sqrt{d(d-1)}}R$  and

$$\tilde{\Phi}^{(0,l)} \equiv \begin{pmatrix} \tilde{y} \\ \tilde{z} \end{pmatrix} \equiv \frac{1}{\sqrt{2}}(1 + i\sigma^1)(-gg^{\zeta\zeta})^{-1/4}\psi^{(0,l)}. \quad (4.79)$$

From (4.78) we can write

$$\begin{aligned} \left( \partial_\zeta - i \frac{\omega + q_f A_t}{f} \right) \tilde{y}^{(0,l)} &= \frac{R_2}{\zeta \sqrt{f}} (-im_f + \tilde{m}) \tilde{z}^{(0,l)} \\ \left( \partial_\zeta + i \frac{\omega + q_f A_t}{f} \right) \tilde{z}^{(0,l)} &= \frac{R_2}{\zeta \sqrt{f}} (im_f + \tilde{m}) \tilde{y}^{(0,l)} \end{aligned} \quad (4.80)$$

Then for the upper component  $\tilde{y}^{(0,l)}$  we obtain the equation

$$\begin{aligned} & \partial_\zeta^2 \tilde{y}^{(0,l)} + \frac{2\zeta^2 - \zeta_0^2}{\zeta(\zeta^2 - \zeta_0^2)} \partial_\zeta \tilde{y}^{(0,l)} \\ & + \left( -\frac{\nu_{k_l}^2}{\zeta^2 - \frac{\zeta^4}{\zeta_0^2}} + \frac{\left[ \omega + qe_d \left( \frac{1}{\zeta} - \frac{1}{\zeta_0} \right) \right]^2}{1 - \frac{2\zeta^2}{\zeta_0^2} + \frac{\zeta^4}{\zeta_0^4}} + \frac{\frac{q^2 e_d^2}{\zeta_0^2} \left( 1 - \frac{1}{\zeta^2} \right) - \frac{iqe_d}{\zeta_0^2} \left( 1 - \frac{1}{\zeta} \right) - \frac{i\omega}{\zeta}}{1 - \frac{2\zeta^2}{\zeta_0^2} + \frac{\zeta^4}{\zeta_0^4}} \right) \tilde{y}^{(0,l)} = 0 \end{aligned} \quad (4.81)$$

where we set  $m_f = 0$  and  $\tilde{m} = -k_l \frac{(-1)^\alpha}{z_* R}$  with  $\alpha = 1, 2$  for  $\tilde{y}$  and  $\tilde{z}$  respectively and  $\nu_{k_l} = \sqrt{\tilde{m}^2 R_2^2 - q^2 e_d^2}$ . From now on we will use  $q_f = q$  for simplicity since the charge of the scalar field doesn't play a role in this part. Then the two independent solutions to this equation are

$$\begin{aligned} \tilde{y}^{(0,l)} \sim & \left( 1 + \frac{\zeta_0}{\zeta} \right)^{\mp \nu_{k_l}} \left( \frac{\zeta_0 + \zeta}{\zeta_0 - \zeta} \right)^{\frac{i\zeta_0 \omega}{2}} \\ & \times {}_2F_1 \left( \pm \nu_{k_l} - iqe_d, \frac{1}{2} \pm \nu_{k_l} + iqe_d - i\zeta_0 \omega; 1 \pm 2\nu_{k_l}; \frac{2\zeta}{\zeta + \zeta_0} \right), \end{aligned} \quad (4.82)$$

or

$$\begin{aligned} \tilde{y}^{(0,l)} = & \left( \frac{\zeta_0 + \zeta}{\zeta_0 - \zeta} \right)^{\frac{i\zeta_0 \omega}{2}} \\ & \times \left[ c_{in} \left( 1 + \frac{\zeta_0}{\zeta} \right)^{-\nu_{k_l}} {}_2F_1 \left( \nu_{k_l} - iqe_d, \frac{1}{2} + \nu_{k_l} + iqe_d - i\zeta_0 \omega; 1 + 2\nu_{k_l}; \frac{2\zeta}{\zeta + \zeta_0} \right) \right. \\ & \left. + c_{out} \left( 1 + \frac{\zeta_0}{\zeta} \right)^{\nu_{k_l}} {}_2F_1 \left( -\nu_{k_l} - iqe_d, \frac{1}{2} - \nu_{k_l} + iqe_d - i\zeta_0 \omega; 1 - 2\nu_{k_l}; \frac{2\zeta}{\zeta + \zeta_0} \right) \right]. \end{aligned} \quad (4.83)$$

These solutions are linear combinations of incoming and outgoing solutions as

$$\begin{aligned}\tilde{y}^{(0,l)} &= (\zeta - \zeta_0)^{-\frac{i\omega}{4\pi T}} c_{in} \tilde{y}_{in}^{(0,l)} + (\zeta - \zeta_0)^{\frac{i\omega}{4\pi T}} c_{out} \tilde{y}_{out}^{(0,l)} \\ &= (\zeta - \zeta_0)^{-\frac{i\omega\zeta_0}{2}} c_{in} \tilde{y}_{in}^{(0,l)} + (\zeta - \zeta_0)^{\frac{i\omega\zeta_0}{2}} c_{out} \tilde{y}_{out}^{(0,l)} .\end{aligned}\quad (4.84)$$

We require the solution to be an incoming wave at the horizon (i.e.  $\sim (\zeta - \zeta_0)^{-\frac{i\omega\zeta_0}{2}}$ ).

Therefore, we expand the solution around  $\zeta_0$  and we find that

$$c_{in} = c_{out} \frac{(-1)^{1-2\nu_{kl}} \Gamma(1 - 2\nu_{kl}) \Gamma(\nu_{kl} - iqe_d) \Gamma\left(\frac{1}{2} + iqe_d + \nu_{kl} - i\zeta_0\omega\right)}{\Gamma(2\nu_{kl} + 1) \Gamma(-iqe_d - \nu_{kl}) \Gamma\left(\frac{1}{2} + iqe_d - \nu_{kl} - i\zeta_0\omega\right)}, \quad (4.85)$$

or substituting  $T = \frac{1}{2\pi\zeta_0}$  and using the identity  $\Gamma(1+t) = t\Gamma(t)$  for Gamma functions we obtain

$$c_{in} = (-1)^{2-2\nu_{kl}} c_{out} \frac{(iqe_d + \nu_{kl})}{(iqe_d - \nu_{kl})} \cdot \frac{\Gamma(-2\nu_{kl}) \Gamma(1 + \nu_{kl} - iqe_d) \Gamma\left(\frac{1}{2} + iqe_d + \nu_{kl} - \frac{i\omega}{2\pi T}\right)}{\Gamma(2\nu_{kl}) \Gamma(1 - iqe_d - \nu_{kl}) \Gamma\left(\frac{1}{2} + iqe_d - \nu_{kl} - \frac{i\omega}{2\pi T}\right)}. \quad (4.86)$$

We can use the transformation of hypergeometric functions which are given by Abramowitz and Stegun, in 1964 as

$$\begin{aligned}F(a, b; c; z) &= (1-z)^{c-a-b} {}_2F_1(c-a, c-b; c; z) \\ &= \frac{\Gamma(c)\Gamma(c-a-b)}{\Gamma(c-a)\Gamma(c-b)} z^{-a} {}_2F_1\left(a, a-c+1; a+b-c+1; 1-\frac{1}{z}\right) \\ &\quad + \frac{\Gamma(c)\Gamma(a+b-c)}{\Gamma(a)\Gamma(b)} (1-z)^{c-a-b} z^{a-c} {}_2F_1\left(c-a, 1-a; c-a-b+1; 1-\frac{1}{z}\right) \\ &\quad \text{with } (|\arg(1-z)| < \pi, |1-z| < 1) .\end{aligned}\quad (4.87)$$



Then the two linearly independent solutions are

$$\begin{aligned}
\tilde{y}^{(0,l)} &= \left(1 + \frac{\zeta_0}{\zeta}\right)^{\frac{1}{2} + iqe_d - \frac{i\omega\zeta_0}{2}} \\
&\times \left[ c_{in} \left(\frac{\zeta_0}{\zeta} - 1\right)^{-\frac{i\omega\zeta_0}{2}} {}_2F_1\left(\frac{1}{2} - \nu_{k_l} + iqe_d - i\omega\zeta_0, \frac{1}{2} + \nu_{k_l} + iqe_d - i\omega\zeta_0; \frac{1}{2} - i\omega\zeta_0; \frac{\zeta - \zeta_0}{2\zeta}\right) \right. \\
&\quad \left. + c_{out} \left(\frac{\zeta_0}{\zeta} - 1\right)^{\frac{1}{2} + \frac{i\omega\zeta_0}{2}} {}_2F_1\left(1 - \nu_{k_l} + iqe_d, 1 + \nu_{k_l} + iqe_d; \frac{3}{2} + i\omega\zeta_0; \frac{\zeta - \zeta_0}{2\zeta}\right) \right]
\end{aligned} \tag{4.88}$$

Similarly, we can find the two linearly independent solutions for lower component  $\tilde{z}$  as the following.

$$\begin{aligned}
\tilde{z}^{(0,l)} &= \left(1 + \frac{\zeta_0}{\zeta}\right)^{\frac{1}{2} - iqe_d + \frac{i\omega\zeta_0}{2}} \\
&\times \left[ c_{in} \left(\frac{\zeta_0}{\zeta} - 1\right)^{\frac{i\omega\zeta_0}{2}} {}_2F_1\left(\frac{1}{2} - \nu_{k_l} - iqe_d + i\omega\zeta_0, \frac{1}{2} + \nu_{k_l} - iqe_d + i\omega\zeta_0; \frac{1}{2} + i\omega\zeta_0; \frac{\zeta - \zeta_0}{2\zeta}\right) \right. \\
&\quad \left. + c_{out} \left(\frac{\zeta_0}{\zeta} - 1\right)^{\frac{1}{2} - \frac{i\omega\zeta_0}{2}} {}_2F_1\left(1 - \nu_{k_l} - iqe_d, 1 + \nu_{k_l} - iqe_d; \frac{3}{2} - i\omega\zeta_0; \frac{\zeta - \zeta_0}{2\zeta}\right) \right]
\end{aligned} \tag{4.89}$$

Earlier we defined (4.79) the spinor field near horizon region can be found by solving the equation for  $\Phi^{(0,l)} = \frac{1}{\sqrt{2}}(1 - i\sigma^1)\tilde{\Phi}^{(0,l)}$ . Near the AdS<sub>2</sub> boundary, i.e.  $\zeta \rightarrow 0$ , Dirac equation becomes

$$(\zeta\partial_\zeta - i\sigma^3qe_d)\tilde{\Phi}^{(0,l)} = R_2(m_f\sigma^2 + \tilde{m}\sigma^1)\tilde{\Phi}^{(0,l)}. \tag{4.90}$$

We write  $\tilde{\Phi}^{(0,l)} = \frac{1}{\sqrt{2}}(1 + i\sigma^1)\Phi^{(0,l)}$  in (4.90) then we find

$$\zeta\partial_\zeta(1 + i\sigma^1)\Phi^{(0,l)} = [R_2(m_f\sigma^2 + \tilde{m}\sigma^1) + i\sigma^3qe_d](1 + i\sigma^1)\Phi^{(0,l)}. \tag{4.91}$$

which gives

$$\zeta \partial_\zeta \begin{pmatrix} y + iz \\ iy + z \end{pmatrix} = \begin{pmatrix} (iqe_d + (m_f + i\tilde{m})R_2) & -(qe_d + (im_f - \tilde{m})R_2) \\ (qe_d + (im_f + \tilde{m})R_2) & -i(qe_d - (im_f + \tilde{m})R_2) \end{pmatrix} \begin{pmatrix} y \\ z \end{pmatrix} \quad (4.92)$$

finally we obtain [120]

$$\zeta \partial_\zeta \Phi^{(0,l)} = U \Phi^{(0,l)}, \quad U = \begin{pmatrix} m_f R_2 & \tilde{m} R_2 - qe_d \\ \tilde{m} R_2 + qe_d & -m_f R_2 \end{pmatrix}. \quad (4.93)$$

The boundary behavior of  $\Phi^{(0,l)}$  can be written as

$$\Phi^{(0,l)} = A v_-^{(0,l)} \zeta^{-\nu_{k_l}} (1 + \mathcal{O}(\zeta)) + B v_+^{(0,l)} \zeta^{\nu_{k_l}} (1 + \mathcal{O}(\zeta)). \quad (4.94)$$

The coefficients  $v_\pm^{(0,l)}$  can be found by substituting (4.94) in (4.93) as

$$v_\pm^{(0,l)} = \begin{pmatrix} m_f R_2 \pm \nu_{k_l} \\ \tilde{m} R_2 + qe_d \end{pmatrix} \quad (4.95)$$

where we chose the normalization so that the bottom components are the same. Then the retarded AdS<sub>2</sub> Green's function is obtained from

$$\mathcal{G}_R = \frac{B}{A} \quad (4.96)$$

near AdS<sub>2</sub> boundary. To find the retarded AdS<sub>2</sub> Green's function let us write

$$\tilde{\Phi}^{(0,l)} = c_{out} \begin{pmatrix} (\tilde{m} - im_f) y_{out}^{(0,l)} \\ -z_{out}^{(0,l)} \end{pmatrix} + c_{in} \begin{pmatrix} -y_{in}^{(0,l)} \\ (\tilde{m} + im_f) z_{in}^{(0,l)} \end{pmatrix} \quad (4.97)$$

where

$$\begin{aligned}
y_{out}^{(0,l)} &= \frac{1}{\sqrt{2}} \left( \tilde{y}_{out}^{(0,l)} - i\tilde{z}_{out}^{(0,l)} \right) \\
y_{in}^{(0,l)} &= \frac{1}{\sqrt{2}} \left( \tilde{y}_{in}^{(0,l)} - i\tilde{z}_{in}^{(0,l)} \right) \\
z_{out}^{(0,l)} &= \frac{1}{\sqrt{2}} \left( -i\tilde{y}_{out}^{(0,l)} + \tilde{z}_{out}^{(0,l)} \right) \\
z_{in}^{(0,l)} &= \frac{1}{\sqrt{2}} \left( -i\tilde{y}_{in}^{(0,l)} + \tilde{z}_{in}^{(0,l)} \right)
\end{aligned} \tag{4.98}$$

with

$$\begin{aligned}
\tilde{y}_{out}^{(0,l)} &= \left( 1 + \frac{\zeta_0}{\zeta} \right)^{\frac{1}{2} + iqe_d - \frac{i\omega\zeta_0}{2}} \left( \frac{\zeta_0}{\zeta} - 1 \right)^{\frac{1}{2} + \frac{i\omega\zeta_0}{2}} \\
&\quad \times {}_2F_1 \left( 1 - \nu_{k_l} + iqe_d, 1 + \nu_{k_l} + iqe_d; \frac{3}{2} + i\omega\zeta_0; \frac{\zeta - \zeta_0}{2\zeta} \right), \\
\tilde{y}_{in}^{(0,l)} &= \left( 1 + \frac{\zeta_0}{\zeta} \right)^{\frac{1}{2} + iqe_d - \frac{i\omega\zeta_0}{2}} \left( \frac{\zeta_0}{\zeta} - 1 \right)^{-\frac{i\omega\zeta_0}{2}} \\
&\quad \times {}_2F_1 \left( \frac{1}{2} - \nu_{k_l} + iqe_d - i\omega\zeta_0, \frac{1}{2} + \nu_{k_l} + iqe_d - i\omega\zeta_0; \frac{1}{2} - i\omega\zeta_0; \frac{\zeta - \zeta_0}{2\zeta} \right), \\
\tilde{z}_{out}^{(0,l)} &= \left( 1 + \frac{\zeta_0}{\zeta} \right)^{\frac{1}{2} - iqe_d + \frac{i\omega\zeta_0}{2}} \left( \frac{\zeta_0}{\zeta} - 1 \right)^{\frac{1}{2} - \frac{i\omega\zeta_0}{2}} \\
&\quad \times {}_2F_1 \left( 1 - \nu_{k_l} - iqe_d, 1 + \nu_{k_l} - iqe_d; \frac{3}{2} - i\omega\zeta_0; \frac{\zeta - \zeta_0}{2\zeta} \right), \\
\tilde{z}_{in}^{(0,l)} &= \left( 1 + \frac{\zeta_0}{\zeta} \right)^{\frac{1}{2} - iqe_d + \frac{i\omega\zeta_0}{2}} \left( \frac{\zeta_0}{\zeta} - 1 \right)^{\frac{i\omega\zeta_0}{2}} \\
&\quad \times {}_2F_1 \left( \frac{1}{2} - \nu_{k_l} - iqe_d + i\omega\zeta_0, \frac{1}{2} + \nu_{k_l} - iqe_d + i\omega\zeta_0; \frac{1}{2} + i\omega\zeta_0; \frac{\zeta - \zeta_0}{2\zeta} \right).
\end{aligned} \tag{4.99}$$

The retarded AdS<sub>2</sub> Green's function can be found by expanding around  $\zeta = 0$ .

Therefore, we obtain

$$\mathcal{G}_R = (4\pi T)^{2\nu_{k_l}} \frac{(m_f - i\tilde{m})R_2 + iqe_d + \nu_{k_l}}{(m_f - i\tilde{m})R_2 + iqe_d - \nu_{k_l}} \frac{\Gamma(-2\nu_{k_l})\Gamma(1 + \nu_{k_l} - iqe_d)\Gamma\left(\frac{1}{2} + iqe_d + \nu_{k_l} - \frac{i\omega}{2T}\right)}{\Gamma(2\nu_{k_l})\Gamma(1 - iqe_d - \nu_{k_l})\Gamma\left(\frac{1}{2} + iqe_d - \nu_{k_l} - \frac{i\omega}{2T}\right)}. \tag{4.100}$$

The zeroth order Dirac equation in the near region at finite temperature can be reorganized as

$$\partial_\zeta \tilde{\Phi}_\alpha^{(0,l)} - i\sigma^3 \frac{\omega + qA_{t0}}{f} \tilde{\Phi}_\alpha^{(0,l)} - \frac{R_2}{\zeta \sqrt{f}} (m_f \sigma^2 + \tilde{m} \sigma^1) \tilde{\Phi}_\alpha^{(0,l)} = 0 \quad (4.101)$$

where  $A_{t0} = \frac{e_d}{\zeta} \left(1 - \frac{\zeta}{\zeta_0}\right)$ . To be able to expand in small  $\omega$  we make a change of variable as  $u = \omega \zeta$  and  $u_0 = \omega \zeta_0$  where the inner region is  $\epsilon < u < \infty$  and outer region is  $u < \epsilon$ , where  $\epsilon \ll 1$ . Then we will compare the solutions in the overlapping region which is  $u \rightarrow 0$ . After the coordinate transformation and setting  $m_f = 0$  we can write

$$\partial_u \tilde{\Phi}_\alpha^{(0,l)} - i\sigma^3 \frac{1 + qe_d \left(\frac{1}{u} - \frac{1}{u_0}\right)}{f(u)} \tilde{\Phi}_\alpha^{(0,l)} - \frac{\tilde{m} R_2}{u \sqrt{f(u)}} \sigma^1 \tilde{\Phi}_\alpha^{(0,l)} = 0 \quad (4.102)$$

where  $f(u) = 1 - \frac{u^2}{u_0^2}$ . Then the second order differential equation is

$$\partial_u^2 \tilde{\Phi}_\alpha^{(0,l)} - \frac{h'_{11}}{h_{11}} \tilde{\Phi}_\alpha^{(0,l)} - \left( h_{11}^2 + h_{22}^2 + (-1)^\alpha \frac{h_{22} h'_{11}}{h_{11}} - (-1)^\alpha h_{22} \right) \tilde{\Phi}_\alpha^{(0,l)} = 0 \quad (4.103)$$

where

$$h_{11} = -\frac{\tilde{m} R_2}{u \sqrt{f(u)}}, \quad h_{22} = i \frac{1 + qe_d \left(\frac{1}{u} - \frac{1}{u_0}\right)}{f(u)}. \quad (4.104)$$

Solving the equations we find the incoming and outgoing solutions as

$$\begin{aligned} \tilde{y}^{(0,l)} = & c_{out} \left( \frac{u + u_0}{u} \right)^{\nu_{k_l}} \left( \frac{u - u_0}{u + u_0} \right)^{-i \frac{u_0}{2}} \\ & \times {}_2F_1 \left( -iqe_d - \nu_{k_l}, \frac{1}{2} + iqe_d - iu_0 - \nu_{k_l}, 1 - 2\nu_{k_l}, \frac{2u}{u + u_0} \right) \\ & + c_{in} \left( \frac{u}{u + u_0} \right)^{\nu_{k_l}} \left( \frac{u - u_0}{u + u_0} \right)^{-i \frac{u_0}{2}} \\ & \times {}_2F_1 \left( -iqe_d + \nu_{k_l}, \frac{1}{2} + iqe_d - iu_0 + \nu_{k_l}, 1 + 2\nu_{k_l}, \frac{2u}{u + u_0} \right) \end{aligned} \quad (4.105)$$

and

$$\begin{aligned} \tilde{z}^{(0,l)} = & c_{out} \left( \frac{u+u_0}{u} \right)^{\nu_{k_l}} \left( \frac{u-u_0}{u+u_0} \right)^{i\frac{u_0}{2}} {}_2F_1 \left( iqe_d - \nu_{k_l}, \frac{1}{2} - iqe_d + iu_0 - \nu_{k_l}, 1 - 2\nu_{k_l}, \frac{2u}{u+u_0} \right) \\ & + c_{in} \left( \frac{u}{u+u_0} \right)^{\nu_{k_l}} \left( \frac{u-u_0}{u+u_0} \right)^{i\frac{u_0}{2}} {}_2F_1 \left( iqe_d + \nu_{k_l}, \frac{1}{2} - iqe_d + iu_0 + \nu_{k_l}, 1 + 2\nu_{k_l}, \frac{2u}{u+u_0} \right). \end{aligned} \quad (4.106)$$

where  $\nu_{k_l} = \sqrt{\tilde{m}^2 - q^2 e_d^2}$ . After transformation of the Hypergeometric function we can also write the upper component of  $\tilde{\Phi}_\alpha^{(0,l)}$  as

$$\begin{aligned} \tilde{y}^{(0,l)} = & c_{in} \left( 1 + \frac{u_0}{u} \right)^{\frac{1}{2} + i(qe_d - \frac{u_0}{2})} \left( \frac{u_0}{u} - 1 \right)^{-\frac{i u_0}{2}} \\ & \times {}_2F_1 \left( \frac{1}{2} + iqe_d - \nu_{k_l} - iu_0, \frac{1}{2} + iqe_d - iu_0 + \nu_{k_l}, \frac{1}{2} - iu_0, \frac{u-u_0}{2u} \right) \\ & + c_{out} \left( 1 + \frac{u_0}{u} \right)^{\frac{1}{2} + i(qe_d - \frac{u_0}{2})} \left( \frac{u_0}{u} - 1 \right)^{1 + i\frac{u_0}{2}} \\ & \times {}_2F_1 \left( 1 + iqe_d - \nu_{k_l}, 1 + iqe_d + \nu_{k_l}, \frac{3}{2} + iu_0, \frac{u-u_0}{2u} \right). \end{aligned} \quad (4.107)$$

#### 4.4.4 First Order Solution to Dirac Equations

##### First Order Numerical Solution to Dirac Equations

Below the critical temperature the first order Dirac equations before rotation are

$$\partial_z \psi_{\alpha j}^{(1,l)} - i \frac{qf\mu_0(1-z) + \omega}{h} \sigma^2 \psi_{\alpha j}^{(1,l)} + \frac{k_x + Kl}{\sqrt{h}} \sigma^3 \psi_{\alpha j}^{(1,l)} - \frac{k_y}{\sqrt{h}} \sigma^1 \psi_{\beta m}^{(1,l)} + \mathcal{A} = 0 \quad (4.108)$$

where

$$\begin{aligned} \mathcal{A} = & - \left( \frac{Q_{zz11}}{4} \psi_{\alpha j}^{(0,l-1)'} + \frac{Q_{zz11}}{4} \psi_{\alpha j}^{(0,l+1)'} + \frac{Q_{zz10}}{2} \psi_{\alpha j}^{(0,l)'} \right) + \mathcal{M}_\alpha^{(0,l-1)} \psi_{\alpha j}^{(0,l-1)} \\ & + \mathcal{M}_{\alpha j}^{(0,l+1)} \psi_{\alpha j}^{(0,l+1)} + \mathcal{M}_{\alpha j}^{(0,l)} \psi_{\alpha j}^{(0,l)} + \frac{Q_{yy11}}{4\sqrt{h}} \sigma^1 \psi_{\beta m}^{(0,l-1)} + \frac{Q_{yy11}}{4\sqrt{h}} \sigma^1 \psi_{\beta m}^{(0,l+1)} + \frac{Q_{yy10}}{2\sqrt{h}} \sigma^1 \psi_{\beta m}^{(0,l)}, \end{aligned} \quad (4.109)$$

$$\mathcal{M}_{\alpha j}^{(0,l)} = i \left[ \frac{(q_f \mu_0 (1-z) + \omega) Q_{tt10}}{2h} - \frac{q_f (1-z) A_{t10}}{h} \right] \sigma^2 - \alpha \frac{(k_x + Kl) Q_{xx10}}{2\sqrt{h}} \sigma^1, \quad (4.110)$$

$$\begin{aligned} \mathcal{M}_{\alpha j}^{(0,l \mp 1)} = & i \left[ \frac{(q_f \mu_0 (1-z) + \omega) Q_{tt11}}{4h} - \frac{q_f (1-z) A_{t11}}{2h} \right] \sigma^2 \pm \frac{\alpha k Q_{zz11}}{4\sqrt{h}} \sigma^1 \\ & - \alpha \frac{(\pm k + k_x + K(l \mp 1)) Q_{xx11}}{4\sqrt{h}} \sigma^1 \end{aligned} \quad (4.111)$$

where  $\alpha = +, -, j = 1, 2$  and  $\beta = -\alpha, m = 3 - j$ .

The first order Dirac equations show us that the  $(l \pm 1)$ , and  $(l)$  modes of the zeroth order spinor fields are mixed with each other.

Applying ingoing boundary conditions at the horizon we can write

$$\begin{aligned} \psi_{+,1}^{(1,l)}(z) &= (1-z)^{-\frac{i\omega}{4\pi T}} F_1^{(1,l)}(z), \\ \psi_{+,2}^{(1,l)}(z) &= (1-z)^{-\frac{i\omega}{4\pi T}} F_2^{(1,l)}(z), \\ \psi_{-,1}^{(1,l)}(z) &= (1-z)^{-\frac{i\omega}{4\pi T}} F_3^{(1,l)}(z), \\ \psi_{-,2}^{(1,l)}(z) &= (1-z)^{-\frac{i\omega}{4\pi T}} F_4^{(1,l)}(z). \end{aligned} \quad (4.112)$$

After doing the similar calculations for the first order and applying the ingoing boundary conditions we obtain the first order Dirac equations. When we calculate the retarded Green's function from (4.49) we see that there is no contribution to the Green's function at first order. We solve the first order equations to use them in solving the second order equations.

### First Order Analytical Solution to Dirac Equations

At the first order we can write the Dirac equations as

$$-\frac{mR_2}{\zeta\sqrt{f}} \sigma^2 \tilde{\Phi}_\alpha^{(1,l)} + \partial_\zeta \tilde{\Phi}_\alpha^{(1,l)} - \frac{i}{f} \sigma^3 (\omega + qA_{t0}) \tilde{\Phi}_\alpha^{(1,l)} + \frac{k_l R_2}{\zeta\sqrt{f}\mu_* R} (-1)^\alpha \sigma^1 \tilde{\Phi}_\alpha^{(1,l)} + \tilde{\mathcal{A}}_{\alpha,\beta}^{(0,l')} = 0 \quad (4.113)$$

where

$$\begin{aligned} \tilde{\mathcal{A}}_{\alpha,\beta}^{(0,l')} = & - \left( \frac{1}{4} Q_{zz11} \tilde{\Phi}_\alpha^{(0,l-1)'} + \frac{1}{4} Q_{zz11} \tilde{\Phi}_\alpha^{(0,l+1)'} + \frac{1}{2} Q_{zz10} \tilde{\Phi}_\alpha^{(0,l)'} \right) + \mathcal{M}_\alpha^{(0,l-1)} \tilde{\Phi}_\alpha^{(0,l-1)} \\ & + \mathcal{M}_\alpha^{(0,l+1)} \tilde{\Phi}_\alpha^{(0,l+1)} + \mathcal{M}_\alpha^{(0,l)} \tilde{\Phi}_\alpha^{(0,l)} + \mathcal{N}_\beta^{(0,l-1)} \tilde{\Phi}_\beta^{(0,l-1)} + \mathcal{N}_\beta^{(0,l+1)} \tilde{\Phi}_\beta^{(0,l+1)} + \mathcal{N}_\beta^{(0,l)} \tilde{\Phi}_\beta^{(0,l)} , \end{aligned} \quad (4.114)$$

with

$$\begin{aligned} \mathcal{M}_\alpha^{(0,l\mp 1)} = & \frac{i \left[ qe_d \left( \frac{\zeta_0}{\zeta} - 1 \right) Q_{tt11} + 2q(\zeta - \zeta_0) A_{t11} \right]}{4\zeta_0 f} \sigma^3 + (-1)^\alpha \frac{\pm k (k_1 + K(l \mp 1)) \tilde{m} R_2 Q_{zz11}}{4z k_{l\mp 1}^2} \sigma^1 \\ & + \frac{(-1)^\alpha \tilde{m} R_2}{4z \sqrt{f} k_{l\mp 1}^2} \\ & \times \left[ (k_{l\mp 1}^2 - (k_1 + K(l \mp 1))^2) Q_{yy11} + (k_1 + K(l \mp 1)) (k_1 \pm k + K(l \mp 1)) Q_{xx11} \right] \sigma^1 , \end{aligned} \quad (4.115)$$

$$\begin{aligned} \mathcal{M}_\alpha^{(0,l)} = & \frac{i \left[ qe_d \left( \frac{\zeta_0}{\zeta} - 1 \right) Q_{tt10} + 2q(\zeta - \zeta_0) A_{t10} \right]}{2\zeta_0 f} \sigma^3 \\ & + (-1)^\alpha \frac{\tilde{m} R_2 [(k_1 + Kl)^2 Q_{xx10} - ((k_1 + Kl)^2 - k_l^2) Q_{yy10}]}{2z k_l \sqrt{f}} \sigma^1 , \end{aligned} \quad (4.116)$$

$$\begin{aligned} \mathcal{N}_\beta^{(0,l\mp 1)} = & \frac{(-1)^\alpha \tilde{m} R_2 (k_1 + K(l \mp 1) + k_{l\mp 1}) [(k_1 \pm k + K(l \mp 1)) Q_{xx11} - (k_1 + K(l \mp 1)) Q_{yy11}]}{4z \sqrt{f} k_{l\mp 1}^2} \sigma^1 \\ & \pm \frac{(-1)^\alpha \tilde{m} R_2 (k_1 + K(l \mp 1) + k_{l\mp 1}) k Q_{zz11}}{4z \sqrt{f} k_{l\mp 1}^2} \sigma^1 , \end{aligned} \quad (4.117)$$

$$\mathcal{N}_\beta^{(0,l)} = (-1)^\alpha \frac{\tilde{m} R_2 (k_1 + Kl - (1)^\alpha k_l) (Q_{xx10} - Q_{yy10})}{2z \sqrt{f} k_l^2} \sigma^1 . \quad (4.118)$$

where we defined  $\tilde{m} = \frac{k_l}{\mu_* R}$ .

As in the zero temperature case [117] we divide the spacetime in two regions, i.e. near region and far region and then compare the solutions in the overlapping region which is  $u \rightarrow 0$ .

In the near region the first order Dirac equation is

$$\begin{aligned} \partial_\zeta \tilde{\Phi}_\alpha^{(1,l)} - i\sigma^3 \frac{\omega + q_f A_t}{f} \tilde{\Phi}_\alpha^{(1,l)} - \frac{R_2}{\zeta \sqrt{f}} (m_f \sigma^2 + \tilde{m} \sigma^1) \tilde{\Phi}_\alpha^{(1,l)} \\ + \frac{iq}{\zeta_0 \left(1 + \frac{\zeta}{\zeta_0}\right)} \sigma^3 \sum_{\beta; l' = l \pm 1} M_{\alpha\beta, l'} \tilde{\Phi}_\beta^{(0,l')} = 0 \end{aligned} \quad (4.119)$$

with

$$M_{\alpha\beta, l'} \tilde{\Phi}_\beta^{(0,l')} = \frac{iq A_{t11}}{2\zeta_0 \left(1 + \frac{\zeta}{\zeta_0}\right)} \sigma^3 \tilde{\Phi}_\beta^{(0,l')} + \frac{iq A_{t10}}{\zeta_0 \left(1 + \frac{\zeta}{\zeta_0}\right)} \sigma^3 \tilde{\Phi}_\beta^{(0,l')} \quad (4.120)$$

where we used the boundary condition that at the boundary of the near region  $Q_{tt} = Q_{zz} = Q_{xx} = Q_{yy} = 1$ . After the coordinate transformation the second order equation is

$$\partial_u^2 \tilde{\Phi}_\alpha^{(1,l)} - \frac{h'_{11}}{h_{11}} \tilde{\Phi}_\alpha^{(1,l)} - \left( h_{11}^2 + h_{22}^2 + (-1)^\alpha \frac{h_{22} h'_{11}}{h_{11}} - (-1)^\alpha h_{22} \right) \tilde{\Phi}_\alpha^{(1,l)} + X_{\alpha j}^l = 0 \quad (4.121)$$

where

$$X_{\alpha j}^l = \sum_{\beta; l' = l \pm 1, l} X_{(\alpha\beta, l')} \quad (4.122)$$

with

$$X_{(\alpha\beta, l')} = \frac{iq(-(-1)^\alpha h_{11} + h_{22}) M_{\alpha\beta, l'} \tilde{\Phi}_\beta^{(0,l')}}{u + u_0} - (-1)^\alpha h_{11} \partial_u \left( \frac{iq M_{\alpha\beta, l'} \tilde{\Phi}_\beta^{(0,l')}}{(u + u_0) h_{11}} \right) \quad (4.123)$$

The first order inhomogeneous Dirac equations can be solved by using the homogeneous solution with the help of Green's function. Let us review the solution of non-homogeneous differential equation with Green's function. For the boundary value problem

$$\frac{d}{du} \left( p(u) \frac{dy(u)}{du} \right) + q(u) y(u) = f(u) , \quad (4.124)$$

with  $y(a) = 0$ ,  $y'(b) = 0$  the solution is of the form

$$y(u) = \int_a^b G(u, u') f(u') du' , \quad (4.125)$$



where Green's function is defined as

$$G(u, u') = \begin{cases} \frac{y_1(u')y_2(u)}{pW} & a \leq u' \leq u \\ \frac{y_1(u)y_2(u')}{pW} & u \leq u' \leq b \end{cases} \quad (4.126)$$

where  $W$  is the Wronskian for homogeneous solution.

As mentioned earlier in zero temperature case the solution for inhomogeneous equations are going to be found in terms of homogeneous solutions at zeroth order. To solve these inhomogeneous differential equations we are going to follow the same steps as followed in [117] and as we followed in zero temperature case. We will use the similar notation. The special solution to the inhomogeneous equation is found from Green's function

$$G_{\alpha j}^{(l)}(u, u') = \frac{\eta_{1\alpha j}^l \eta_{2\alpha j}^l \theta(u - u') + \eta_{1\alpha j}^l \eta_{2\alpha j}^l \theta(u' - u)}{W(u)}. \quad (4.127)$$

where we defined  $\eta_{1\alpha j}^l = \tilde{\Phi}_{\alpha j}^{(0,l),\text{in}}$  and  $\eta_{2\alpha j}^l = \tilde{\Phi}_{\alpha j}^{(0,l),\text{out}}$ . The  $W(u)$  term in the Green's function above is the Wronskian determinant of the system which can be stated as

$$W(u) = \eta_{1\alpha j}^l \partial_u \eta_{2\alpha j}^l - \eta_{2\alpha j}^l \partial_u \eta_{1\alpha j}^l. \quad (4.128)$$

Then the near horizon region Wronskian is found to be

$$W(u) = c_0 \frac{-5u + 9u_0}{\sqrt{u - u_0}}. \quad (4.129)$$

Then the special solution to the first order Dirac equations at finite temperature is

$$\eta_{s,\text{canonical}}^{(1,l)}(\alpha j, \beta l')(u) = \eta_{1\alpha j}^l \int_0^u du' \frac{\eta_{2\alpha j}^l X_{(\alpha j, \beta l')}}{W(u')} + \eta_{2\alpha j}^l \int_x^\infty du' \frac{\eta_{1\alpha j}^l X_{(\alpha j, \beta l')}}{W(u')}. \quad (4.130)$$

To fix the coefficients of ingoing homogeneous solutions we change the integration limits and set the upper limit of the first integral to  $\infty$ . Then we find the special

solution as

$$\eta_{s(\alpha_j, \beta^{l'})}^{(1,l)}(u) = -\eta_{1\alpha_j}^l \int_u^\infty du' \frac{\eta_{2\alpha_j}^l X_{(\alpha_j, \beta^{l'})}}{W(u')} + \eta_{2\alpha_j}^l \int_u^\infty du' \frac{\eta_{1\alpha_j}^l X_{(\alpha_j, \beta^{l'})}}{W(u')} . \quad (4.131)$$

The near region solution can be written with the contribution from infalling homogeneous solution as

$$\tilde{\Phi}_{\alpha_j}^{(1,l)} = \eta_{s(\alpha_j)}^{(1,l)}(u) + c_4 \eta_{1\alpha_j}^l(u) \quad (4.132)$$

with an arbitrary constant  $c_4$  which can be set to zero due to the fact that Green's functions are independent of normalization.

Remember that we use matching method therefore we need the behavior of this special solution at the boundary of the near horizon region, i.e.  $u \ll 1$ . To analyze the boundary of the near region we separate the integral in the special solution into two parts as following.

$$\begin{aligned} \eta_{s(\alpha_j, \beta^{l'})}^{(1,l)}(u) = & -\eta_{1\alpha_j}^l \int_\epsilon^\infty du' \frac{\eta_{2\alpha_j}^l X_{(\alpha_j, \beta^{l'})}}{W(u')} + \eta_{2\alpha_j}^l \int_\epsilon^\infty du' \frac{\eta_{1\alpha_j}^l X_{(\alpha_j, \beta^{l'})}}{W(u')} \\ & -\eta_{1\alpha_j}^l \int_u^\epsilon du' \frac{\eta_{2\alpha_j}^l X_{(\alpha_j, \beta^{l'})}}{W(u')} + \eta_{2\alpha_j}^l \int_u^\epsilon du' \frac{\eta_{1\alpha_j}^l X_{(\alpha_j, \beta^{l'})}}{W(u')} . \end{aligned} \quad (4.133)$$

The first two terms can be calculated as constants as  $\epsilon$  is a non-zero constant. Now, we will analyze the  $u$ -dependence of the third and the fourth terms above by using the asymptotic values of the homogeneous solutions, i.e.

$$\eta_{1\alpha_j}^l \sim \omega^{\nu_{k_l}} \left( u^{-\nu_{k_l}} + \tilde{\mathcal{G}}_{IR} u^{\nu_{k_l}} \right) , \quad \eta_{2\alpha_j}^l \sim \omega^{\nu_{k_l}} \left( u^{-\nu_{k_l}} + \tilde{\mathcal{G}}_{IR}^\dagger u^{\nu_{k_l}} \right) . \quad (4.134)$$

To obtain the  $\omega$ -dependence of the non-homogeneous solution we make a linear transformation in which the special solution is invariant, i.e.

$$\eta_{1\alpha_j}^l = a_{1\alpha_j} u^{-\nu_{k_l}} + a_{2\alpha_j} u^{\nu_{k_l}} , \quad \eta_{2\alpha_j}^l = a_{1\alpha_j} u^{-\nu_{k_l}} + a_{2\alpha_j} u^{\nu_{k_l}} . \quad (4.135)$$

Therefore, we find the  $\omega$ -dependence of the special solution at the boundary of the near region as

$$\begin{aligned} \eta_{s(\alpha j, \beta l')}^{(1, l)}(u) \approx & u^{\nu_{k_l}} \omega^{\nu_{k_{l'}}} n_{1(\alpha j, \beta l')}^{(1, l)} + u^{-\nu_{k_l}} \omega^{\nu_{k_{l'}}} n_{2(\alpha j, \beta l')}^{(1, l)} \\ & + u^{\nu_{k_{l'}}} \omega^{\nu_{k_l}} n_{3(\alpha j, \beta l')}^{(1, l)} + u^{-\nu_{k_{l'}}} \omega^{\nu_{k_l}} n_{4(\alpha j, \beta l')}^{(1, l)} \end{aligned} \quad (4.136)$$

where the coefficients are calculated as

$$\begin{aligned} n_{1(\alpha j, \beta l')}^{(1, l)} = & \omega^{-\nu_{k_{l'}}} \int_{\infty}^{\epsilon} dz \frac{\eta_{1\alpha j}^l X_{(\alpha j, \beta l')}^l}{W(z)} \\ & + \frac{iqM_{\alpha\beta, ll'}}{9(-u_0)^{3/2}} [-2(-1)^\alpha + 2iqe_d + (-1)^\alpha \tilde{m}R_2 + (-1)^\alpha \tilde{m}'R_2] \\ & \times \left[ \frac{\epsilon^{-\nu_{k_l} - \nu_{k_{l'}}}}{\nu_{k_l} + \nu_{k_{l'}}} v_{-\beta j}^{(0, l')} + \frac{\epsilon^{\nu_{k_l} + \nu_{k_{l'}}}}{\nu_{k_l} - \nu_{k_{l'}}} \tilde{\mathcal{G}}_{\beta}^{\prime} v_{+\beta j}^{(0, l')} \right], \end{aligned} \quad (4.137)$$

$$\begin{aligned} n_{2(\alpha j, \beta l')}^{(1, l)} = & -\omega^{-\nu_{k_{l'}}} \int_{\infty}^{\epsilon} dz \frac{\eta_{2\alpha j}^l X_{(\alpha j, \beta l')}^l}{W(z)} \\ & + \frac{iqM_{\alpha\beta, ll'}}{9(-u_0)^{3/2}} [-2(-1)^\alpha + 2iqe_d + (-1)^\alpha \tilde{m}R_2 + (-1)^\alpha \tilde{m}'R_2] \\ & \times \left[ \frac{\epsilon^{\nu_{k_l} - \nu_{k_{l'}}}}{\nu_{k_l} - \nu_{k_{l'}}} v_{-\beta j}^{(0, l')} + \frac{\epsilon^{\nu_{k_l} + \nu_{k_{l'}}}}{\nu_{k_l} + \nu_{k_{l'}}} \tilde{\mathcal{G}}_{\beta}^{\prime} v_{+\beta j}^{(0, l')} \right], \end{aligned} \quad (4.138)$$

$$n_{3(\alpha j, \beta l')}^{(1, l)} = \frac{2iqM_{\alpha\beta, ll'}}{9(-u_0)^{3/2}} [-2(-1)^\alpha + 2iqe_d + (-1)^\alpha \tilde{m}R_2 + (-1)^\alpha \tilde{m}'R_2] \tilde{\mathcal{G}}_{\beta}^{\prime} v_{+\beta j}^{(0, l')}, \quad (4.139)$$

$$n_{4(\alpha j, \beta l')}^{(1, l)} = -\frac{2iqM_{\alpha\beta, ll'}}{9(-u_0)^{3/2}} [-2(-1)^\alpha + 2iqe_d + (-1)^\alpha \tilde{m}R_2 + (-1)^\alpha \tilde{m}'R_2] v_{-\beta j}^{(0, l')} \quad (4.140)$$

The explicit  $\omega$  dependence of this solution scales as  $\omega^{\nu_{k_l} + \nu_{k_{l'}}$ ,  $\omega^{\nu_{k_{l'}} - \nu_{k_l}}$ ,  $\omega^{2\nu_{k_{l'}}$ , and  $\omega^0$ . The non-analyticity due to the possibility of having  $\nu_{k_{l'}} - \nu_{k_l} < 0$  can be overcome by adding a homogeneous solution. Then the non-homogeneous solution is

$$\tilde{\psi}_{\alpha j, \beta l'}^{(1, l)}(u) = \eta_{s(\alpha j, \beta l')}^{(1, l)}(u) + c_4 \eta_{\alpha j}^{(0, l)}(u). \quad (4.141)$$

Substituting  $\eta_{\alpha j}^{(0,l)}(u) = (u^{-\nu_{k_l}} + \tilde{\mathcal{G}}_{IR} u^{\nu_{k_l}})$  one will see that the best choice for  $c_4$  is

$$c_4 = -\omega^{\nu_{k_{l'}}} n_{2\alpha j \beta l'}^l . \quad (4.142)$$

Finally, the first order near region solution is obtained as

$$\begin{aligned} \tilde{\psi}_{\alpha j, \beta l'}^{(1,l)}(u) &\simeq u^{\nu_{k_l}} \omega^{\nu_{k_{l'}}} \tilde{n}_{1\alpha j \beta l'}^l + u^{\nu_{k_{l'}}} \omega^{\nu_{k_l}} n_{3\alpha j \beta l'}^l + u^{-\nu_{k_{l'}}} \omega^{\nu_{k_l}} n_{4\alpha j \beta l'}^l \\ &\simeq u^{\nu_{k_l}} \omega^{\nu_{k_l} + \nu_{k_{l'}}} \tilde{n}_{1\alpha j \beta l'}^l + u^{\nu_{k_{l'}}} \omega^{2\nu_{k_{l'}}} n_{3\alpha j \beta l'}^l + u^{-\nu_{k_{l'}}} \omega^{\nu_{k_l}} n_{4\alpha j \beta l'}^l \end{aligned} \quad (4.143)$$

where

$$\tilde{n}_{1\alpha j \beta l'} = n_{1\alpha j \beta l'}^l - (-1)^j \tilde{\mathcal{G}}_{IR} n_{2\alpha j \beta l'}^l . \quad (4.144)$$

We were able to eliminate the non-analyticity of first order solution in the near region due to  $\omega$  terms but looking at the coefficients (4.138), (4.139), (4.140) we can see that this solution blows up in the degenerate case, i.e.  $\nu_{k_l} = \nu_{k_{l'}}$ .

**Degenerate case**  $\nu_{k_l} = \nu_{k_{l'}}$ :

The issue of divergency in the degenerate case in the near region solutions can be addressed by expanding the first order (4.136) solution in  $\nu_{k_l} \rightarrow \nu_{k_{l'}}$  limit. Then we find at first order

$$\begin{aligned} \eta_{s(\alpha j, \beta l')}^{(1,l)}(u) &\approx u^{\nu_{k_l}} \omega^{\nu_{k_l}} d_{1(\alpha j, \beta l')}^{(1,l)} + u^{-\nu_{k_l}} \omega^{\nu_{k_l}} d_{2(\alpha j, \beta l')}^{(1,l)} + u^{\nu_{k_l}} \omega^{\nu_{k_l}} (\ln \omega) d_{3(\alpha j, \beta l')}^{(1,l)} \\ &\quad + u^{\nu_{k_l}} \omega^{\nu_{k_l}} (\ln \zeta) d_{3(\alpha j, \beta l')}^{(1,l)} + u^{-\nu_{k_l}} \omega^{\nu_{k_l}} (\ln \omega) d_{4(\alpha j, \beta l')}^{(1,l)} \\ &\quad + u^{-\nu_{k_l}} \omega^{\nu_{k_l}} (\ln \zeta) d_{4(\alpha j, \beta l')}^{(1,l)} \end{aligned} \quad (4.145)$$

with the coefficients

$$d_{1(\alpha j, \beta l')}^{(1,l)} = \omega^{-\nu_{k_l}} \int_{\infty}^{\epsilon} dz \frac{\eta_{1\alpha j}^l X_{(\alpha j, \beta l')}^l}{W(z)} - m_{\alpha j, \beta l'}^l \left[ \frac{\epsilon^{-2\nu_{k_l}}}{-2\nu_{k_l}} v_{-\beta j}^{(0,l')} + \left( \frac{1}{2\nu_{k_l}} + \ln \epsilon \right) \tilde{\mathcal{G}}_{\beta}^{l'} v_{+\beta j}^{(0,l')} \right] , \quad (4.146)$$

$$d_{2(\alpha j, \beta l') }^{(1, l)} = -\omega^{-\nu_{k_l}} \int_{\infty}^{\epsilon} dz \frac{\eta_{2\alpha j}^l X_{(\alpha j, \beta l')}^l}{W(z)} + m_{\alpha j, \beta l'}^l \left[ \left( -\frac{1}{2\nu_{k_l}} + \ln \epsilon \right) v_{-\beta j}^{(0, l')} + \frac{\epsilon^{2\nu_{k_l}}}{2\nu_{k_l}} \tilde{\mathcal{G}}_{\beta}^{\prime} v_{+\beta j}^{(0, l')} \right], \quad (4.147)$$

$$d_{3(\alpha j, \beta l') }^{(1, l)} = m_{\alpha j, \beta l'}^l \tilde{\mathcal{G}}_{\beta}^{\prime} v_{+\beta j}^{(0, l')}, \quad (4.148)$$

$$d_{4(\alpha j, \beta l') }^{(1, l)} = -m_{\alpha j, \beta l'}^l v_{-\beta j}^{(0, l')} \quad (4.149)$$

where we defined

$$m_{\alpha j, \beta l'}^l = qM_{\alpha\beta, l l'} \left[ -2(-1)^{\alpha} + 2iqe_d + (-1)^{\alpha} \tilde{m}R_2 + (-1)^{\beta} \tilde{m}'R_2 \right]. \quad (4.150)$$

We repeat the procedure for eliminating irregular terms as  $\omega \rightarrow 0$  for degenerate case as well.

$$\begin{aligned} \tilde{\psi}_{s(\alpha j, \beta l')}^{(1, l)}(u) &\approx u^{\nu_{k_l}} \omega^{\nu_{k_l}} \tilde{d}_{1(\alpha j, \beta l')}^{(1, l)} + 2u^{\nu_{k_l}} \omega^{\nu_{k_l}} (\ln \omega) d_{3(\alpha j, \beta l')}^{(1, l)} \\ &\quad + u^{\nu_{k_l}} \omega^{\nu_{k_l}} (\ln \zeta) d_{3(\alpha j, \beta l')}^{(1, l)} + u^{-\nu_{k_l}} \omega^{\nu_{k_l}} (\ln \omega) d_{4(\alpha j, \beta l')}^{(1, l)} \\ &\quad + u^{-\nu_{k_l}} \omega^{\nu_{k_l}} (\ln \zeta) d_{4(\alpha j, \beta l')}^{(1, l)} \end{aligned} \quad (4.151)$$

or the explicit  $\omega$  dependence can be written as

$$\begin{aligned} \tilde{\psi}_{s(\alpha j, \beta l')}^{(1, l)} &\approx \zeta^{\nu_{k_l}} \omega^{2\nu_{k_l}} \tilde{d}_{1(\alpha j, \beta l')}^{(1, l)} + 2\zeta^{\nu_{k_l}} \omega^{2\nu_{k_l}} (\ln \omega) d_{3(\alpha j, \beta l')}^{(1, l)} \\ &\quad + \zeta^{\nu_{k_l}} \omega^{2\nu_{k_l}} (\ln \zeta) d_{3(\alpha j, \beta l')}^{(1, l)} + \zeta^{-\nu_{k_l}} (\ln \zeta) d_{4(\alpha j, \beta l')}^{(1, l)} \end{aligned} \quad (4.152)$$

where we added the terms  $\left( -\omega^{\nu_{k_l}} d_{2(\alpha j, \beta l')}^{(1, l)} \eta_{\alpha j}^{(0, l)}(u) \right)$  and  $\left( -\omega^{\nu_{k_l}} \ln \omega d_{4(\alpha j, \beta l')}^{(1, l)} \frac{v_{+\beta j}^{(0, l')}}{v_{-\beta j}^{(0, l')}} \eta_{\alpha j}^{(0, l)}(u) \right)$  respectively and remembering that  $d_{3(\alpha j, \beta l')}^{(1, l)} = \frac{v_{+\beta j}^{(0, l')}}{v_{-\beta j}^{(0, l')}} \mathcal{G}_{\beta}^{\prime} d_{4(\alpha j, \beta l')}^{(1, l)}$ . We also defined

$$\tilde{d}_{1(\alpha j, \beta l')}^{(1, l)} = d_{1(\alpha j, \beta l')}^{(1, l)} - (-1)^j d_{2(\alpha j, \beta l')}^{(1, l)} \mathcal{G}_{\alpha}^l. \quad (4.153)$$

## 4.4.5 Second Order Solution to Dirac Equations

### Second Order Numerical Solution to Dirac Equations

The second order Dirac equations are

$$\partial_z \psi_{\alpha j}^{(2,l)} - i \frac{q_f \mu_0 (1-z) + \omega}{h} \sigma^2 \psi_{\alpha j}^{(2,l)} + \frac{k_x + Kl}{\sqrt{h}} \sigma^3 \psi_{\alpha j}^{(2,l)} - \frac{k_y}{\sqrt{h}} \sigma^1 \psi_{\beta m}^{(2,l)} + \mathcal{B} = 0 \quad (4.154)$$

where

$$\begin{aligned} \mathcal{B} = & - \left( \frac{Q_{zz11}}{4} \psi_{\alpha j}^{(1,l-1)'} + \frac{Q_{zz11}}{4} \psi_{\alpha j}^{(1,l+1)'} + \frac{Q_{zz10}}{2} \psi_{\alpha j}^{(1,l)'} \right) + \frac{3}{32} Q_{zz11}^2 \left( \psi_{\alpha j}^{(0,l-2)'} + \psi_{\alpha j}^{(0,l+2)'} \right) \\ & + \frac{3}{8} Q_{zz10} Q_{zz11} \left( \psi_{\alpha j}^{(0,l-1)'} + \psi_{\alpha j}^{(0,l+1)'} \right) + \frac{3}{16} (2Q_{zz10}^2 + Q_{zz11}^2) \psi_{\alpha j}^{(0,l)'} \\ & + \mathcal{M}_{\alpha j}^{(0,l-1)} \psi_{\alpha j}^{(1,l-1)} + \mathcal{M}_{\alpha j}^{(0,l+1)} \psi_{\alpha j}^{(1,l+1)} + \mathcal{M}_{\alpha j}^{(0,l)} \psi_{\alpha j}^{(1,l)} + \mathcal{M}_{\alpha j}^{(0,l-2)} \psi_{\alpha j}^{(0,l-2)} + \mathcal{M}_{\alpha j}^{(0,l+2)} \psi_{\alpha j}^{(0,l+2)} \\ & + \mathcal{M}_{\alpha j}^{(2,l)} \psi_{\alpha j}^{(0,l)} + \frac{Q_{yy11}}{4\sqrt{h}} \sigma^1 \psi_{\beta m}^{(1,l-1)} + \frac{Q_{yy11}}{4\sqrt{h}} \sigma^1 \psi_{\beta m}^{(1,l+1)} + \frac{Q_{yy10}}{2\sqrt{h}} \sigma^1 \psi_{\beta m}^{(1,l)} \\ & + \mathcal{N}_{\beta m}^{(0,l-1)} \psi_{\beta m}^{(0,l-1)} + \mathcal{N}_{\beta m}^{(0,l+1)} \psi_{\beta m}^{(0,l+1)} + \mathcal{N}_{\beta m}^{(0,l)} \psi_{\beta m}^{(0,l)} + \mathcal{N}_{\beta m}^{(0,l-2)} \psi_{\beta m}^{(0,l-2)} + \mathcal{N}_{\beta m}^{(0,l+2)} \psi_{\beta m}^{(0,l+2)}, \end{aligned} \quad (4.155)$$

$$\begin{aligned} \mathcal{M}_{\alpha j}^{(2,l)} = & -i \left[ \frac{3(q_f \mu_0 (1-z) + \omega) (2Q_{tt10}^2 + Q_{tt11}^2)}{16h} - \frac{q_f (1-z) (2Q_{tt10} A_{t10} + Q_{tt11} A_{t11})}{4h} \right] \sigma^2 \\ & + \alpha \frac{3(k_x + Kl) (2Q_{xx10}^2 + Q_{xx11}^2)}{16\sqrt{h}} \sigma^1, \end{aligned} \quad (4.156)$$

$$\begin{aligned} \mathcal{M}_{\alpha j}^{(0,l \mp 2)} = & i \left[ -\frac{3(q_f \mu_0 (1-z) + \omega) Q_{tt11}^2}{32h} + \frac{q_f (1-z) Q_{tt11} A_{t11}}{8h} \right] \sigma^2 \mp \frac{\alpha k Q_{zz11}^2}{8\sqrt{h}} \sigma^1 \\ & + \alpha \frac{3(\pm 2k + k_x + K(l \mp 2)) Q_{xx11}^2}{32\sqrt{h}} \sigma^1 \mp \alpha \frac{k Q_{xx11} Q_{zz11}}{16\sqrt{h}} \sigma^1 \end{aligned} \quad (4.157)$$

$$\mathcal{N}_{\beta m}^{(0,l \pm 2)} = -\frac{3Q_{yy11}^2}{32\sqrt{h}} \sigma^1, \quad \mathcal{N}_{\beta m}^{(0,l \pm 1)} = -\frac{3Q_{yy11} Q_{yy10}}{8\sqrt{h}} \sigma^1, \quad \mathcal{N}_{\beta m}^{(0,l)} = -\frac{3(2Q_{yy10}^2 + Q_{yy11}^2)}{16\sqrt{h}} \sigma^1, \quad (4.158)$$

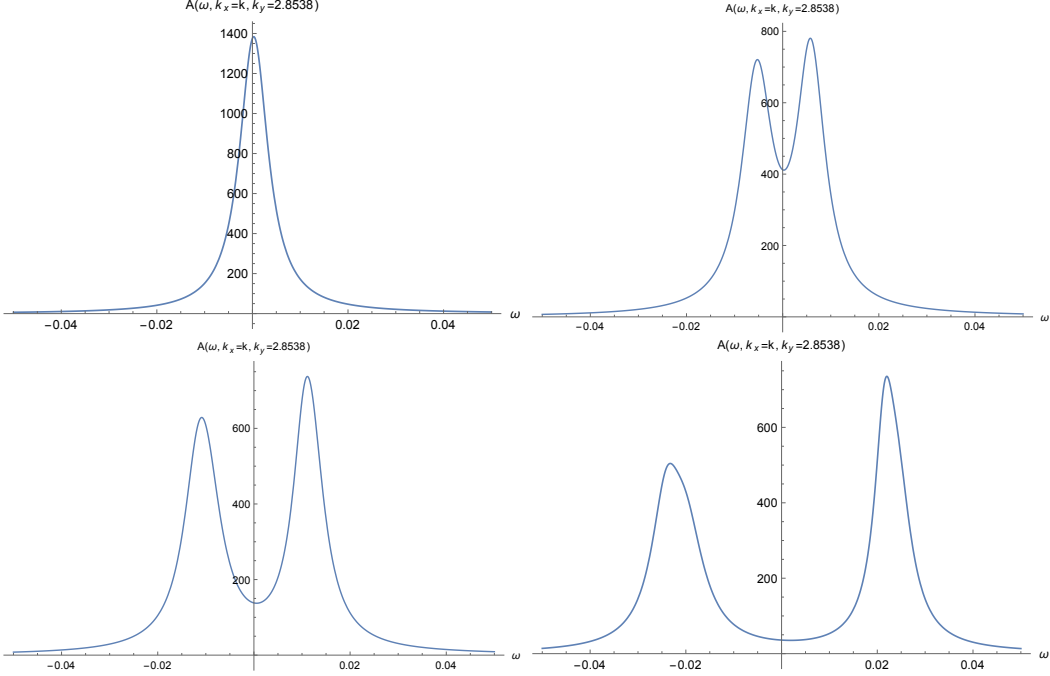


**Figure 4.7:** Plot of spectral function  $A(\omega, k_x = k, k_y = 2.8538)$  vs.  $\omega$  for parameters  $\frac{\eta}{\mu_0^2} = 0.25$ ,  $\frac{\eta'}{\mu_0^4} = 0.005$ ,  $q = 0$ ,  $\Delta = 1$ ,  $q_f = 2$ ,  $\mu_0 = 2.25072$ ,  $\frac{T}{\mu_0} = 0.0613$  and for  $\xi = 0.0, 0.05, 0.07, 0.1$  respectively.

where  $\alpha = +, -$ ,  $j = 1, 2$  and  $\beta = -\alpha$ ,  $m = 3 - j$ . The coefficients  $\mathcal{M}_{\alpha j}^{(0,l)}$ ,  $\mathcal{M}_{\alpha j}^{(0,l \mp 1)}$  are given in (4.110) and (4.111) respectively.

The first order Dirac equations show us that the  $(l \pm 1)$ ,  $(l)$ , and  $(l \pm 2)$  modes of the zeroth and first order spinor fields are mixed with each other.

The most general form of the retarded Green's function for both degenerate and non-degenerate cases is provided in [117] as

$$G_R \simeq \frac{B_{\alpha l, \alpha l}^{(0)} + \mathcal{O}(\xi^4)}{A_{\alpha l, \alpha l}^{(0)} + \xi^4 A_{\alpha l, \alpha l}^{(2)} - \xi^4 \sum_{\beta=1,2} \left( \frac{A_{\beta l-1, \alpha l}^{(1)} A_{\alpha l, \beta l-1}^{(1)}}{A_{\beta l-1, \beta l-1}^{(0)}} + \frac{A_{\beta l+1, \alpha l}^{(1)} A_{\alpha l, \beta l+1}^{(1)}}{A_{\beta l+1, \beta l+1}^{(0)}} \right)}. \quad (4.159)$$

We do numerical calculation to find the spectral function from this retarded Green's function and see that there is no band gap formed in near  $k_l \rightarrow k_F$  for non-degenerate case.

Retarded Green's function gives a pole at the Fermi surface where  $k_l = k_F$ . Near the Fermi surface we can write the retarded Green's function for degenerate case  $\nu_{k_l} \rightarrow \nu_{k'_l}$  as

$$G_{Ral,\alpha l} = \frac{A_{\alpha l,\alpha l}^{(0)} B_{\alpha l,\alpha l}^{(0)}}{(A_{\alpha l,\alpha l}^{(0)} + \xi^4 A_{\alpha l,\alpha l}^{(2)})^2 - \xi^4 A_{\alpha l,\alpha l-1}^{(1)} A_{\alpha l-1,\alpha l}^{(1)} + \mathcal{O}(\xi^6)} \quad (4.160)$$

To find the retarded Green's function we solve second order Dirac equations, i.e. (4.154), at the boundary choosing the ingoing boundary conditions at the horizon. Remember that near the Fermi surface the retarded Green's functions has the form

$$G_R = \frac{Z}{\omega - v_F(k - k_F) + \Sigma(\omega, k)} \quad (4.161)$$

where  $\Sigma$  is the self energy for fermionic excitations near Fermi surface and  $Z$  is the residue of the pole or in other words the quasiparticle weight. Therefore, we can write  $A_{\alpha l,\alpha l}^{(0)} + \xi^4 A_{\alpha l,\alpha l}^{(2)} = \omega - v_F(k_l - k_F) + i(c_1 - ic_2)\omega^{2\nu_{k_l}}$  where  $v_F, c_1, c_2$  are real constants and are determined from boundary data.

The retarded Green's function has three different cases depending on the parameters.

For  $\nu_{k_l} > \frac{1}{2}$ , the system has fermionic quasiparticles and the effective theory is a Fermi liquid. In this case the imaginary part of the self-energy behaves as  $\propto \omega^2$ . Also in this case the spectral function has a nice Lorentzian distribution centered around  $\omega = 0$ . For  $\nu_{k_l} > \frac{1}{2}$  the dominant linear term leads dispersion and we obtain

$$G_{Ral,\alpha l} \simeq \frac{(\omega - v_F(k_l - k_F)) B_{\alpha l,\alpha l}^{(0)}}{(\omega - v_F(k_l - k_F))^2 - \Delta^2 + ic_1(\omega - v_F(k_l - k_F))\omega^{2\nu_{k_l}}} . \quad (4.162)$$

Near Fermi surface and small  $\omega$  there are two peaks in the spectral function ( $A(\omega, k_x, k_y) = \Im[G_{R1l,1l} + G_{R2l,2l}]$ ) of the system are found in  $\omega = v_F(k_l - k_F) \pm \Delta$



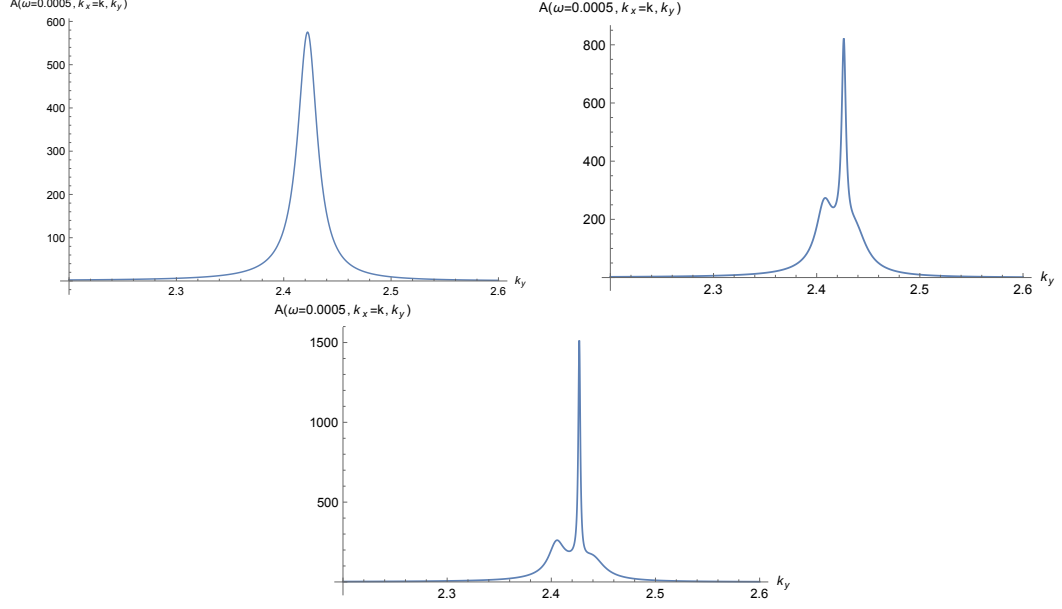


**Figure 4.8:** Plot of spectral function  $A(\omega = 0.0005, k_x = k, k_y)$  vs.  $k_y$  for parameters  $\frac{\eta}{\mu_0^2} = 0.25$ ,  $\frac{\eta'}{\mu_0^4} = 0.005$ ,  $q = 0$ ,  $\Delta = 1$ ,  $q_f = 1.8$ ,  $\mu_0 = 2.25072$ ,  $\frac{T}{\mu_0} = 0.0613$  and for  $\xi = 0.0, 0.07, 0.075$  respectively.

as seen in Fig.4.7. Here the band gap,  $\Delta$  is first order in  $\xi^2$  and is given by

$$\Delta^2 = \xi^4 A_{\alpha l, \alpha l-1}^{(1)} A_{\alpha l-1, \alpha l}^{(1)} \quad (4.163)$$

and its width can be changed by taking second order terms into account. Fig. 4.7 also shows us that the order of the gap is in the order of  $\xi$ , i.e.  $\omega \sim \Delta \sim \xi^2$ .  $\xi = 0$  corresponds to above critical temperature case. As we increase the  $\xi$  value the magnitude of the gap also increases. But after a certain  $\xi$  value the perturbation breaks down. The width of the peaks in the order of  $\xi^{2\nu_{k_i}}$  therefore they can be ignored and they will seem to be sharp peaks. For the parameters used for plotting Fig.4.7,  $\nu_{k_i} = 1.5064$  which is greater than 0.5 and shows the Fermi liquid property.

We can also observe the presence of the gap in  $A(\omega, k_x, k_y)$  vs.  $k_y$  graph as seen in Fig.4.8 at small  $\omega$  near Fermi surface region. Again perturbation breaks down near  $\xi \sim 0.08$ .

On the other hand, for  $\nu_{k_l} < \frac{1}{2}$ , i.e. in non-Fermi liquid case the non-analytic term dominates non-linear dispersion and we can write  $A_{\alpha l, \alpha l}^{(0)} + \xi^4 A_{\alpha l, \alpha l}^{(2)} = c_2 \omega^{2\nu_{k_l}} - v_F(k_l - k_F) + ic_1 - \omega^{2\nu_{k_l}}$  which gives the retarded Green's function

$$G_{R\alpha l, \alpha l} \simeq \frac{(\omega^{2\nu_{k_l}} - v_F(k_l - k_F))}{(\omega^{2\nu_{k_l}} - v_F(k_l - k_F))^2 - \Delta^2 + ic_1(\omega^{2\nu_{k_l}} - v_F(k_l - k_F))\omega^{2\nu_{k_l}}}, \quad (4.164)$$

where the two peaks are at  $\omega^{2\nu_{k_l}} = v_F(k_l - k_F) \pm \Delta$  and as opposed to the Fermi liquid case both the width of the non-linear dispersion and band gap are in the order of  $\xi^{1/2\nu_{k_l}}$ .

Finally, for  $\nu_{k_l} = \frac{1}{2}$ , leads too marginal Fermi liquid. There is still a Fermi surface but the self energy scaling is not quadratic in  $\omega$  but  $\Im\Sigma \propto \omega \ln \omega$ . Therefore, near Fermi surface and  $\omega = 0$  the  $\omega$  dependence of matrix elements of  $A$  are  $A_{\alpha l, \alpha l} = \omega + c_2 \omega \ln \omega - v_F(k_l - k_F) + ic_1 \omega \ln \omega$ .

## Second Order Analytical Solution to Dirac Equations

In the near region the second order Dirac equation is

$$\begin{aligned} \partial_\zeta \tilde{\Phi}_\alpha^{(2,l)} - i\sigma^3 \frac{\omega + qA_t}{f} \tilde{\Phi}_\alpha^{(2,l)} - \frac{R_2}{\zeta\sqrt{f}} (m\sigma^2 + \tilde{m}\sigma^1) \tilde{\Phi}_\alpha^{(2,l)} \\ + \frac{iq}{\zeta_0 \left(1 + \frac{\zeta}{\zeta_0}\right)} \sigma^3 \sum_{\beta; l'=l\pm 1} M_{\alpha\beta, ll'} \tilde{\Phi}_\beta^{(1,l')} = 0 \end{aligned} \quad (4.165)$$

with

$$M_{\alpha\beta, ll'} \tilde{\Phi}_\beta^{(1,l')} = \frac{iqA_{t11}}{2\zeta_0 \left(1 + \frac{\zeta}{\zeta_0}\right)} \sigma^3 \tilde{\Phi}_\beta^{(1,l')} + \frac{iqA_{t10}}{\zeta_0 \left(1 + \frac{\zeta}{\zeta_0}\right)} \sigma^3 \tilde{\Phi}_\beta^{(1,l')} \quad (4.166)$$

where we used the boundary condition that at the boundary of the near region  $Q_{tt} = Q_{zz} = Q_{xx} = Q_{yy} = 1$ . After the coordinate transformation the second order equation is

$$\partial_u^2 \tilde{\Phi}_\alpha^{(2,l)} - \frac{h'_{11}}{h_{11}} \tilde{\Phi}_\alpha^{(2,l)} - \left( h_{11}^2 + h_{22}^2 + (-1)^\alpha \frac{h_{22} h'_{11}}{h_{11}} - (-1)^\alpha h_{22} \right) \tilde{\Phi}_\alpha^{(2,l)} + Y_{\alpha j}^l = 0 \quad (4.167)$$

where

$$Y_{\alpha j}^l = \sum_{\beta; l' = l \pm 1, l} Y_{(\alpha\beta, l')} \quad (4.168)$$

with

$$Y_{(\alpha\beta, l')} = \frac{iq(-(-1)^\alpha h_{11} + h_{22})M_{\alpha\beta, l'} \tilde{\Phi}_\beta^{(1, l')}}{u + u_0} - (-1)^\alpha h_{11} \partial_u \left( \frac{iqM_{\alpha\beta, l'} \tilde{\Phi}_\beta^{(1, l')}}{(u + u_0)h_{11}} \right) \quad (4.169)$$

Similar to the first order case the special solution at second order can be written as

$$\begin{aligned} \eta_{s(\alpha j, \beta l')}^{(2, l)}(u) = & -\eta_{1\alpha j}^l \int_\epsilon^\infty du' \frac{\eta_{2\alpha j}^l Y_{(\alpha j, \beta l')}}{W(u')} + \eta_{2\alpha j}^l \int_\epsilon^\infty du' \frac{\eta_{1\alpha j}^l Y_{(\alpha j, \beta l')}}{W(u')} \\ & - \eta_{1\alpha j}^l \int_u^\epsilon du' \frac{\eta_{2\alpha j}^l Y_{(\alpha j, \beta l')}}{W(u')} + \eta_{2\alpha j}^l \int_u^\epsilon du' \frac{\eta_{1\alpha j}^l Y_{(\alpha j, \beta l')}}{W(u')} . \end{aligned} \quad (4.170)$$

We substitute (4.143) and (4.135) in (4.170) and find

$$\begin{aligned} \eta_{s(\alpha j, \beta l')}^{(2, l)}(u) \approx & u^{\nu_{k_l}} \omega^{\nu_{k_l}} s_{1(\alpha j, \beta l')}^{(2, l)} + u^{-\nu_{k_l}} \omega^{\nu_{k_l}} s_{2(\alpha j, \beta l')}^{(2, l)} + \sum_{l' = l \pm 1} u^{\nu_{k_{l'}}} \omega^{\nu_{k_l}} s_{3(\alpha j, \beta l')}^{(2, l)} \\ & + u^{\nu_{k_l}} \omega^{\nu_{k_l}} (\ln \zeta) s_{4(\alpha j, \beta l')}^{(2, l)} + u^{-\nu_{k_l}} \omega^{\nu_{k_l}} (\ln \zeta) s_{5(\alpha j, \beta l')}^{(2, l)} \\ & + u^{\nu_{k_l}} \omega^{\nu_{k_l}} (\ln \omega) s_{4(\alpha j, \beta l')}^{(2, l)} + u^{-\nu_{k_l}} \omega^{\nu_{k_l}} (\ln \omega) s_{5(\alpha j, \beta l')}^{(2, l)} + \dots \end{aligned} \quad (4.171)$$

where the coefficients are found as the following.

$$\begin{aligned} s_{1(\alpha j, \beta l')}^{(2, l)} = & \omega^{-\nu_{k_l}} \int_\infty^\epsilon dz \frac{\eta_{1\alpha j}^l Y_{(\alpha j)}^l}{W(z)} \\ & + q \sum_{\beta; l' = l \pm 1} M_{\alpha\beta, l'} \left[ \frac{\epsilon^{\nu_{k_{l'}} - \nu_{k_l}}}{\nu_{k_{l'}} - \nu_{k_l}} N_{1\beta j, \alpha l'}^{l'} + N_{3\beta j, \alpha l'}^{l'} \left( \ln \epsilon + \frac{1}{2\nu_{k_l}} \right) - \frac{\epsilon^{-2\nu_{k_l}}}{2\nu_{k_l}} N_{4\beta j, \alpha l'}^{l'} \right] , \end{aligned} \quad (4.172)$$

$$\begin{aligned} s_{2(\alpha j, \beta l')}^{(2, l)} = & -\omega^{-\nu_{k_l}} \int_\infty^\epsilon dz \frac{\eta_{2\alpha j}^l Y_{(\alpha j)}^l}{W(z)} \\ & - q \sum_{\beta; l' = l \pm 1} M_{\alpha\beta, l'} \left[ \frac{\epsilon^{\nu_{k_{l'}} + \nu_{k_l}}}{\nu_{k_{l'}} + \nu_{k_l}} N_{1\beta j, \alpha l'}^{l'} + \frac{\epsilon^{2\nu_{k_l}}}{2\nu_{k_l}} N_{3\beta j, \alpha l'}^{l'} + N_{4\beta j, \alpha l'}^{l'} \left( \ln \epsilon - \frac{1}{2\nu_{k_l}} \right) \right] , \end{aligned} \quad (4.173)$$

$$s_{3(\alpha j, \beta l')}^{(2,l)} = q \sum_{\beta; l' = l \pm 1} M_{\alpha \beta, l l'} \frac{2\nu_{k_l}}{\nu_{k_l}^2 - \nu_{k_{l'}}^2} N_{1\beta j, \alpha l}^{l'} , \quad (4.174)$$

$$s_{4(\alpha j, \beta l')}^{(2,l)} = -q \sum_{\beta; l' = l \pm 1} M_{\alpha \beta, l l'} N_{3\beta j, \alpha l}^{l'} , \quad (4.175)$$

$$s_{5(\alpha j, \beta l')}^{(2,l)} = q \sum_{\beta; l' = l \pm 1} M_{\alpha \beta, l l'} N_{4\beta j, \alpha l}^{l'} \quad (4.176)$$

where we defined

$$\begin{aligned} N_{1\beta j, \alpha l}^{l'} &= \frac{(-1)^\alpha}{9(-u_0)^{3/2}} \left( -i\tilde{m}R_2 + (-1)^{-\alpha} qe_d + i(1 + \nu_{k_{l'}}) \right) \tilde{n}_1 , \\ N_{3\beta j, \alpha l}^{l'} &= \frac{(-1)^\alpha}{9(-u_0)^{3/2}} \left( -i\tilde{m}R_2 + (-1)^{-\alpha} qe_d + i(1 + \nu_{k_l}) \right) \tilde{n}_3 , \\ N_{4\beta j, \alpha l}^{l'} &= \frac{(-1)^\alpha}{9(-u_0)^{3/2}} \left( -i\tilde{m}R_2 + (-1)^{-\alpha} qe_d - i(-1 + \nu_{k_l}) \right) \tilde{n}_4 . \end{aligned} \quad (4.177)$$

Due to the coefficients of  $s_{2(\alpha j, \beta l')}^{(2,l)}$  and  $s_{5(\alpha j, \beta l')}^{(2,l)}$  terms in the second order special solution

$\omega \rightarrow 0$  limit is not regular therefore we add  $(-\omega^{\nu_{k_l}} \eta_{\alpha j}^l s_{2(\alpha j, \beta l')}^{(2,l)})$  and  $(-\omega^{\nu_{k_l}} \eta_{\alpha j}^l s_{5(\alpha j, \beta l')}^{(2,l)})$  respectively. Therefore, we can write the second order solution at zero temperature as

$$\begin{aligned} \tilde{\psi}_{(\alpha j)}^{(2,l)}(u) &\approx u^{\nu_{k_l}} \omega^{\nu_{k_l}} \tilde{s}_{1(\alpha j, \beta l')}^{(2,l)} + \sum_{l' = l \pm 1} u^{\nu_{k_{l'}}} \omega^{\nu_{k_l}} s_{3(\alpha j, \beta l')}^{(2,l)} + u^{\nu_{k_l}} \omega^{\nu_{k_l}} (\ln \zeta) s_{4(\alpha j, \beta l')}^{(2,l)} \\ &+ u^{-\nu_{k_l}} \omega^{\nu_{k_l}} (\ln \zeta) s_{5(\alpha j, \beta l')}^{(2,l)} + u^{\nu_{k_l}} \omega^{\nu_{k_l}} (\ln \omega) \tilde{s}_{4(\alpha j, \beta l')}^{(2,l)} + \dots \end{aligned} \quad (4.178)$$

or we can also write

$$\begin{aligned} \tilde{\psi}_{(\alpha j)}^{(2,l)}(\zeta) &\approx \zeta^{\nu_{k_l}} \omega^{2\nu_{k_l}} \tilde{s}_{1(\alpha j, \beta l')}^{(2,l)} + \sum_{l' = l \pm 1} \zeta^{\nu_{k_{l'}}} \omega^{\nu_{k_l} + \nu_{k_{l'}}} s_{3(\alpha j, \beta l')}^{(2,l)} \\ &+ \zeta^{\nu_{k_l}} \omega^{2\nu_{k_l}} (\ln \zeta) s_{4(\alpha j, \beta l')}^{(2,l)} + \zeta^{-\nu_{k_l}} (\ln \zeta) s_{5(\alpha j, \beta l')}^{(2,l)} \\ &+ \zeta^{\nu_{k_l}} \omega^{2\nu_{k_l}} (\ln \omega) \tilde{s}_{4(\alpha j, \beta l')}^{(2,l)} + \dots \end{aligned} \quad (4.179)$$

with

$$\tilde{s}_{1(\alpha j, \beta l')}^{(2,l)} = s_{1(\alpha j, \beta l')}^{(2,l)} - (-1)^j s_{2(\alpha j, \beta l')}^{(2,l)} \mathcal{G}_\alpha^l, \quad \tilde{s}_{4(\alpha j, \beta l')}^{(2,l)} = s_{4(\alpha j, \beta l')}^{(2,l)} - (-1)^j s_{5(\alpha j, \beta l')}^{(2,l)} \mathcal{G}_\alpha^l. \quad (4.180)$$

We managed to eliminate of irregular solution due to  $\omega$  terms but the coefficients (4.172), (4.174) are not regular in the degenerate case, i.e.  $\nu_{k_l} = \nu_{k_{l'}}$  as in the first order case. Next, we will try to resolve the divergent coefficients problem for the degenerate case.

**Degenerate case  $\nu_{k_l} = \nu_{k_{l'}}$ :**

Now, we repeat the same steps for second order near region solution (4.171).

$$\begin{aligned} \eta_{s(\alpha j, \beta l')}^{(2,l)}(u) &\approx u^{\nu_{k_l}} \omega^{\nu_{k_l}} \mathbf{s}_{1(\alpha j, \beta l')}^{(2,l)} + u^{-\nu_{k_l}} \omega^{\nu_{k_l}} \mathbf{s}_{2(\alpha j, \beta l')}^{(2,l)} + u^{\nu_{k_l}} \omega^{\nu_{k_l}} (\ln \omega) \mathbf{s}_{3(\alpha j, \beta l')}^{(2,l)} \\ &\quad + u^{-\nu_{k_l}} \omega^{\nu_{k_l}} (\ln \omega) \mathbf{s}_{4(\alpha j, \beta l')}^{(2,l)} + u^{\nu_{k_l}} \omega^{\nu_{k_l}} (\ln \zeta) \mathbf{s}_{5(\alpha j, \beta l')}^{(2,l)} + u^{-\nu_{k_l}} \omega^{\nu_{k_l}} (\ln \zeta) \mathbf{s}_{6(\alpha j, \beta l')}^{(2,l)} \\ &\quad + u^{\nu_{k_l}} \omega^{\nu_{k_l}} \ln \omega (\ln \zeta) \mathbf{s}_{7(\alpha j, \beta l')}^{(2,l)} + u^{-\nu_{k_l}} \omega^{\nu_{k_l}} \ln \omega (\ln \zeta) \mathbf{s}_{8(\alpha j, \beta l')}^{(2,l)} \\ &\quad + u^{\nu_{k_l}} \omega^{\nu_{k_l}} (\ln \omega)^2 \mathbf{s}_{9(\alpha j, \beta l')}^{(2,l)} + u^{\nu_{k_l}} \omega^{\nu_{k_l}} (\ln \zeta)^2 \mathbf{s}_{10(\alpha j, \beta l')}^{(2,l)} \\ &\quad + u^{-\nu_{k_l}} \omega^{\nu_{k_l}} (\ln \zeta)^2 \mathbf{s}_{11(\alpha j, \beta l')}^{(2,l)} \end{aligned} \quad (4.181)$$

with the coefficients

$$\mathbf{s}_{1(\alpha j, \beta l')}^{(2,l)} = \omega^{-\nu_{k_l}} \int_{\infty}^{\epsilon} dz \frac{\eta_{1\alpha j}^l Y_{(\alpha j, \beta l')}^l}{W(z)} + q \sum_{\beta} M_{\alpha j, \beta l'}^l \tilde{D}_{1\beta} \left( 1 + \frac{1}{2\nu_{k_l}} \ln \epsilon \right), \quad (4.182)$$

$$\mathbf{s}_{2(\alpha j, \beta l')}^{(2,l)} = -\omega^{-\nu_{k_l}} \int_{\infty}^{\epsilon} dz \frac{\eta_{2\alpha j}^l Y_{(\alpha j, \beta l')}^l}{W(z)} - q \sum_{\beta} M_{\alpha j, \beta l'}^l \frac{\tilde{D}_{1\beta}}{2\nu_{k_l}} \epsilon^{2\nu_{k_l}}, \quad (4.183)$$

$$\mathbf{s}_{3(\alpha j, \beta l')}^{(2,l)} = q \sum_{\beta} M_{\alpha j, \beta l'}^l \left[ -\tilde{D}_{1\beta} + D_{3\beta} \left( \frac{1}{\nu_{k_l}} + 2 \ln \epsilon \right) \right], \quad (4.184)$$

$$\mathbf{s}_{4(\alpha j, \beta l')}^{(2,l)} = -q \sum_{\beta} M_{\alpha j, \beta l'}^l \frac{D_{3\beta}}{\nu_{k_l}} \epsilon^{2\nu_{k_l}}, \quad (4.185)$$

$$\mathbf{s}_5^{(2,l)}(\alpha_j, \beta l') = q \sum_{\beta} M_{\alpha_j, \beta l'}^l \left[ -\tilde{D}_{1\beta} + D_{3\beta} \left( \frac{1}{2\nu_{k_l}} + \ln \epsilon \right) - D_{4\beta} \frac{\epsilon^{-2\nu_{k_l}}}{2\nu_{k_l}} \right], \quad (4.186)$$

$$\mathbf{s}_6^{(2,l)}(\alpha_j, \beta l') = q \sum_{\beta} M_{\alpha_j, \beta l'}^l \left[ -D_{3\beta} \frac{\epsilon^{-2\nu_{k_l}}}{2\nu_{k_l}} + D_{4\beta} \left( \frac{1}{2\nu_{k_l}} - \ln \epsilon \right) \right], \quad (4.187)$$

$$\mathbf{s}_7^{(2,l)}(\alpha_j, \beta l') = -q \sum_{\beta} M_{\alpha_j, \beta l'}^l 3D_{3\beta}, \quad (4.188)$$

$$\mathbf{s}_8^{(2,l)}(\alpha_j, \beta l') = q \sum_{\beta} M_{\alpha_j, \beta l'}^l D_{4\beta}, \quad (4.189)$$

$$\mathbf{s}_9^{(2,l)}(\alpha_j, \beta l') = -q \sum_{\beta} M_{\alpha_j, \beta l'}^l 2D_{3\beta}, \quad (4.190)$$

$$\mathbf{s}_{10}^{(2,l)}(\alpha_j, \beta l') = -q \sum_{\beta} M_{\alpha_j, \beta l'}^l D_{3\beta}, \quad (4.191)$$

$$\mathbf{s}_{11}^{(2,l)}(\alpha_j, \beta l') = q \sum_{\beta} M_{\alpha_j, \beta l'}^l D_{4\beta}, \quad (4.192)$$

where we defined

$$\tilde{D}_{1\beta} = \frac{(-1)^\alpha}{9(-u_0)^{3/2}} \left( -i\tilde{m}R_2 + (-1)^{-\alpha} qe_d + i(1 + \nu_{k_l}) \right) \tilde{d}_{1\beta j, \alpha l}'^l, \quad (4.193)$$

$$D_{3\beta} = \frac{(-1)^\alpha}{9(-u_0)^{3/2}} \left( -i\tilde{m}R_2 + (-1)^{-\alpha} qe_d + i(1 + \nu_{k_l}) \right) d_{3\beta j, \alpha l}'^l, \quad (4.194)$$

$$D_{4\beta} = \frac{(-1)^\alpha}{9(-u_0)^{3/2}} \left( -i\tilde{m}R_2 + (-1)^{-\alpha} qe_d + i(1 - \nu_{k_l}) \right) d_{4\beta j, \alpha l}'^l. \quad (4.195)$$

To regularize the second order solution in  $\omega$  for degenerate case we repeat the same procedure with the  $u^{-\nu_{k_l}} \omega^{\nu_{k_l}}$  terms and find

$$\begin{aligned} \tilde{\psi}_{(\alpha_j, \beta l')}^{(2,l)}(u) &\approx \zeta^{\nu_{k_l}} \omega^{2\nu_{k_l}} \tilde{\mathbf{s}}_1^{(2,l)}(\alpha_j, \beta l') + \zeta^{\nu_{k_l}} \omega^{2\nu_{k_l}} (\ln \omega) \tilde{\mathbf{s}}_3^{(2,l)}(\alpha_j, \beta l') \\ &\quad + \zeta^{\nu_{k_l}} \omega^{2\nu_{k_l}} (\ln \zeta) \mathbf{s}_5^{(2,l)}(\alpha_j, \beta l') + \zeta^{-\nu_{k_l}} (\ln \zeta) \mathbf{s}_6^{(2,l)}(\alpha_j, \beta l') \\ &\quad + \zeta^{\nu_{k_l}} \omega^{2\nu_{k_l}} \ln \omega (\ln \zeta) \mathbf{s}_7^{(2,l)}(\alpha_j, \beta l') + \zeta^{-\nu_{k_l}} \ln \omega (\ln \zeta) \mathbf{s}_8^{(2,l)}(\alpha_j, \beta l') \\ &\quad + \zeta^{\nu_{k_l}} \omega^{2\nu_{k_l}} (\ln \omega)^2 \mathbf{s}_9^{(2,l)}(\alpha_j, \beta l') + \zeta^{\nu_{k_l}} \omega^{2\nu_{k_l}} (\ln \zeta)^2 \mathbf{s}_{10}^{(2,l)}(\alpha_j, \beta l') \\ &\quad + \zeta^{-\nu_{k_l}} \omega^{2\nu_{k_l}} (\ln \zeta)^2 \mathbf{s}_{11}^{(2,l)}(\alpha_j, \beta l') \end{aligned} \quad (4.196)$$

where

$$\begin{aligned}\tilde{\mathbf{s}}_{\mathbf{1}(\alpha j, \beta l') }^{(2,l)} &= \mathbf{s}_{\mathbf{1}(\alpha j, \beta l') }^{(2,l)} - (-1)^j \mathbf{s}_{\mathbf{2}(\alpha j, \beta l') }^{(2,l)} \tilde{\mathcal{G}}_{\alpha}^l, & \tilde{\mathbf{s}}_{\mathbf{3}(\alpha j, \beta l') }^{(2,l)} &= \mathbf{s}_{\mathbf{3}(\alpha j, \beta l') }^{(2,l)} - (-1)^j \mathbf{s}_{\mathbf{4}(\alpha j, \beta l') }^{(2,l)} \tilde{\mathcal{G}}_{\alpha}^l, \\ \tilde{\mathbf{s}}_{\mathbf{8}(\alpha j, \beta l') }^{(2,l)} &= \mathbf{s}_{\mathbf{8}(\alpha j, \beta l') }^{(2,l)} - (-1)^j \mathbf{s}_{\mathbf{9}(\alpha j, \beta l') }^{(2,l)} \tilde{\mathcal{G}}_{\alpha}^l.\end{aligned}\tag{4.197}$$

#### 4.4.6 The Far Region

The reason for us to use the matching method is that expanding in small  $\omega$  is problematic at zero or at  $T \ll \mu$  temperatures due to the fact that  $\omega$ -term is dominant in the near horizon region. To find the leading order equation in the far region we set  $\omega = 0$  at zeroth, first, and second orders. In the far region, i.e. as  $z \rightarrow 0$  the solution to the leading order equations can be written as

$$\tilde{\psi}_{\alpha}^{(s,l)}(z) = A_{\alpha}^{(s,l)} z^{-mR} \begin{pmatrix} 0 \\ 1 \end{pmatrix} + B_{\alpha}^{(s,l)} z^{mR} \begin{pmatrix} 1 \\ 0 \end{pmatrix} + \dots\tag{4.198}$$

where  $s = 0, 1, 2, \dots$  is the order of perturbation. Now, we use the matching method to find the coefficients  $A_{\alpha}^{(s,l)}$  and  $B_{\alpha}^{(s,l)}$  since the retarded Green's function is  $G_R = BA^{-1}$ . The matching method is applied in the overlap region, i.e. the inner boundary of the far region and the boundary of the near horizon region. In general the small  $\omega$  expansion of the retarded Green's function is

$$G_R(\omega, k) = K \frac{B_+^{(0)} + \omega B_+^{(1)} + \mathcal{O}(\omega^2) + \mathcal{G}_{IR}(\omega) \left( B_-^{(0)} + \omega B_-^{(1)} + \mathcal{O}(\omega^2) \right)}{A_+^{(0)} + \omega A_+^{(1)} + \mathcal{O}(\omega^2) + \mathcal{G}_{IR}(\omega) \left( A_-^{(0)} + \omega A_-^{(1)} + \mathcal{O}(\omega^2) \right)}\tag{4.199}$$

where  $K$  is the normalization factor but it does not affect the result, thus can be set  $K = 1$  [120]. In the following calculations we will be interested in the leading order but they can be generalized to higher orders in  $\omega$ .

The non-degenerate case the far region solutions read

$$\begin{aligned}
A_{\alpha l, \alpha l}^{(0)} &= A_{\alpha l, \alpha l}^{(0)-} v_{-\alpha 2}^{(0, l)} + \tilde{\mathcal{G}}_{\alpha I R}^l A_{\alpha l, \alpha l}^{(0)+} v_{+\alpha 2}^{(0, l)} \omega^{2\nu_{k_l}} , \\
B_{\alpha l, \alpha l}^{(0)} &= B_{\alpha l, \alpha l}^{(0)-} v_{-\alpha 1}^{(0, l)} + \tilde{\mathcal{G}}_{\alpha I R}^l B_{\alpha l, \alpha l}^{(0)+} v_{+\alpha 1}^{(0, l)} \omega^{2\nu_{k_l}} , \\
A_{\alpha l, \beta l'}^{(1)} &= A_{\alpha l, \beta l'}^{(1, 1)} \tilde{n}_{1\alpha 2\beta l'}^l \omega^{\nu_{k_l} + \nu_{k_{l'}}} + A_{\alpha l, \beta l'}^{(1, 3)} n_{3\alpha 2\beta l'}^l \omega^{2\nu_{k_{l'}}} + A_{\alpha l, \beta l'}^{(1, 4)} n_{4\alpha 2\beta l'}^l , \\
B_{\alpha l, \beta l'}^{(1)} &= B_{\alpha l, \beta l'}^{(1, 1)} \tilde{n}_{1\alpha 2\beta l'}^l \omega^{\nu_{k_l} + \nu_{k_{l'}}} + B_{\alpha l, \beta l'}^{(1, 3)} n_{3\alpha 2\beta l'}^l \omega^{2\nu_{k_{l'}}} + B_{\alpha l, \beta l'}^{(1, 4)} n_{4\alpha 2\beta l'}^l , \\
A_{\alpha l, \alpha l}^{(2)} &= \left( A_{\alpha l}^{(2, 1)} \tilde{s}_{1\alpha 2}^l + A_{\alpha l}^{(2, 4)} s_{4\alpha 2}^l \right) \omega^{2\nu_{k_l}} + \sum_{l'} A_{\alpha l, l'}^{(2, 3)} s_{3\alpha 2, l'}^l \omega^{\nu_{k_l} + \nu_{k_{l'}}} + \tilde{A}_{\alpha l}^{(2, 4)} \tilde{s}_{4\alpha 2}^l \omega^{2\nu_{k_l}} \ln \omega \\
&\quad + A_{\alpha l}^{(2, 5)} s_{5\alpha 2}^l , \\
B_{\alpha l, \alpha l}^{(2)} &= \left( B_{\alpha l}^{(2, 1)} \tilde{s}_{1\alpha 2}^l + B_{\alpha l}^{(2, 4)} s_{4\alpha 2}^l \right) \omega^{2\nu_{k_l}} + \sum_{l'} B_{\alpha l, l'}^{(2, 3)} s_{3\alpha 2, l'}^l \omega^{\nu_{k_l} + \nu_{k_{l'}}} + \tilde{B}_{\alpha l}^{(2, 4)} \tilde{s}_{4\alpha 2}^l \omega^{2\nu_{k_l}} \ln \omega \\
&\quad + B_{\alpha l}^{(2, 5)} s_{5\alpha 2}^l .
\end{aligned} \tag{4.200}$$

For degenerate case

$$\begin{aligned}
A_{\alpha l, \alpha l}^{(0)} &= A_{\alpha l, \alpha l}^{(0)-} v_{-\alpha 2}^{(0, l)} + \tilde{\mathcal{G}}_{\alpha I R}^l A_{\alpha l, \alpha l}^{(0)+} v_{+\alpha 2}^{(0, l)} \omega^{2\nu_{k_l}} , \\
B_{\alpha l, \alpha l}^{(0)} &= B_{\alpha l, \alpha l}^{(0)-} v_{-\alpha 1}^{(0, l)} + \tilde{\mathcal{G}}_{\alpha I R}^l B_{\alpha l, \alpha l}^{(0)+} v_{+\alpha 1}^{(0, l)} \omega^{2\nu_{k_l}} , \\
A_{\alpha l, \beta l'}^{(1)} &= \left( A_{\alpha l, \beta l'}^{(1, 1)} \tilde{d}_{1\alpha 2\beta l'}^l + A_{\alpha l, \beta l'}^{(1, 3)} d_{3\alpha 2\beta l'}^l \right) \omega^{2\nu_{k_l}} + A_{\alpha l, \beta l'}^{(1, 4)} d_{4\alpha 2\beta l'}^l + 2A_{\alpha l, \beta l'}^{(1, 3)} d_{3\alpha 2\beta l'}^l \omega^{2\nu_{k_l}} \ln \omega , \\
B_{\alpha l, \beta l'}^{(1)} &= \left( B_{\alpha l, \beta l'}^{(1, 1)} \tilde{d}_{1\alpha 2\beta l'}^l + B_{\alpha l, \beta l'}^{(1, 3)} d_{3\alpha 2\beta l'}^l \right) \omega^{2\nu_{k_l}} + B_{\alpha l, \beta l'}^{(1, 4)} d_{4\alpha 2\beta l'}^l + 2B_{\alpha l, \beta l'}^{(1, 3)} d_{3\alpha 2\beta l'}^l \omega^{2\nu_{k_l}} \ln \omega , \\
A_{\alpha l, \alpha l}^{(2)} &= \left( A_{\alpha l}^{(2, 1)} \tilde{\mathbf{s}}_{1\alpha 2}^l + A_{\alpha l}^{(2, 5)} \mathbf{s}_{5\alpha 2}^l + A_{\alpha l}^{(2, 10)} \mathbf{s}_{10\alpha 2}^l \right) \omega^{2\nu_{k_l}} + \left( A_{\alpha l}^{(2, 3)} \tilde{\mathbf{s}}_{3\alpha 2}^l + A_{\alpha l}^{(2, 7)} \mathbf{s}_{7\alpha 2}^l \right) \omega^{2\nu_{k_l}} \ln \omega \\
&\quad + \left( A_{\alpha l}^{(2, 6)} \mathbf{s}_{6\alpha 2}^l + A_{\alpha l}^{(2, 11)} \mathbf{s}_{11\alpha 2}^l \right) + A_{\alpha l}^{(2, 8)} \mathbf{s}_{8\alpha 2}^l \ln \omega + A_{\alpha l}^{(2, 9)} \mathbf{s}_{9\alpha 2}^l \omega^{2\nu_{k_l}} (\ln \omega)^2 \\
&\quad + (\text{terms from non-degenerate } l'') , \\
B_{\alpha l, \alpha l}^{(2)} &= \left( B_{\alpha l}^{(2, 1)} \tilde{\mathbf{s}}_{1\alpha 2}^l + B_{\alpha l}^{(2, 5)} \mathbf{s}_{5\alpha 2}^l + B_{\alpha l}^{(2, 10)} \mathbf{s}_{10\alpha 2}^l \right) \omega^{2\nu_{k_l}} + \left( B_{\alpha l}^{(2, 3)} \tilde{\mathbf{s}}_{3\alpha 2}^l + B_{\alpha l}^{(2, 7)} \mathbf{s}_{7\alpha 2}^l \right) \omega^{2\nu_{k_l}} \ln \omega \\
&\quad + \left( B_{\alpha l}^{(2, 6)} \mathbf{s}_{6\alpha 2}^l + B_{\alpha l}^{(2, 11)} \mathbf{s}_{11\alpha 2}^l \right) + B_{\alpha l}^{(2, 8)} \mathbf{s}_{8\alpha 2}^l \ln \omega + B_{\alpha l}^{(2, 9)} \mathbf{s}_{9\alpha 2}^l \omega^{2\nu_{k_l}} (\ln \omega)^2 \\
&\quad + (\text{terms from non-degenerate } l'')
\end{aligned} \tag{4.201}$$



as given in [117].

## 4.5 Conclusion

In this study, we have explored the holographic fermionic spectral function to see the band gap structure due to the presence of a spontaneously generated holographic lattice structure. Holographic fermionic field was put into a finite but small temperature black hole and the Einstein, Maxwell, scalar, and Dirac equations were solved both analytically and numerically using perturbation theory. The results of our calculations are consistent with the lattice effect in a periodic potential and we found out that there is a band gap formed at the edge of the Brillouin zone, i.e. degenerate case with  $\nu_{k_l} = \nu_{k_{l'}}$  due to the interaction between different levels. The magnitude of this gap increases as we increase magnitude of the order parameter,  $\xi$ , up to a certain value in which the perturbation breaks down.

A similar system was studied in papers [117] and [118] to analyze the holographic lattice effect on the Fermi surface. The contribution of our paper to these studies is that in our system the holographic lattice structure was spontaneously generated by a higher order derivative term which we studied previously in [12].

In [121] and [122] they introduced the dipole coupling in Q-lattice background to dynamically generate the Mott gap and analyze its behavior as a function of dipole coupling and the effects of lattice parameters and to analyze the metal-insulator transitions. As a future study, it would be interesting to explore the Mott gap and the metal-insulator transitions by studying our system in Chapter 3 in a spontaneously generated holographic lattice background.

# Chapter 5

## Conclusion and Outlook

In this PhD thesis holographic duals of the spatially inhomogeneous phases, a robust phase diagram, and fermionic system with lattice effects have been presented. The summary of these studies are as follows.

We started with presenting a holographic model which includes a  $U(1)$  gauge field and a scalar field coupled to a charged AdS black hole with a spatially homogeneous chemical potential in Chapter 2. As we turned on the higher derivative interaction term between the  $U(1)$  gauge field and the scalar field a spatially dependent scalar field and a spatially inhomogeneous charge density at the boundary was spontaneously generated below a transition temperature,  $T$ . We discussed the dependence of the critical temperature to parameters like wavenumber ( $k$ ), higher derivative coupling constant ( $\frac{\eta}{\mu^2}$ ), charge of the  $U(1)$  gauge field ( $q$ ), scaling dimension ( $\Delta$ ), and second higher-derivative coupling constant ( $\frac{\eta'}{\mu^4}$ ). Plotting the transition temperature as a function of wavenumber,  $k$ , shows that the maximum transition temperature corresponds to the critical temperature,  $T_c$ , of the system. The scaling dimension does not make a significant difference in our results. We also found out that inhomogeneous solution is more dominant for small enough  $q$  value. Finally, the second higher derivative term plays the UV-cutoff role to obtain a finite wavenumber,  $k$ . In addition to these results we explored the fully backreacted system below the critical

temperature using the perturbation theory and our analytical results confirm that the spatial dependent charge density was spontaneously generated at the boundary gauge theory.

In Chapter 4 we analyzed the behavior of the Fermi surface in spatially inhomogeneous background that was spontaneously generated by higher derivative coupling term studied in Chapter 2. To this end, we needed the numerical results of the previously analytically studied system. By using the perturbation theory we numerically solved the Einstein, Maxwell, scalar field equation system which gave us the opportunity to observe the spatial variation of metric functions due to the backreaction of the spatially dependent gauge field. We were also able to see the spatial variation of the charge density of the boundary gauge field theory numerically. These results confirmed our claim in Chapter 2 that the holographic lattice structure was spontaneously generated at the boundary. To study the Fermi surface we added holographic fermions to the system and analyzed the single fermion spectral function. As a result of the degeneracy the interaction of different momentum levels leads to the band gap structure which is well defined in condensed matter physics.

Another interesting application of gauge/gravity duality was studied in Chapter 3 where a robust holographic dual of phase diagram was explored. The holographic dual of the phase diagram was formed by using a dipole coupling between the fermion and gauge fields in the bulk. A pole in the spectral function of the holographic fermionic system is an indicator of a Fermi and non-Fermi liquid depending on the scaling dimension  $\nu_k$  and a zero is an indicator of a Mott insulator. The coexistence of both poles and zeroes indicates the pseudo-gap phase in the phase diagram. The important contribution of this study was pointing out that since there is duality between zeroes and poles of the Green's function,  $G_R$ , the Mott phase can be studied by mapping it to the Fermi liquid phase by applying a sign change to dipole coupling constant between the massless fermion and the gauge field.

To finalize this thesis we will present an outlook for future studies based on the work presented in this thesis.

One interesting work that can be done is generalizing the spontaneously generated one-dimensional holographic lattice structure to two-dimensional lattice effect which in general can be anisotropic in  $x - y$  plane.

In most of the gauge/gravity duality studies probe limit is studied and lattice effects are ignored. Therefore, to see the lattice effects we can apply our spontaneously generated holographic lattice model to different systems to analyze the lattice effect to different mechanisms. One of the implications of the spontaneously generated holographic lattice effect can be to study the lattice effect on the optical conductivity. This work has been done by Horowitz et. al. in [62] and [63]. They added the lattice by introducing a neutral scalar field with boundary conditions corresponding to a periodic source and also by a spatially varying chemical potential in both  $AdS_4$  and  $AdS_5$  spacetimes. Their studies revealed that adding the lattice to the background leads to broadening of the delta function at  $\omega = 0$  of the real part of the optical conductivity. Also the real and imaginary parts of the optical conductivity obeys the simple Drude form at low frequencies and then they show a power-law dependence on frequency,  $\sigma \sim \omega^{-2/3}$  in the mid-infrared regime. Given these findings, it would be interesting to analyze the frequency dependent optical conductivity of a lattice in both spatial directions.

Another possible follow up study can be to explore the Mott metal-insulator transition which involves strongly correlated system and requires methods other than conventional techniques. We can study the effect of lattice constant to this transition by putting the holographic fermions with dipole coupling system into a spatially inhomogeneous background. This was done in [121] by introducing a Q-lattice instead of the spontaneously generating the holographic lattice structure. As a result of their study they found out that the lattice amplitude and the wave number provides a wider parameter space and this leads to an abundant Mott physics. Since in our holographic lattice system we have more parameters we believe that we will be able to analyze the Mott physics in more detail.

The ultimate goal of the gauge/gravity duality is to become an alternate solution for understanding the strongly correlated electron systems where conventional methods cannot be used. The phase diagram of high- $T_c$  superconductors has a variety of phases like Mott insulator, strange metal, pseudo-gap phase which are not well understood yet due to their strongly coupled nature. We hope that gauge/gravity duality studies will expand our understanding of these phases and contribute to condensed matter physics.

# Bibliography

- [1] J. J. Quinn and K. S. Yi, “Solid State Physics, Principles and Modern Applications,” Springer-Verlag, Berlin Heidelberg (2009) 534 p [xi](#), [3](#), [4](#), [12](#), [14](#)
- [2] J. Sólyom, “Fundamentals of the Physics of Solids, Volume 2 Electronic Properties ” Springer-Verlag, Berlin Heidelberg New York (2007) [xi](#), [14](#), [15](#), [16](#)
- [3] J. M. Maldacena, “The large N limit of superconformal field theories and supergravity,” Adv. Theor. Math. Phys. **2** (1998) 231 [Int. J. Theor. Phys. **38** (1999) 1113] [arXiv:hep-th/9711200]. [30](#), [51](#)
- [4] G. 't Hooft, Nucl. Phys. B **72**, 461 (1974). [17](#)
- [5] E. Witten, “Anti de Sitter space and holography,” Adv. Theor. Math. Phys. **2**, 253-291, (1998). [21](#)
- [6] P. Kerner, “Gauge/Gravity duality: A Road Towards Reality,” PhD Thesis, Ludwig-Maximilians-Universität München , (2012). [18](#), [21](#)
- [7] G. T. Horowitz, “Theory of Superconductivity,” Lect. Notes Phys. **828**, 313 (2011) [arXiv:1002.1722 [hep-th]]. [xi](#), [24](#), [27](#), [29](#), [30](#)
- [8] S. S. Gubser, “Breaking an Abelian gauge symmetry near a black hole horizon,” Phys. Rev. D **78**, 065034 (2008) [arXiv:0801.2977 [hep-th]]. [24](#), [30](#)
- [9] S. A. Hartnoll, C. P. Herzog and G. T. Horowitz, “Building a Holographic Superconductor,” Phys. Rev. Lett. **101**, 031601 (2008) [arXiv:0803.3295 [hep-th]]. [31](#)
- [10] S. A. Hartnoll, C. P. Herzog and G. T. Horowitz, “Holographic Superconductors,” JHEP **0812**, 015 (2008) [arXiv:0810.1563 [hep-th]]. [31](#)
- [11] G. Koutsoumbas, E. Papantonopoulos and G. Siopsis, “Exact Gravity Dual of a Gapless Superconductor,” JHEP **0907**, 026 (2009) [arXiv:0902.0733 [hep-th]]. [31](#), [52](#)

- [12] J. Alsup, E. Papantonopoulos, G. Siopsis and K. Yeter, “Spontaneously Generated Inhomogeneous Phases via Holography,” *Phys. Rev. D* **88**, no. 10, 105028 (2013) [arXiv:1305.2507 [hep-th]]. [2](#), [68](#), [69](#), [71](#), [118](#)
- [13] J. Alsup, E. Papantonopoulos, G. Siopsis and K. Yeter, “Duality between zeroes and poles in holographic systems with massless fermions and a dipole coupling,” *Phys. Rev. D* **90**, no. 12, 126013 (2014) [arXiv:1404.4010 [hep-th]]. [2](#), [77](#)
- [14] M. Tinkham, “Introduction to Superconductivity,” Second Edition, Dover: New York (1996) [3](#), [7](#)
- [15] F. London and H. London, “Electromagnetic Equations of the Supraconductor,” *Proc. Roy. Soc., (London)* **A149**, no. 71, (1935) [4](#)
- [16] L. D. Landau , “On the Theory of Phase Transitions,” *Zh. Eksp. Teor. Fiz.*, **7**, 19-32, (1937) [5](#)
- [17] V. L. Ginzburg and L. D. Landau, “On the Theory of Superconductivity,” *Zh. Eksp. Teor. Fiz.*, **20**, no. 1064, (1950) [6](#)
- [18] J. Bardeen and L. N. Cooper and J. R. Schrieffer, “Microscopic Theory of Superconductivity,” *Phys. Rev.*, **108**, no. 1175, (1957) [7](#)
- [19] J. L. Tallon and J. W. Loram, “The doping dependence of  $T^*$ - what is the real high- $T_c$  phase diagram?,” *J. W. Physica C*, **349**, (2001)
- [20] J. G. Bednorz and K. A. Müller, “Possible High  $T_c$  Superconductivity in the Ba-La-Cu-O System,” *Z. Phys.*, **B64**, no.189, (1986) [8](#)
- [21] A. Schilling and M. Cantoni and J. D. Guo and H. R. Ott, “Superconductivity above 130 K in the Hg-Ba-Ca-Cu-O System,” *Nature*, **363**, (1993), 56 [8](#)
- [22] D. M. Broun, “What lies beneath the dome?,” *Nature*, **4**, (2008) [xi](#), [9](#), [10](#)
- [23] G. Grüner, “Density Waves in Solids,” Addison-Wesley Publishing Company, (1994) [10](#), [12](#)
- [24] G. Grüner, “The dynamics of charge-density waves,” *Reviews of Modern Physics*, **60**, no. 4, (1998) [10](#), [12](#)



- [25] M. Dressel and G. Grüner, “Electrodynamics of Solids,” Cambridge University Press, (2002) [xi](#), [11](#)
- [26] J. Erdmenger, “Introduction to gauge/gravity duality,” *Lect. Notes Phys.* **851**, 99 (2012). [16](#)
- [27] J. de Boer, “Introduction to the AdS/CFT correspondence,” [16](#)
- [28] R. Emparan, H. S. Reall, “Black hole in higher dimensions”, *Living Rev. Rel.* **8**, 6 (2008), [arXiv:0801.3471v2](#). [21](#)
- [29] M. Natsuume, “AdS/CFT Duality User Guide,” [arXiv:1409.3575 \[hep-th\]](#). [8](#), [9](#), [20](#), [22](#), [29](#)
- [30] A. V. Ramallo, “Introduction to the AdS/CFT correspondence,” *Springer Proc. Phys.* **161**, 411 (2015) [arXiv:1310.4319 \[hep-th\]](#). [20](#)
- [31] M. Hanada, Y. Hyakutake, G. Ishiki and J. Nishimura, “Holographic description of quantum black hole on a computer,” *Science* **344**, 882 (2014) [[arXiv:1311.5607 \[hep-th\]](#)]. [17](#)
- [32] Y. Hyakutake, “Quantum near-horizon geometry of a black 0-brane,” *PTEP* **2014**, 033B04 (2014) [arXiv:1311.7526 \[hep-th\]](#). [17](#)
- [33] R. Cowen, “Simulations back up theory that Universe is a hologram,” *Nature* (2013). [17](#)
- [34] J. Maldacena, “Testing gauge/gravity duality on a quantum black hole,” *Science* **344**, 806 (2014). [17](#)
- [35] S. S. Gubser, I. R. Klebanov and A. M. Polyakov, “Gauge theory correlators from noncritical string theory,” *Phys. Lett. B* **428**, 105 (1998) [[hep-th/9802109](#)]. [22](#)
- [36] J. Zaanen, Y. W. Sun, Y. Liu, K. Schalm “The AdS/CMT manual for plumbers and electricians”, [Lecture Notes](#). [xi](#), [23](#)
- [37] G. T. Horowitz, “Introduction to Holographic Superconductors,” *Lect. Notes Phys.* **828**, 313 (2011) [arXiv:1002.1722 \[hep-th\]](#). [xi](#), [24](#), [27](#), [29](#), [30](#)

- [38] S. S. Gubser, “Breaking an Abelian gauge symmetry near a black hole horizon,” Phys. Rev. D **78**, 065034 (2008) [arXiv:0801.2977 \[hep-th\]](#). 24, 30
- [39] P. Breitenlohner and D. Z. Freedman, “Stability in Gauged Extended Supergravity,” Annals Phys. **144**, 249 (1982). 26
- [40] I. Martin, D. Podolsky, and S. A. Kivelson, “Enhancement of superconductivity by local inhomogeneity”, Phys. Rev. B **72** (2005) 060502, [cond-mat/0501659](#). 31
- [41] C. S. Hellberg and E. Manousakis, “Phase separation at all interaction strengths in the t-j model”, Phys. Rev. Lett. **78** (1997) 4609, [cond-mat/9611195](#). 31
- [42] S. R. White and D. Scalapino, “Dmrg study of the striped phase in the 2d t-j model”, Phys. Rev. Lett. **80** (1998) 1272, [cond-mat/9705128](#). 31
- [43] E. Berg, E. Fradkin, S. A. Kivelson, and J. Tranquada, “Striped superconductors: How the cuprates intertwine spin, charge and superconducting orders”, New J. Phys. **11** (2009) 115004, [arXiv:0901.4826](#). 31
- [44] S. Baruch and D. Orgad, “Spectral signatures of modulated d-wave superconducting phases”, Phys. Rev. B **77** (2008) 174502, [arXiv:0801.2436](#). 31
- [45] L. Radzihovsky and A. Vishwanath, “Quantum liquid crystals in imbalanced fermi gas: fluctuations and fractional vortices in larkin-ovchinnikov states”, Phys. Rev. Lett. **103** (2009) 010404, [arXiv:0812.3945](#). 31
- [46] R. Flauger, E. Pajer and S. Papanikolaou, “A Striped Holographic Superconductor,” Phys. Rev. D **83**, 064009 (2011). [[arXiv:1010.1775 \[hep-th\]](#)]. 31, 32
- [47] J. A. Hutasoit, S. Ganguli, G. Siopsis and J. Therrien, “Strongly Coupled Striped Superconductor with Large Modulation,” JHEP **1202**, 086 (2012). [[arXiv:1110.4632 \[cond-mat.str-el\]](#)]. 31
- [48] S. Ganguli, J. A. Hutasoit and G. Siopsis, “Enhancement of Critical Temperature of a Striped Holographic Superconductor,” [arXiv:1205.3107 \[hep-th\]](#). 31

- [49] A. Donos and J. P. Gauntlett, “Holographic striped phases,” JHEP **1108**, 140 (2011), [arXiv:1106.2004 [hep-th]]. [31](#)
- [50] A. Donos and J. P. Gauntlett, “Holographic charge density waves,” [arXiv:1303.4398 [hep-th]]. [31](#), [33](#), [50](#)
- [51] A. M. Gabovich *et al*, “Charge- and spin-density-wave superconductors ,” Supercond. Sci. Technol. **14**, R1 (2001). [32](#)
- [52] A. Aperis, G. Varelogiannis, and P. B. Littlewood “Magnetic-Field-Induced Pattern of Coexisting Condensates in the Superconducting State of CeCoIn<sub>5</sub>,” Phys. Rev. Lett. **104**, 216403 (2010). [32](#)
- [53] G. Grüner, “The dynamics of charge-density waves,” Rev. Mod. Phys. **60**, 1129 (1988); “The dynamics of spin-density waves,” Rev. Mod. Phys. **66**, 1 (1994). [32](#)
- [54] L. P. Gorkov and A. G. Lebed, “On the stability of the quasi-one dimensional metallic phase in magnetic fields against the spin density wave formation,” J. Phys. Lett. **45**, L433 (1984); M. Héritier, G. Montambaux and P. Lederer, J. Phys. Lett. **45**, L943 (1984). [32](#)
- [55] A. Aperis *et al*, “New field-induced spin density wave phenomena from the Pauli terms in excitonic insulators,” Europhys. Lett. **83**, 67008 (2008). [32](#)
- [56] G. Varelogiannis and M. Héritier, “Confined field induced density waves in unconventional superconductors,” J. Phys.: Condens. Matter **15**, L673 (2003). [32](#)
- [57] P. Thalmeier, “Classification of unconventional electron-hole condensates ,” Z. Phys. B **100**, 387 (1996); C. Nayak, “Density-wave states of nonzero angular momentum,” Phys. Rev. B **62**, 4880 (2000). [32](#)
- [58] A. Aperis, P. Kotetes, E. Papantonopoulos, G. Siopsis, P. Skamagoulis and G. Varelogiannis, “Holographic Charge Density Waves,” Phys. Lett. B **702**, 181 (2011) [arXiv:1009.6179 [hep-th]]. [32](#), [34](#)

- [59] K. Maeda, T. Okamura and J. -i. Koga, “Inhomogeneous charged black hole solutions in asymptotically anti-de Sitter spacetime,” *Phys. Rev. D* **85**, 066003 (2012) [arXiv:1107.3677 [gr-qc]]. [32](#)
- [60] N. Iizuka and K. Maeda, “Towards the Lattice Effects on the Holographic Superconductor,” *JHEP* **1211**, 117 (2012) [arXiv:1207.2943 [hep-th]]. [32](#)
- [61] A. Donos and S. A. Hartnoll, “Universal linear in temperature resistivity from black hole superradiance,” *Phys. Rev. D* **86**, 124046 (2012) [arXiv:1208.4102 [hep-th]]. [32](#)
- [62] G. T. Horowitz, J. E. Santos and D. Tong, “Optical Conductivity with Holographic Lattices,” *JHEP* **1207**, 168 (2012) [arXiv:1204.0519 [hep-th]]. [32](#), [121](#)
- [63] G. T. Horowitz, J. E. Santos and D. Tong, “Further Evidence for Lattice-Induced Scaling,” *JHEP* **1211**, 102 (2012) [arXiv:1209.1098 [hep-th]]. [32](#), [121](#)
- [64] J. Alsup, E. Papantonopoulos and G. Siopsis, “A Novel Mechanism to Generate FFLO States in Holographic Superconductors,” *Phys. Lett. B* **720**, 379 (2013) [arXiv:1210.1541 [hep-th]]. [33](#), [34](#), [50](#)
- [65] X. -M. Kuang, E. Papantonopoulos, G. Siopsis and B. Wang, “Building a Holographic Superconductor with Higher-derivative Couplings,” arXiv:1303.2575 [hep-th]. [33](#), [34](#)
- [66] A. Donos and J. P. Gauntlett, “Black holes dual to helical current phases ,” *Phys. Rev. D* **86**, 064010 (2012) [arXiv:1204.1734 [hep-th]]. [33](#), [50](#)
- [67] S. Nakamura, H. Ooguri, and C.-S. Park, “Gravity Dual of Spatially Modulated Phase,” *Phys. Rev. D* **81**, 044018 (2010) [arXiv:0911.0679 [hep-th]]. [33](#), [50](#)
- [68] J. Alsup, J. Therrien and G. Siopsis, “Hair on near-extremal Reissner-Nordstrom AdS black holes,” *Phys. Rev. D* **86**, 025002 (2012) [arXiv:1110.3342 [hep-th]]. [38](#)
- [69] S. A. Hartnoll, C. P. Herzog and G. T. Horowitz, “Building a Holographic Superconductor,” *Phys. Rev. Lett.* **101**, 031601 (2008) [arXiv:0803.3295];

- S. A. Hartnoll, C. P. Herzog and G. T. Horowitz, “Holographic Superconductors,” JHEP **0812**, 015 (2008) [arXiv:0810.1563]. [51](#)
- [70] M. Cubrovic, J. Zaanen and K. Schalm, “String Theory, Quantum Phase Transitions and the Emergent Fermi-Liquid,” Science **325**, 439 (2009). [arXiv:0904.1993 [hep-th]]. [51](#), [54](#)
- [71] S. Bhattacharyya *et al*, V. E. Hubeny, S. Minwalla and M. Rangamani, “Non-linear Fluid Dynamics from Gravity,” JHEP **0802**, 045 (2008). [arXiv:0712.2456 [hep-th]]. [51](#)
- [72] N. Iqbal, H. Liu, M. Mezei and Q. Si, “Quantum phase transitions in holographic models of magnetism and superconductors,” Phys. Rev. D **82**, 045002 (2010). [arXiv:1003.0010 [hep-th]]. [51](#)
- [73] C. P. Herzog, P. Kovtun, S. Sachdev and D. T. Son, “Quantum critical transport, duality, and M-theory,” Phys. Rev. D **75**, 085020 (2007). [arXiv:hep-th/0701036]. [52](#)
- [74] G. Koutsoumbas, E. Papantonopoulos and G. Siopsis, “Exact Gravity Dual of a Gapless Superconductor,” JHEP **0907**, 026 (2009), [arXiv:0902.0733 [hep-th]]; Q. Pan, B. Wang, E. Papantonopoulos, J. Oliveira and A. B. Pavan, “Holographic Superconductors with various condensates in Einstein-Gauss-Bonnet gravity,” Phys. Rev. D **81**, 106007 (2010). [arXiv:0912.2475 [hep-th]]; G. Siopsis and J. Therrien, “Analytic Calculation of Properties of Holographic Superconductors,” JHEP **1005**, 013 (2010), [arXiv:1003.4275 [hep-th]]. [31](#), [52](#)
- [75] H. Liu, J. McGreevy and D. Vegh, “Non-Fermi liquids from holography,” Phys. Rev. D **83**, 065029 (2011) [arXiv:0903.2477 [hep-th]]. [52](#), [54](#)
- [76] T. Faulkner, H. Liu, J. McGreevy and D. Vegh, “Emergent quantum criticality, Fermi surfaces, and AdS(2),” Phys. Rev. D **83**, 125002 (2011) [arXiv:0907.2694 [hep-th]]. [52](#), [54](#), [59](#), [60](#), [90](#)
- [77] S. A. Hartnoll, J. Polchinski, E. Silverstein and D. Tong, “Towards strange metallic holography,” JHEP **1004**, 120 (2010) [arXiv:0912.1061 [hep-th]]. [52](#)

- [78] S. A. Hartnoll and A. Tavanfar, “Electron stars for holographic metallic criticality,” *Phys. Rev. D* **83**, 046003 (2011) [arXiv:1008.2828 [hep-th]]. [52](#)
- [79] A. Allais and J. McGreevy, “How to construct a gravitating quantum electron star,” *Phys. Rev. D* **88**, no. 6, 066006 (2013) [arXiv:1306.6075 [hep-th]]. [52](#)
- [80] M. Cubrovic, J. Zaanen and K. Schalm, “Constructing the AdS Dual of a Fermi Liquid: AdS Black Holes with Dirac Hair,” *JHEP* **1110**, 017 (2011) [arXiv:1012.5681 [hep-th]]. [52](#)
- [81] S. Sachdev, “A model of a Fermi liquid using gauge-gravity duality,” *Phys. Rev. D* **84**, 066009 (2011) [arXiv:1107.5321 [hep-th]]. [52](#)
- [82] M. Edalati, R. G. Leigh and P. W. Phillips, “Dynamically Generated Mott Gap from Holography,” *Phys. Rev. Lett.* **106**, 091602 (2011) [arXiv:1010.3238 [hep-th]]. [52](#), [57](#), [60](#), [64](#)
- [83] M. Edalati, R. G. Leigh, K. W. Lo and P. W. Phillips, “Dynamical Gap and Cuprate-like Physics from Holography,” *Phys. Rev. D* **83**, 046012 (2011) [arXiv:1012.3751 [hep-th]]. [52](#), [57](#), [60](#), [64](#)
- [84] W. J. Li and H. Zhang, “Holographic non-relativistic fermionic fixed point and bulk dipole coupling,” *JHEP* **1111**, 018 (2011) [arXiv:1110.4559 [hep-th]]. [52](#)
- [85] X. M. Kuang, B. Wang and J. P. Wu, “Dipole Coupling Effect of Holographic Fermion in the Background of Charged Gauss-Bonnet AdS Black Hole,” *JHEP* **1207**, 125 (2012) [arXiv:1205.6674 [hep-th]]. [52](#)
- [86] L. Q. Fang, X. H. Ge and X. M. Kuang, “Holographic fermions with running chemical potential and dipole coupling,” *Nucl. Phys. B* **877**, 807 (2013) [arXiv:1304.7431 [hep-th]]. [52](#)
- [87] J. P. Wu, “The charged Lifshitz black brane geometry and the bulk dipole coupling,” *Phys. Lett. B* **728**, 450 (2014). [52](#)
- [88] P. W. Phillips, B. W. Langle, J. A. Hutasoit, “Un-Fermi liquids: Unparticles in strongly correlated electron matter,” *Phys. Rev. B* **88**, 115129 (2013),

- [arXiv:1305.0006 [cond-mat]]. [52](#)
- [89] D. Guarrera and J. McGreevy, “Holographic Fermi surfaces and bulk dipole couplings,” [arXiv:1102.3908 [hep-th]]. [52](#)
- [90] J. M. Luttinger, “Fermi Surface and Some Simple Equilibrium Properties of a System of Interacting Fermions,” *Phys. Rev.* **119**, 1153 (1960). [53](#)
- [91] T. D. Stanescu, P. W. Phillips, and T. Choy, P “Theory of the Luttinger surface in doped Mott insulators,” *Phys. Rev. B* **75**, 104503 (2007), [arXiv:cond-mat/0602280]. [53](#), [54](#)
- [92] I. Dzyaloshinskii, “Some consequences of the Luttinger theorem: The Luttinger surfaces in non-Fermi liquids and Mott insulators,” *Phys. Rev. B* **68**, 085113 (2003). [53](#), [54](#)
- [93] G. ’t Hooft, “A Two-Dimensional Model for Mesons,” *Nucl. Phys. B* **75**, 461 (1974). [54](#)
- [94] T. D. Stanescu and G. Kotliar, “Fermi arcs and hidden zeros of the Green function in the pseudogap state,” *Phys. Rev. B* **74**, 125110 (2006), [arXiv:cond-mat/0508302]; R. M. Konik, T. M. Rice, and A. M. Tsvelik, “Doped Spin Liquid: Luttinger Sum Rule and Low Temperature Order,” *Phys. Rev. Lett.* **96**, 086407 (2006), [arXiv:cond-mat/0511268]. [54](#)
- [95] S. Hong and P. W. Phillips, “Towards the standard model for Fermi arcs from a Wilsonian reduction of the Hubbard model,” *Phys. Rev. B* **86**, 115118 (2012), [arXiv:1110.0440 [cond-mat.str-el]]. [54](#)
- [96] S. Sakai, Y. Motome, and M. Imada, “Evolution of Electronic Structure of Doped Mott Insulators: Reconstruction of Poles and Zeros of Green’s Function,” *Phys. Rev. Lett.* **102**, 056404 (2009), [arXiv:0809.0950v1 [cond-mat.str-el]]. [54](#)
- [97] S. Sakai, Y. Motome, and M. Imada, “Doped high-Tc cuprate superconductors elucidated in the light of zeros and poles of the electronic Green’s function,” *Phys. Rev. B* **82**, 134505 (2010), [arXiv:1004.2569 [cond-mat.str-el]]. [54](#)

- [98] S. S. Lee, “A Non-Fermi Liquid from a Charged Black Hole: A Critical Fermi Ball,” *Phys. Rev. D* **79**, 086006 (2009) [arXiv:0809.3402 [hep-th]]. [54](#)
- [99] T. Faulkner, N. Iqbal, H. Liu, J. McGreevy and D. Vegh, “From Black Holes to Strange Metals,” [arXiv:1003.1728 [hep-th]]. [55](#), [61](#), [78](#)
- [100] S. S. Gubser, F. D. Rocha and A. Yarom, “Fermion correlators in non-abelian holographic superconductors,” *JHEP* **1011**, 085 (2010) [arXiv:1002.4416 [hep-th]]; M. Ammon, J. Erdmenger, M. Kaminski and A. O’Bannon, “Fermionic Operator Mixing in Holographic p-wave Superfluids,” *JHEP* **1005**, 053 (2010) [arXiv:1003.1134 [hep-th]]. [55](#)
- [101] F. Benini, C. P. Herzog and A. Yarom, “Holographic Fermi arcs and a d-wave gap,” *Phys. Lett. B* **701**, 626 (2011) [arXiv:1006.0731 [hep-th]]. [55](#), [80](#)
- [102] Y. Liu, K. Schalm, Y. W. Sun and J. Zaanen, “Lattice Potentials and Fermions in Holographic non Fermi-Liquids: Hybridizing Local Quantum Criticality,” *JHEP* **1210**, 036 (2012) [arXiv:1205.5227 [hep-th]]. [55](#)
- [103] S. S. Gubser, C. P. Herzog, S. S. Pufu and T. Tesileanu, “Superconductors from Superstrings,” *Phys. Rev. Lett.* **103**, 141601 (2009) [arXiv:0907.3510 [hep-th]]. [55](#)
- [104] J. P. Gauntlett, S. Kim, O. Varela and D. Waldram, “Consistent supersymmetric Kaluza–Klein truncations with massive modes,” *JHEP* **0904** (2009) 102 [arXiv:0901.0676 [hep-th]]. [55](#)
- [105] J. P. Gauntlett, J. Sonner and T. Wiseman, “Holographic superconductivity in M-Theory,” *Phys. Rev. Lett.* **103** (2009) 151601 [arXiv:0907.3796 [hep-th]]. [55](#)
- [106] J. P. Gauntlett, J. Sonner and T. Wiseman, “Quantum Criticality and Holographic Superconductors in M-theory,” *JHEP* **1002**, 060 (2010) [arXiv:0912.0512 [hep-th]]. [55](#)
- [107] N. Bobev, N. Halmagyi, K. Pilch and N. P. Warner, “Supergravity Instabilities of Non-Supersymmetric Quantum Critical Points,” *Class. Quant. Grav.* **27**,



- 235013 (2010); N. Bobev, A. Kundu, K. Pilch and N. P. Warner, “Minimal Holographic Superconductors from Maximal Supergravity,” JHEP **1203**, 064 (2012). [55](#)
- [108] I. Bah, A. Faraggi, J. I. Jottar, R. G. Leigh and L. A. Pando Zayas, “Fermions and  $D = 11$  Supergravity On Squashed Sasaki-Einstein Manifolds,” JHEP **1102**, 068 (2011) [arXiv:1008.1423 [hep-th]]. [55](#)
- [109] I. Bah, A. Faraggi, J. I. Jottar and R. G. Leigh, “Fermions and Type IIB Supergravity On Squashed Sasaki-Einstein Manifolds,” JHEP **1101**, 100 (2011) [arXiv:1009.1615 [hep-th]]. [55](#)
- [110] O. DeWolfe, S. S. Gubser, and C. Rosen, “Fermi surfaces in N=4 Super-Yang-Mills theory,” Phys. Rev. D **86**, (2012) 106002 , [arXiv:1207.3352 [hep-th]]; O. DeWolfe, S. S. Gubser, and C. Rosen,, “Minding the Gap in N=4 Super-Yang-Mills,” [arXiv:1312.7347 [hep-th]]. [55](#)
- [111] G. Vanacore, P. W. Phillips, “Minding the Gap in Holographic Models of Interacting Fermions,” Phys. Rev. D **90**, 044022 (2014), [arXiv:1405.1041 [cond-mat]]. [60](#)
- [112] S. Ryu and T. Takayanagi, “Holographic derivation of entanglement entropy from AdS/CFT,” Phys. Rev. Lett. **96**, 181602 (2006) [hep-th/0603001]. [65](#)
- [113] S. Ryu and T. Takayanagi, “Aspects of Holographic Entanglement Entropy,” JHEP **0608**, 045 (2006) [hep-th/0605073]. [65](#)
- [114] X. M. Kuang, E. Papantonopoulos and B. Wang, “Entanglement Entropy as a Probe of the Proximity Effect in Holographic Superconductors,” JHEP **1405**, 130 (2014) [arXiv:1401.5720 [hep-th]]. [65](#)
- [115] T. Albash and C. V. Johnson, “Holographic Studies of Entanglement Entropy in Superconductors,” JHEP **1205**, 079 (2012) [arXiv:1202.2605 [hep-th]]. [65](#)
- [116] C. M. Varma, P. B. Littlewood, and S. Schmitt-Rink, E. Abrahams and A. E. Ruckenstein, "Phenomenology of the Normal State of Cu-O High-Temperature

- Superconductors", Phys. Rev. Lett. 63, 1996, (1989) [67](#)
- [117] Y. Liu, K. Schalm, Y. W. Sun, and J. Zaanen, "Lattice potentials and fermions in holographic non Fermi-liquids: hybridizing local quantum criticality," JHEP **1210**, 036 (2012) [arXiv:1205.5227v2 [hep-th]]. [81](#), [100](#), [102](#), [108](#), [118](#)
- [118] Y. Ling, C. Niu and J. -P. Wu and Z. -Y. Xian and H. Zhang, "Holographic fermionic liquid with lattices," JHEP **1307**, 045 (2013) [arXiv:1304.2128 [hep-th]]. [80](#), [118](#)
- [119] T. Faulkner, G. T. Horowitz, J. McGreevy, M. M. Roberts and D. Vegh, "Photoemission 'experiments' on holographic superconductors," JHEP **1003**, 121 (2010) [arXiv:0911.3402 [hep-th]]. [68](#)
- [120] T. Faulkner, H. Liu, J. McGreevy, and D. Vegh, "Holographic non-Fermi liquid fixed points", [arXiv:1101.0597[hep-th]]. [95](#), [116](#)
- [121] Y. Ling, P. Liu, C. Niu, J. P. Wu and Z. Y. Xian, "Holographic fermionic system with dipole coupling on Q-lattice," JHEP **1412**, 149 (2014) [arXiv:1410.7323 [hep-th]]. [118](#), [121](#)
- [122] Y. Ling, P. Liu, C. Niu, J. P. Wu, "Building a doped Mott system by holography," [arXiv:1507.02514 [hep-th]]. [118](#)

# Appendix

# Appendix A

## Calculation of the metric functions

$$Q_{tt10}(z) = \frac{z^3}{4(1-z)P(z)} \times \int_1^z \left[ 2\mu_0 A_{t10}(w) - 2(1-w)\mu_0 A'_{t10}(w) - \frac{12\mathcal{A}_{t1}(w)}{w^4} + \frac{w^{2\Delta-4}}{16P(w)} \mathcal{A}_{t2}(w) \right] dw \quad (\text{A.1})$$

where

$$\mathcal{A}_{t1}(z) = - \int_0^z dw w^{2\Delta+1} \frac{q^2 \mu_0^2 F^2(w) + w^{-2} [P^2(w)(\Delta F(w) + wF'(w))^2]}{2P^2(w)}, \quad (\text{A.2})$$

and

$$\begin{aligned} \mathcal{A}_{t2}(z) &= 16(z-1)z^2 P(z)^2 [F'(z)]^2 + 32\Delta(z-1)zP^2(z)F(z)F'(z) \\ &+ [16\mu_0^2 q^2 (z-1)z^2 + \Delta^2 z^3 (4(\mu_0^2 + 4) + \mu_0^4 z^4 - (\mu_0^2 + 8)\mu_0^2 z^3 + 16z^2 + 16z)] F^2(z) \\ &+ 16k^2 z^2 P(z) (\eta\mu_0^2 z^4 + 1) F^2(z) - 48\Delta P(z) F^2(z). \end{aligned} \quad (\text{A.3})$$

Similarly,

$$Q_{zz10}(z) = \frac{z^3}{4(1-z)P(z)} \times \int_1^z [-2\mu_0 A_{t10}(w) + 2(1-w)\mu_0 A'_{t10}(w) + \mu_0^2 \mathcal{A}_{z1}(w) + w^{2\Delta-4} \mathcal{A}_{z2}(w)] dw \quad (\text{A.4})$$

where

$$\mathcal{A}_{z1}(z) = - \int_0^z dw w^{2\Delta+1} \frac{q^2 \mu_0^2 F^2(w) + w^{-2} [P^2(w)(\Delta F(w) + wF'(w))^2]}{2P^2(w)}, \quad (\text{A.5})$$

and

$$\begin{aligned} \mathcal{A}_{z2}(z) = & - \frac{[q^2(1-z)z^2\mu_0^2 + ((\Delta-3)\Delta + k^2z^2(1+z^4\eta\mu_0^2))P(z)]}{P(z)} \\ & + (1-z)P(z) [\Delta F(z) + zF'(z)]^2. \end{aligned} \quad (\text{A.6})$$

$$Q_{xx10}(z) = \int_0^z dw \frac{w^2}{P(w)(1-w)} \int_1^{w'} \frac{1}{2} k^2 w'^{2\Delta-2} (w'^4 \eta \mu_0^2 - 1) F^2(w') dw' \quad (\text{A.7})$$

and calculations show us that  $Q_{yy10}(z) = -Q_{xx10}(z)$ . Therefore, we find

$$Q_{yy10}(z) = - \int_0^z dw \frac{w^2}{P(w)(1-w)} \int_1^{w'} \frac{1}{2} k^2 w'^{2\Delta-2} (w'^4 \eta \mu_0^2 - 1) F^2(w') dw'. \quad (\text{A.8})$$

Maxwell's, and Einstein's equations for the remaining first-order modes, i.e.  $Q_{tt11}$ ,  $Q_{zz11}$ ,  $Q_{xx11}$ ,  $Q_{yy11}$  and  $Q_{xz11}$ , are reduced to the following equations.

$$\begin{aligned}
& Q''_{xx11} + Q''_{yy11} + \frac{Q_{zz11} [z(8k^2z + 4(z-1)P' + \mu_0^2z^3) + (12-8z)P]}{2(z-1)z^2P} + \frac{4k^2Q_{yy11}}{(z-1)P} \\
& - \frac{2kz^2Q_{xz11}((z-1)P' + P)}{(z-1)P} - 4kz^2Q'_{xz11} + \frac{((z-1)zP' + (4-3z)P)Q'_{xx11}}{2(z-1)zP} + \frac{2Q'_{zz11}}{z} \\
& + \frac{((z-1)zP' + (4-3z)P)Q'_{yy11}}{2(z-1)zP} + \frac{\mu_0^2z^2Q_{tt11}}{2(z-1)P} - \frac{\mu_0z^2A'_{t11}}{P} + \frac{\mu_0z^2A_{t11}}{P-zP} + \mathcal{A}_1 = 0,
\end{aligned} \tag{A.9}$$

$$\begin{aligned}
& Q'_{xx11} + Q'_{yy11} - 4kz^2Q_{xz11}(z) + \frac{(8k^2z + \mu_0^2z^3)Q_{tt11}}{(z-1)zP' + (4-3z)P} + \frac{8k^2zQ_{yy11}}{(z-1)zP' + (4-3z)P} \\
& - \frac{4(z-1)PQ'_{tt11}}{(z-1)zP' + (4-3z)P} + \frac{[z(4(z-1)P' + \mu_0^2z^3) + (12-8z)P]Q_{zz11}}{z((z-1)zP' + (4-3z)P)} \\
& - \frac{2\mu_0z^3A_{t11}}{(z-1)zP' + (4-3z)P} - \frac{2\mu_0(z-1)z^3A'_{t11}}{(z-1)zP' + (4-3z)P} + \mathcal{A}_2 = 0,
\end{aligned} \tag{A.10}$$

$$\begin{aligned}
& Q'_{tt11} + Q'_{yy11} + \frac{[(z-1)P' + P]Q_{tt11}}{2(z-1)P} + \frac{[(3z-4)P - (z-1)zP']Q_{zz11}}{2(z-1)zP} \\
& + \frac{\mu_0z^2A_{t11}}{P} + \mathcal{A}_3 = 0,
\end{aligned} \tag{A.11}$$

$$\begin{aligned}
& Q''_{tt11} + Q''_{yy11} + \frac{[3(z-1)zP' - (z-4)P]Q'_{tt11}}{2(z-1)zP} + \frac{[(z-1)zP' - (z-2)P]Q'_{yy11}}{(z-1)zP} \\
& - \frac{[(z-1)zP' + (4-3z)P]Q'_{zz11}}{2(z-1)zP} + \frac{\mu_0^2z^2Q_{tt11}}{2P-2zP} + \frac{\mu_0z^2A'_{t11}}{P} \\
& - \frac{[z(z(2(z-1)P'' + \mu_0^2z^2) - 4(z-2)P') + 4(z-3)P]Q_{zz11}}{2(z-1)z^2P} + \frac{\mu_0z^2A_{t11}}{(z-1)P} + \mathcal{A}_4 = 0
\end{aligned} \tag{A.12}$$

$$\begin{aligned}
& Q''_{tt11} + Q''_{xx11} - \frac{[z(z(-8k^2 + 2(z-1)P'' + \mu_0^2 z^2) - 4(z-2)P') + 4(z-3)P] Q_{zz11}}{2(z-1)z^2 P} \\
& + \frac{Q_{tt11}(8k^2 - \mu_0^2 z^2)}{2(z-1)P} - \frac{4kz^2 Q_{xz11}((z-1)P' + P)}{(z-1)P} + \frac{(3(z-1)zP' - (z-4)P) Q'_{tt11}}{2(z-1)zP} \\
& + \frac{((z-1)zP' - (z-2)P) Q'_{xx11}}{(z-1)zP} - \frac{((z-1)zP' + (4-3z)P) Q'_{zz11}}{2(z-1)zP} \\
& + \frac{\mu_0 z^2 A'_{t11}}{P} + \frac{\mu_0 z^2 A_{t11}}{(z-1)P} - 4kz^2 Q'_{xz11} + \mathcal{A}_5 = 0,
\end{aligned} \tag{A.13}$$

and from Maxwell's equation

$$\begin{aligned}
A''_{t11} + \frac{4k^2 A_{t11}}{(z-1)P} + \frac{2A'_{t11}}{z-1} - \frac{2k\mu_0 z^2 Q_{xz11}}{z-1} + \frac{\mu_0 Q'_{tt11}}{2(1-z)} + \frac{\mu_0 Q'_{xx11}}{2(z-1)} + \frac{\mu_0 Q'_{yy11}}{2(z-1)} \\
+ \frac{\mu_0 Q'_{zz11}}{2(1-z)} + \mathcal{A}_6 = 0
\end{aligned} \tag{A.14}$$

where

$$\begin{aligned}
\mathcal{A}_1 = & \frac{F^2 z^{2\Delta-2} [P(k^2(\eta\mu_0^2 z^6 + z^2) - (\Delta-3)\Delta) + \Delta^2(z-1)P^2 + \mu_0^2 q^2(z-1)z^2]}{2(z-1)P^2} \\
& + \frac{1}{2} z^{2\Delta} F'^2 + \Delta F z^{2\Delta-1} F',
\end{aligned} \tag{A.15}$$

$$\begin{aligned}
\mathcal{A}_2 = & -\frac{2\Delta(z-1)Pz^{2\Delta}FF'}{(z-1)zP' + (4-3z)P} - \frac{(z-1)Pz^{2\Delta+1}F'^2}{(z-1)zP' + (4-3z)P} \\
& - \frac{z^{2\Delta-1} \left[ (\Delta-3)\Delta - k^2(\eta\mu_0^2 z^6 + z^2) + \frac{\mu_0^2 q^2(z-1)z^2}{P} + \Delta^2(z-1)P \right] F^2}{(z-1)zP' + (4-3z)P},
\end{aligned} \tag{A.16}$$

$$\mathcal{A}_3 = \frac{1}{2} F z^{2\Delta-1} (zF' + \Delta F), \tag{A.17}$$

$$\begin{aligned}
\mathcal{A}_4 = & \frac{1}{2} z^{2\Delta} F'^2 + \Delta z^{2\Delta-1} F F' \\
& + \frac{z^{2\Delta-2} [P((\Delta-3)\Delta + k^2 z^2 (1 - \eta \mu_0^2 z^4)) - \Delta^2 (z-1) P^2 + \mu_0^2 q^2 (z-1) z^2]}{2(1-z) P^2} F^2 ,
\end{aligned} \tag{A.18}$$

$$\begin{aligned}
\mathcal{A}_5 = & \frac{1}{2} z^{2\Delta} F'^2 + \Delta z^{2\Delta-1} F F' \\
& + \frac{z^{2\Delta-2} [P((\Delta-3)\Delta + k^2 z^2 (\eta \mu_0^2 z^4 - 1)) - \Delta^2 (z-1) P^2 + \mu_0^2 q^2 (z-1) z^2]}{2(1-z) P^2} F^2 ,
\end{aligned} \tag{A.19}$$

$$\mathcal{A}_6 = \frac{\mu_0 z^{2\Delta-2} (q^2 - 2\eta k^2 z^3 P)}{(z-1) P} F^2 . \tag{A.20}$$



## Appendix B

The first order scalar equation below

$T_C$

$$C_2 = -\frac{z^3 \mu_0}{2P} , \quad (\text{B.1})$$

$$C_1 = -\frac{\mu_0 z^3 P'}{2P^2} + \frac{\mu_0 z^2 [8\Delta + (2\Delta - 1)\mu_0^2 z^4 - 2z^3 (\Delta (\mu_0^2 + 4) - \mu_0^2) - 8z^2 - 8z + 4]}{8(z-1)P^2} , \quad (\text{B.2})$$

$$C_0 = \frac{2q^2 \mu_0 (1 + z + z^2)}{P^3} - \frac{z^2 \Delta \mu_0 P'}{2P^2} - \frac{2k^2 z^4 \eta \mu_0}{(z-1)P} + \frac{\Delta \mu_0 z [z^4 (\Delta - 2)\mu_0^2 + z^3 (4 + 3\mu_0^2 - \Delta(4 + \mu_0^2)) - 8z(z+1) + 4\Delta]}{8(z-1)P^2} , \quad (\text{B.3})$$

$$\mathcal{D}_2 = -\mathbf{q}_{zz10} - \frac{1}{2} Q_{zz11} , \quad (\text{B.4})$$

$$\mathcal{D}_1 = \mathbf{q}_{zz10} \left[ \frac{(2\Delta - 2\Delta z + z - 2)}{(z-1)z} - \frac{P'}{P} \right] + \frac{1}{4} Q_{zz11} \left[ \frac{2(2\Delta - 2\Delta z + z - 2)}{(z-1)z} - \frac{2P'}{P} \right] + \frac{\mathbf{q}_{tt10}'}{2} + \frac{Q'_{tt11}}{4} + \frac{Q'_{xx10}}{2} + \frac{Q'_{xx11}}{4} + \frac{Q'_{yy10}}{2} + \frac{Q'_{yy11}}{4} - \frac{\mathbf{q}_{zz10}'}{2} - \frac{Q'_{zz11}}{4} , \quad (\text{B.5})$$

$$\begin{aligned}
\mathcal{D}_0 = & \frac{\mathbf{q}_{zz10} (z(\eta k^2 \mu_0^2 z^5 + (\Delta - \Delta z)P') + \Delta P(\Delta + (\Delta - 2)(-z) - 3))}{(z-1)z^2 P} \\
& - \frac{Q_{zz11} (z(k^2 z + \Delta(z-1)P') + \Delta P(-\Delta + (\Delta - 2)z + 3))}{2(z-1)z^2 P} \\
& + \frac{\mu_0^2 \mathbf{q}_{tt10} \left( \frac{\eta k^2 z^4 P}{z-1} - q^2 \right)}{P^2} + \frac{Q_{tt11} \left( -\frac{k^2 P}{z-1} - \mu_0^2 q^2 \right)}{2P^2} + \frac{2\mu_0 \mathbf{v}_{10} \left( q^2 - \frac{\eta k^2 z^4 P}{z-1} \right)}{P^2} \\
& + \frac{\mu_0 A_{t11} (q^2 - 2\eta k^2 z^3 P)}{P^2} + \frac{k^2 Q_{xx10} (\eta \mu_0^2 z^4 - 1)}{(z-1)P} + \frac{k^2 Q_{yy11} (\eta \mu_0^2 z^4 - 1)}{2(z-1)P} \\
& + \frac{\Delta (2\mathbf{q}_{tt10}' - 2\mathbf{q}_{zz10}' + 2Q'_{xx10} + 2Q'_{yy10} + Q'_{tt11} - Q'_{zz11} + Q'_{xx11} + Q'_{yy11})}{4z} \\
& - \frac{2\eta k^2 \mu_0 z^4 \mathbf{v}_{10}'}{P(z)}.
\end{aligned} \tag{B.6}$$

where  $\mathbf{q}_{tt10}, \mathbf{q}_{zz10}, \mathbf{v}_{10}$  is found by setting  $C \rightarrow 0$  in (A.1), (A.4), and (4.22) respectively.

# Appendix C

## Details of Spinor Rotation

Consider the Dirac equations

$$\begin{aligned}
\sqrt{h}\psi'_{+1} + \frac{m_f}{z}\psi_{+1} + \left[ k_x + Kl - \frac{\mu q_f(1-z) + \omega}{\sqrt{h}} \right] \psi_{+2} - k_y \psi_{-2} &= 0, \\
\sqrt{h}\psi'_{+2} - \frac{m_f}{z}\psi_{+2} + \left[ k_x + Kl + \frac{\mu q_f(1-z) + \omega}{\sqrt{h}} \right] \psi_{+1} - k_y \psi_{-1} &= 0, \\
\sqrt{h}\psi'_{-1} + \frac{m_f}{z}\psi_{-1} + \left[ -k_x - Kl - \frac{\mu q_f(1-z) + \omega}{\sqrt{h}} \right] \psi_{-2} - k_y \psi_{+2} &= 0, \\
\sqrt{h}\psi'_{-2} - \frac{m_f}{z}\psi_{-2} + \left[ -k_x - Kl + \frac{\mu q_f(1-z) + \omega}{\sqrt{h}} \right] \psi_{-1} - k_y \psi_{+1} &= 0. \quad (\text{C.1})
\end{aligned}$$

The first and third equations can be combined into

$$\begin{aligned}
\sqrt{h}(\psi_{+1} + \lambda\psi_{-1})' + \frac{m_f}{z}(\psi_{+1} + \lambda\psi_{-1}) - \left[ \frac{\mu q_f(1-z) + \omega}{\sqrt{h}} \right] (\psi_{+2} + \lambda\psi_{-2}) \\
+ (k_x - \lambda k_y)\psi_{+2} + (-k_y - \lambda k_x)\psi_{-2} = 0. \quad (\text{C.2})
\end{aligned}$$

Let  $k_x + Kl = k_l \cos \theta$ ,  $k_y = k_l \sin \theta$  with  $k_l = \sqrt{(k_x + Kl)^2 + k_y^2}$  and choose

$$\lambda = -\tan \frac{\theta}{2} \quad (\text{C.3})$$

Then (C.2) becomes

$$\sqrt{h}(\psi_{+1} + \lambda\psi_{-1})' + \frac{m_f}{z}(\psi_{+1} + \lambda\psi_{-1}) + \left[ k_l - \frac{\mu q_f(1-z) + \omega}{\sqrt{h}} \right] (\psi_{+2} + \lambda\psi_{-2}) = 0, \quad (\text{C.4})$$

which is identical to the first equation with  $k_y = 0$ . Similarly, we obtain

$$\sqrt{h}(\psi_{+2} + \lambda\psi_{-2})' - \frac{m_f}{z}(\psi_{+2} + \lambda\psi_{-2}) + \left[ k_l + \frac{\mu q_f(1-z) + \omega}{\sqrt{h}} \right] (\psi_{+1} + \lambda\psi_{-1}) = 0. \quad (\text{C.5})$$

Similarly, choosing  $\delta = \cot\left(\frac{\theta}{2}\right)$  we obtain

$$\sqrt{h}(\psi_{+1} + \delta\psi_{-1})' + \frac{m_f}{z}(\psi_{+1} + \delta\psi_{-1}) + \left[ -k_l - \frac{\mu q_f(1-z) + \omega}{\sqrt{h}} \right] (\psi_{+2} + \delta\psi_{-2}) = 0, \quad (\text{C.6})$$

$$\sqrt{h}(\psi_{+2} + \delta\psi_{-2})' - \frac{m_f}{z}(\psi_{+2} + \delta\psi_{-2}) + \left[ -k_l + \frac{\mu q_f(1-z) + \omega}{\sqrt{h}} \right] (\psi_{+1} + \delta\psi_{-1}) = 0, \quad (\text{C.7})$$

i.e., the modes decouple and the equations are the same as with  $k_y = 0$ . Solutions only depend on  $k_l$  and we define

$$\tilde{\psi}_1^{(l)} = \psi_{+1}^{(l)} + \lambda\psi_{-1}^{(l)}, \quad \tilde{\psi}_2^{(l)} = \psi_{+2}^{(l)} + \lambda\psi_{-2}^{(l)}, \quad (\text{C.8})$$

$$\tilde{\psi}_3^{(l)} = \psi_{+1}^{(l)} + \delta\psi_{-1}^{(l)}, \quad \tilde{\psi}_4^{(l)} = \psi_{+2}^{(l)} + \delta\psi_{-2}^{(l)}. \quad (\text{C.9})$$

which is given in (4.45).

# Vita

Kübra Yeter-Aydeniz was born in Eskişehir, Turkey, in 1985. She grew up in Eskişehir and completed her undergraduate studies in Physics Education at Gazi University, Ankara, Turkey in 2008. She started working as a Graduate Research Assistant in Physics Department at Anadolu University, Eskişehir, Turkey where she received a scholarship from Turkish Higher Education Council to study abroad. Following that she continued her graduate education in August 2010 in Department of Physics and Astronomy at the University of Tennessee, Knoxville where she worked both as a Graduate Teaching Assistant and Graduate Research Assistant. She conducted her studies under supervision of Professor George Siopsis on projects in condensed matter applications of AdS/CFT correspondence. She completed her PhD in 2015.